

Final Design Report

*MAE 162E –
Mechanical Engineering Design II*

Instructors: Robert Shaefer, Herrick Chang, and Sarah Warren

Teaching Assistants: Christopher Kang, Sandeep Singh Rai, and Kuo-Tai Teng

Miracle Robot

Group Number 1

Daniel Lee

Layne Sakamoto

Austin Liu

Sonny Pham

Jonathan Harrison

University of California Los Angeles

Mechanical and Aerospace Engineering Department

6/14/2013

ABSTRACT

This report explores the preliminary design considerations as well as the final design specifications for the autonomous disc transporter robot, "Miracle Robot." The design specifications are changed as the new dimensions and weight of the robot is: 11.37 in x 8.64 in x 14.25 in and the loaded weight with 6 disks is 49.36 lb. According to our approximated center of masses, RWD has lower minimum friction coefficients than FWD with loaded and unloaded values of (0.258, 0.371) compared to (0.583, 0.75). With the steepest ramp angle being 14.036°, the required force to climb the incline is 4.138 lb for unloaded case and 12.085 lb for loaded case. The calculated total traction forces using a friction coefficient of 0.50 is 8.275 lb and 24.171 lb for unloaded and loaded cases. The maximum required torque is 13.966 lb-in, which is less than the optimal torque output for our chosen drive motor, the Hennkwell PD264M Planetary Gear Motor. The drivetrain system is a direct-drive system due to the low optimal RPM of the motor. The unloading mechanism consists of a motorized force gate that drops down to allow the discs to roll off and re-lifts the gate after unloading. In the product testing and evaluation, we performed six test runs using five discs, and the average complete run time was 78.6 seconds and the deviation between runs was small. Overall, the "Miracle Robot" final design adheres to all of the high level requirements.

TEAM PICTURE



Pictured from left to right: Austin Liu, Jonathan Harrison, Layne Sakamoto, Daniel Lee, Sonny Pham

TABLE OF CONTENTS

MIRACLE ROBOT	I
ABSTRACT.....	II
TEAM PICTURE	II
TABLE OF CONTENTS.....	III
LIST OF FIGURES.....	V
LIST OF TABLES.....	VIII
LIST OF SYMBOLS	IX
I. INTRODUCTION	1
I. NEED STATEMENT	1
II. HIGH-LEVEL DESIGN REQUIREMENTS	1
III. PRIOR STATE-OF-THE-ART.....	2
IV. STRUCTURE OF REPORT	2
II. DESIGN DESCRIPTION	3
I. DESIGN CONCEPT DEVELOPMENT.....	3
II. DESIGN OVERVIEW.....	6
III. SYSTEMS SPECIFICATIONS	10
IV. OVERALL SYSTEM DESIGN.....	11
IV. MECHANICAL SYSTEM OPERATION	16
V. CONTROL SYSTEM OPERATION.....	16
III. SUBSYSTEMS DESIGN DESCRIPTION	18
IV. DESIGN ANALYSIS.....	24
I. TORQUE CALCULATIONS.....	30
II. UNLOADING MECHANISMS	34
V. CONTROL SYSTEM DESIGN.....	38
I. MOTOR SELECTION FROM TORQUE CALCULATIONS.....	38
II. UNLOADING MECHANISMS	38
III. SENSORS AND THEORY OF OPERATIONS	39
IV. STATE DIAGRAMS.....	40
VI. PRODUCT FABRICATION	47
I. MACHINING OF SELECTED PARTS.....	47
II. ASSEMBLY	49

VII.	PRODUCT TESTING AND EVALUATION	53
VIII.	WORK BREAKDOWN SCHEDULE	58
IX.	BILL OF MATERIALS AND COST ANALYSIS.....	62
I.	BILL OF MATERIALS	62
II.	COST ANALYSIS.....	64
X.	DESIGN REQUIREMENT SATISFACTION	64
XI.	CONCLUSIONS.....	65
XII.	REFERENCES.....	65
XIII.	APPENDIX.....	67
A.	LENGTHY CALCULATIONS	67
B.	DETAILED FIGURES/LONG TABLES.....	71
C.	CONTROL SOFTWARE	75
D.	ENGINEERING DRAWINGS	77

LIST OF FIGURES

Figure 1: Isometric View of “Catapult” Concept Design #1	3
Figure 2: Motor Placement in “Catapult” Concept Design #1	3
Figure 3: Isometric View of “Disc Roller” Concept Design #2.....	4
Figure 4: Isometric view of “Dump Truck” Concept Design #3 ..	4
Figure 5: Motors in the front and back will drive all of the wheels for “Dump Truck” design #3..	5
Figure 6: Sensor Placement for “Dump Truck” Design #3	5
Figure 7: Isometric View	7
Figure 8: Top View	8
Figure 9: Bottom View	9
Figure 10: Side View.....	10
Figure 11: Isometric View of Developed Design without Discs	12
Figure 12: Bottom View of Developed Design.....	12
Figure 13: Internal Gate Mechanism Used to Hold Discs in Place.....	13
Figure 14: Isometric View of Structural Base for Developed Design.....	13
Figure 15: Isometric View of Electronics and Circuit Board Mount.....	14
Figure 16: Isometric View of Drive Train for Developed Design.....	15
Figure 17: Isometric View of Unloading Mechanism for Developed Design	15
Figure 18: Exploded View of Electronics Board and Mount	18
Figure 19: Motor Driver	18
Figure 20: Exploded View of Sensors.....	19
Figure 21: Isometric View of Unloading Mechanism	20
Figure 22: Exploded View of Unloading Mechanism	21
Figure 23: Exploded View of Unloading Mechanism Servo	21
Figure 24: Isometric View of Servo Under Gate	22
Figure 25: Exploded View of Drive Train.....	23
Figure 26: Friction Coefficient Comparison Chart without Load	25
Figure 27: Friction Coefficient Comparison Chart with Full Load	26
Figure 28: Motor Performance Curves	32
Figure 29: Free body diagram for forced gate after unloading disks	35
Figure 30: Disk rolling down the slope.....	36
Figure 31: Motor Circuit Diagram	38
Figure 32: Sensor and Servo Circuit Diagram	40
Figure 33: LabVIEW Statechart Diagram for Whole Demonstration Code & Testing Code	41
Figure 34: State Diagram between Demonstration Code and Testing Code.....	42
Figure 35: Demonstration Code Statechart Diagram	43
Figure 36: Testing Code Statechart Diagram	44
Figure 37: Wall Follow Going Up Starting Area Sub-Statechart Diagram.....	44

Figure 38: Wall Follow Going Up Ramp Sub-Statechart Diagram.....	45
Figure 39: Turn 180° deg. In Counter Loop Sub-Statechart Diagram	46
Figure 40: Move in Reverse to Edge of Ramp Sub-Statechart Diagram	46
Figure 41: Section wall CAD drawing (top), Section wall finished piece (bottom).....	47
Figure 42: Motor mount CAD drawing (top), Motor mount finished piece (bottom).....	48
Figure 43: Ramp Extender.....	49
Figure 44: Drive train subsystem showing the attachment of the motors	50
Figure 45: Two views of the shaft coupler press-fitted into the rear wheel.....	50
Figure 46: Side view of toggle mechanism used for unloading	51
Figure 47: Fully Assembled Robot	52
Figure 48: Up times using five discs.....	54
Figure 49: Unloading Times using five discs	54
Figure 50: Down times using five discs	55
Figure 51: Total times using five discs	55
Figure 52: Up times using three discs	56
Figure 53: Unloading times using three discs	56
Figure 54: Down times using three discs	57
Figure 55: Total times using three discs	57
Figure 56: Work Breakdown Schedule.....	58
Figure 57: Gantt Chart	61
Figure 58: Exploded Robot Materials	62
Figure 59: Free Body Diagram of Vehicle on Incline Plane [1].....	67
Figure 60: Ramp Isometric View [4].....	69
Figure 61: Ramp Engineering Drawing [4]	69
Figure 62: Side Dimension of Ramp 1.....	70
Figure 63: Side Dimension of Ramp 2	70
Figure 64: LabVIEW Front Panel	76
Figure 65: LabVIEW Main Block Diagram.....	77
Figure 66: SB-RIO L-bracket Mount	77
Figure 67: Gate Servo Arm.....	78
Figure 68: Mount Mounting Strip	78
Figure 69: Rear Shaft Support for Motor	79
Figure 70: Rear Shaft Support Base	79
Figure 71: Servo Mount	80
Figure 72: Shaft Coupler to Rear Wheel	80
Figure 73: Back U-Channel.....	81
Figure 74: Front U-Channel.....	81
Figure 75: Left U-Channel	82

Figure 76: Right U-Channel	82
Figure 77: Ultrasonic Sensor Mount	83
Figure 78: Force Gate Toggle Bar	83
Figure 79: Force Gate	84
Figure 80: Pin Bracket	84
Figure 81: Servo Bar	85
Figure 82: Servo Connecting Linkage	85
Figure 83: Ramp	86
Figure 84: Ramp Extender	86
Figure 85: Section Base	87
Figure 86: Section Wall	87

LIST OF TABLES

Table 1: Parameters used in friction coefficient calculation with and without load	24
Table 2: Drive Systems and their respective friction coefficients with and without load.....	24
Table 3: Normal and Traction Forces without Load	27
Table 4: Normal and Traction Forces with Full Load	27
Table 5: Center of mass lengths for loaded and unloaded cases ($g = 386.088 \text{ in/s}^2$)	28
Table 6: Weight Fraction Tables	28
Table 7: Inertial accelerations for each section.....	28
Table 8: Propulsion Force for each Section	29
Table 9: Required propulsion torque for each section ($R_{\text{DriveWheel}} = 1.00 \text{ in}$)	30
Table 10: Force and Torque Needed per Path Due to Weight (Forward)	31
Table 11: Motor Specifications	31
Table 12: Drive torque and required torque comparison table	32
Table 13: Wheel and Motor Dimensions	33
Table 14: Torque Required per Track Path (Forward)	33
Table 15: Torque Required per Track Path (Back)	34
Table 16: HD High-torque Servo Specifications	37
Table 17: Miracle Robot Run-Times with Five Discs	53
Table 18: Miracle Robot Run-Times with Three Discs	55
Table 19: WBS Dictionary.....	58
Table 20: Bill of Materials	63
Table 21: Subsystem Design Requirement Satisfaction	64
Table 22: Ramp Section Parameters.....	70
Table 23: Pairwise Comparison Chart.....	71
Table 24: Weighted Design Scores.....	71
Table 25: Types used in Objectives Tree Chart.....	71
Table 26: Objectives Tree Chart.....	72
Table 27: Bill of Materials Sorted by Parts.....	73
Table 28: Error Analysis Tables for Five Discs	75

LIST OF SYMBOLS

Symbol	Definition	Units
$v_{initial}$	Velocity at the section start	in/s
v_{final}	Velocity at the section end	in/s
v_{ave}	Average velocity at the section	in/s
t	Time to travel through section	s
v_{max}	Maximum velocity at section	in/s
θ	Ramp section elevation angle	Degrees °
β	Weight fraction over wheels	
L	Length of wheelbase	in
CG	Center of gravity	
L_c	Distance between rear wheelbase to CG	in
h	Height from base to CG	in
γ_f	value used to indicate front-wheel drive (value of 1 for FWD and AWD, a 0 for RWD)	
γ_r	value used to indicate rear-wheel drive (value of 1 for RWD and AWD, a 0 for FWD)	
μ_{rol}	Rolling friction coefficient	
μ_f	Friction coefficient between wheel and ramp	
N	Normal force	lbf
$F_{inertia}$	Inertial force	lbf
F_m	Weight force	lbf
F_w	Weight force along slope	lbf
F_{rol}	Rolling force	lbf
F_f	Friction force	lbf
F_T	Traction force	lbf
F_{prop}	Propulsion force	lbf
ϵ	Efficiency of the motor	
r	Drive wheel radius	in
m	Robot mass	lbm
m_d	Disc mass	lbm
$F_{vertical}$	Force acting along vertical line	lbf
F_{req}	Required force that the motor delivers	lbf
T_{req}	Total propulsion torque	lb-in
F_t	Tension force	lbf
E_{total}	Total Energy	Btu
$E_{potential}$	Potential Energy	Btu
$E_{kinetic}$	Kinetic Energy	Btu
g	gravity	ft/s ²
V_d	Velocity of the disk in unloading mechanism	ft/s
V_{dx}	Disk velocity in horizontal direction	ft/s

v_{dy}	Disk velocity in vertical direction	ft/s
x_f	Final disk horizontal position	ft
x_i	Initial disk horizontal position	ft
y_f	Final disk vertical position	ft
y_i	Initial disk vertical position	ft
a_x	Horizontal acceleration	ft/s ²
a_y	Vertical acceleration	ft/s ²

I. INTRODUCTION

I. Need Statement

The design need of our project is to design an autonomous vehicle that performs bulk material transportation within the team budget of \$350. The vehicle must autonomously deliver lead-disc cargo up a ramp path, unload the cargo into a collection bin, and come down the ramp to receive additional cargo loads and re-perform this cycle.

II. High-Level Design Requirements

The High Level Design Requirements discussed in this section are requirements that each team must follow. These requirements were already set from the beginning of the quarter.

The High Level Design Requirements are as follows:

1. The vehicle can move up and down the pre-designed ramp path autonomously through several cycles.
2. The vehicle can load multiples (minimum 3 per run) of the cargo (lead discs – 6lbs) and store them throughout its movement path and deliver the cargo through the delivery mechanism in the collection bin area through several cycles. The lead discs are loaded manually. The vehicle is only allowed to unload when completely inside the unloading area marked on the top platform.
3. The whole device must fit inside a rectangular box of 12" x 12" x 16". If your box is part of your design, then external dimensions can be no larger than 12" x 12" x 16". The device must be fully assembled when it fits inside the box.
4. Vehicles must be powered by ordinary & readily available batteries, which can be disposable (13 max) or rechargeable (15 max) but not both types. No other sources of energy are permitted. Battery packs are allowed as long as the batteries comply with above rules & are easily verifiable by judges.
5. All powered devices must have a readily accessible and clearly labeled emergency kill switch to shut off the device.
6. One on/off switch can be installed on the vehicle and it can only be accessed in the starting/ loading area to start or to end a load delivery trip.
7. Except those on the vehicle, no other devices or sensors are allowed to be on or around the pathway.
8. For the conceptual design, the primary design parameters are: device dimensions, cargo delivery system, load capacity, drive system, wheel size, wheel position, wheel material, motor power requirements, and gear ratio. Choice of design parameters must be based on engineering fundamentals.
9. The total budget for the project is \$350.

III. Prior State-of-the-art

There are various examples in the real world of bulk transporters. A few examples of prior work in this area include: freight trains, ships, tank truck, and dump trucks. Each transport bulk material, but the type of material they transport is what differentiates them from one another. Considering a tank truck as an example, its main purpose is for “delivering gasoline, chemicals, foodstuff, and other products” [1]. Tank trucks, as well as the other bulk transporters mentioned previously, were a result of the increasingly need to transport bulk items from one place to another. Likewise, dump trucks are used to transport bulk materials, such as construction materials, and then dump its contents at its desired destination. Our design is similar to these bulk transporters in terms of its purpose, but unlike dump trucks, our unloading mechanism does not require the carrier to be raised and tilted, since we will have an incline already built in, thus requiring less energy than traditional bulk transporters. In addition, our bulk transport will be autonomous, whereas the prior examples are all controlled by human operators.

IV. Structure of Report

This report will be structured as follows. First, in Section II we provide a detailed description of our design and our system operations followed by Section III where we provide a detailed description of our subsystems’ designs. Next, in Section IV we provide our design analysis which shows our power requirements along with our calculations that we used to size our motors and our unloading mechanism. Section V shows our control system design for motor selection, unloading mechanism, and sensors. We also introduce the entire state diagram that was designed to run our robot. In Section VI, we describe our product fabrication and assembly. In section VII, we go into product testing and evaluation, as well as provide a simple error analysis calculation regarding our run times. In section VIII, we show the work breakdown schedule. Next, in section IX, we go into our cost analysis and bill of materials. In section X, we go into details regarding our design requirement satisfaction. This is followed by our Conclusion section which summarizes our final design product along with analysis.

II. DESIGN DESCRIPTION

I. Design Concept Development

In order to arrive at a final design we first considered three possible concepts depicted below.

Concept #1 “Catapult” Robot

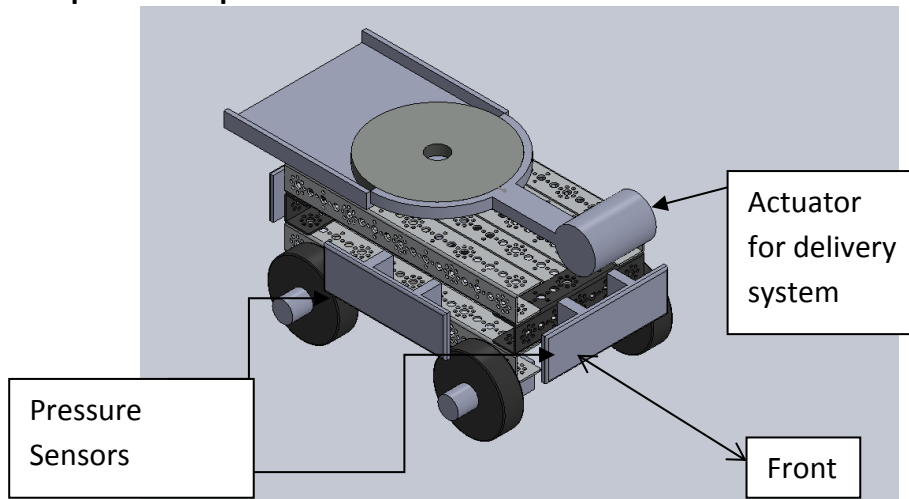


Figure 1: Isometric View of “Catapult” Concept Design #1

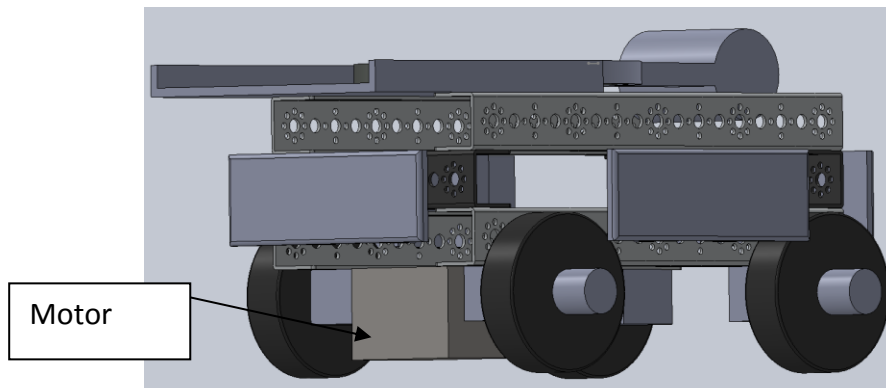


Figure 2: Motor Placement in “Catapult” Concept Design #1

Our first concept is based on a catapult delivery system. For this concept, the robot will be loaded with 2 lead discs and travel along the defined path using the pressure sensors around its body in order to detect walls and send signals to turn robot. Figure 1 shows the delivery system as a plate with a sliding actuator to push the lead discs into the targeted area. As seen, the discs will be placed horizontally in the slot and when the robot senses it is at the end of the track it will actuate the delivery system. Figure 2 shows this concept will be a front wheel drive and because of the lighter load this unit carries it will be able to make faster and more trips within the allotted time.

Concept #2 “Disc Roller” Robot

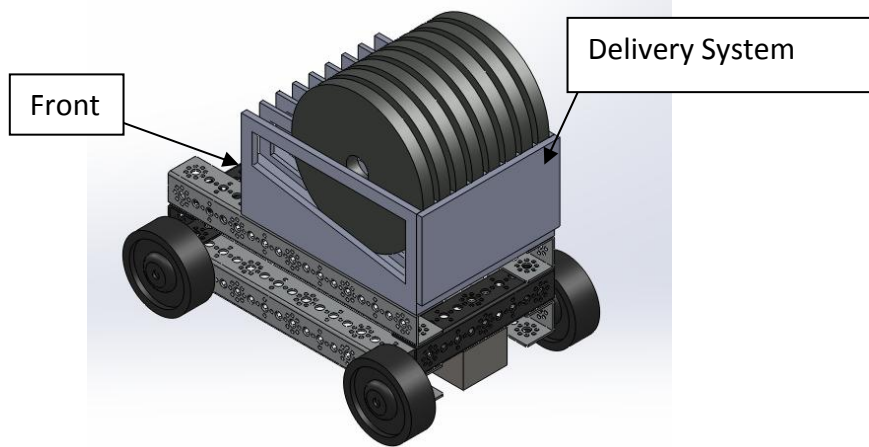


Figure 3: Isometric View of “Disc Roller” Concept Design #2

This concept uses a slot system to hold the lead discs standing vertically on their round sides. There are two advantages to this way of carrying the lead discs. First, this method makes it easy to load multiple discs quickly and transport up to 8 per run. It also uses less energy to release the payload into the box at the end of the run because no force need be applied from the battery. The back plate will just drop down and allow the plates to roll out of the carrier, due to the slope of the carrier base. This concept is driven by a rear-wheel drivetrain (two motors, each on the back two wheels). Varying the speeds of these motors can steer the robot while in motion. Three ultrasonic detectors on the bottom of the vehicle, each spaced equally apart (with separation distance equaling the thickness of the black tape), will be able to tell if the robot is steering off course as it travels up the ramp from the start to the drop-off destination.

Concept #3 “Dump Truck” Robot

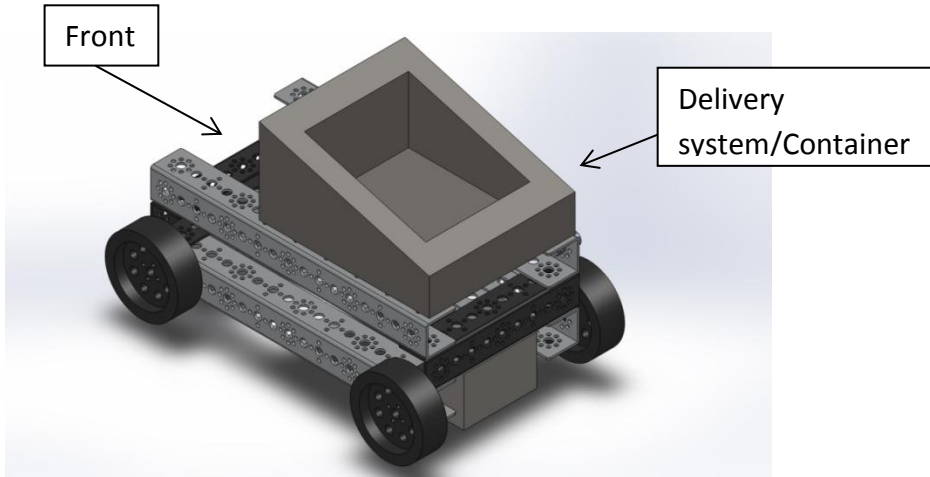


Figure 4: Isometric view of “Dump Truck” Concept Design #3

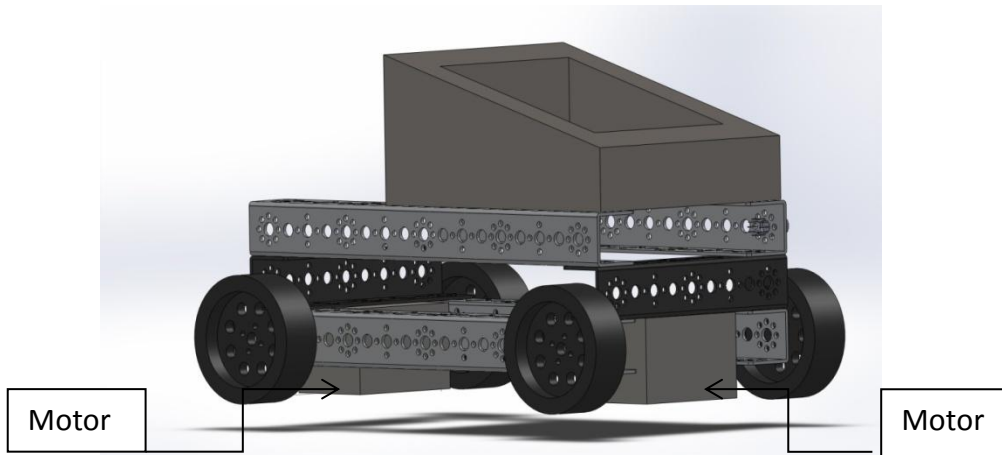


Figure 5: Motors in the front and back will drive all of the wheels for “Dump Truck” design #3

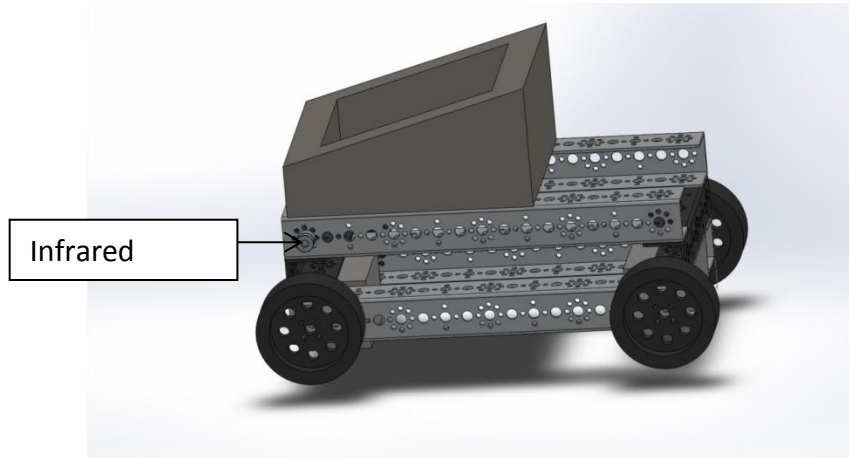


Figure 6: Sensor Placement for “Dump Truck” Design #3

Our third concept is based on a dump truck. The basic idea behind this concept design is that it unloads the disks by dumping the disks as a dump truck would. Figure 4 shows the isometric view of this design. As shown, the container that holds the lead disks has an inclined top surface that allows for easy delivery. There will be a hydraulic mechanism that allows the container to have this “dumping” feature. A pressure sensor will be placed on the container that will signal the robot to go once the container has reached its full capacity (or weight). Furthermore, Figure 5 indicates that this design is an all-wheel drive. As a result, this design will require more energy to power the additional motor compared to if it was a rear-wheel or front-wheel drive. Thus, this design may be more complicated than the previous ones. In addition to the pressure sensor, we will also put in some infrared sensors as shown in Figure 6. The infrared sensor will be used to find the walls. Even though the figures shown do not depict it, this overall appearance of this design will be tank shaped to give it the more robust look. The most beneficial reason for using this design is that its storage capacity is larger than the other designs. This allows for us to transport more lead disks than if we were using the previous designs. Of course, this design may require more power and energy to perform such tasks.

In order to arrive at a final decision between our three concepts we created a pairwise comparison chart and decided as a team what criterion was important for our design. We considered the cost, load capacity, power available, durability, aesthetics, and sensitivity of the design. After weighing each criterion appropriately, we distributed points to each design concept deservedly. The pairwise comparison chart, objectives tree chart and all other accompanying charts are provided in the Appendix.

Once we made our pairwise comparison chart, we were able to begin our objectives tree chart for each of our three designs. From here, we assigned evaluation marks from 0 to 10 for each design concept. Then we were able to assign order of merits based on which design was best. We decided to continue development of our second design concept, since it had the highest score, as shown in Tables 24 and 26 in the Appendix.

II. **Design Overview**

Our overall system design is based around a unidirectional vehicle that will be doing a 360 degree turn. The idea is based off of our second conceptual in which we have a sloped ramp, but instead of an external gate, we added an internal gate that is a detached ramp that pops up to hold the discs in place. To further iterate the basis of the unloading mechanism, we are using a four-bar toggle mechanism. Instead of slots, we are holding the discs together using bolts and nuts and in doing so the cargo will be able to keep itself upright. In terms of drive train, our robot will be rear wheel drive because most of the load is more towards the rear end and this will provide more traction on the wheels. Also having a rear wheel drive train allows for sharper turns. Because of the availability of reasonably sized and powerful motors, we are able to utilize a direct drive system. The front wheels are casters because of the ease of usage and this allows all control to be done using the rear wheels. Images and further explanation of each component is detailed later in this report.

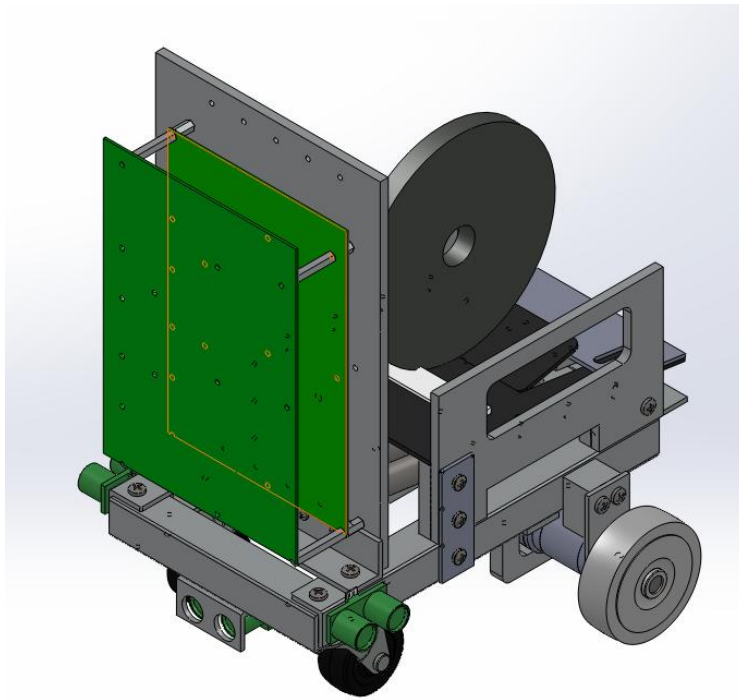


Figure 7: Isometric View

As noted in the picture, we are using three ultrasonic sensors for our navigation and under the shown lead disc is a contact sensor. This sensor is used to detect the existence of a load on the robot. On the backside are 2 more contact sensors used to detect the walls once the robot backs up against the edge of the ramp.

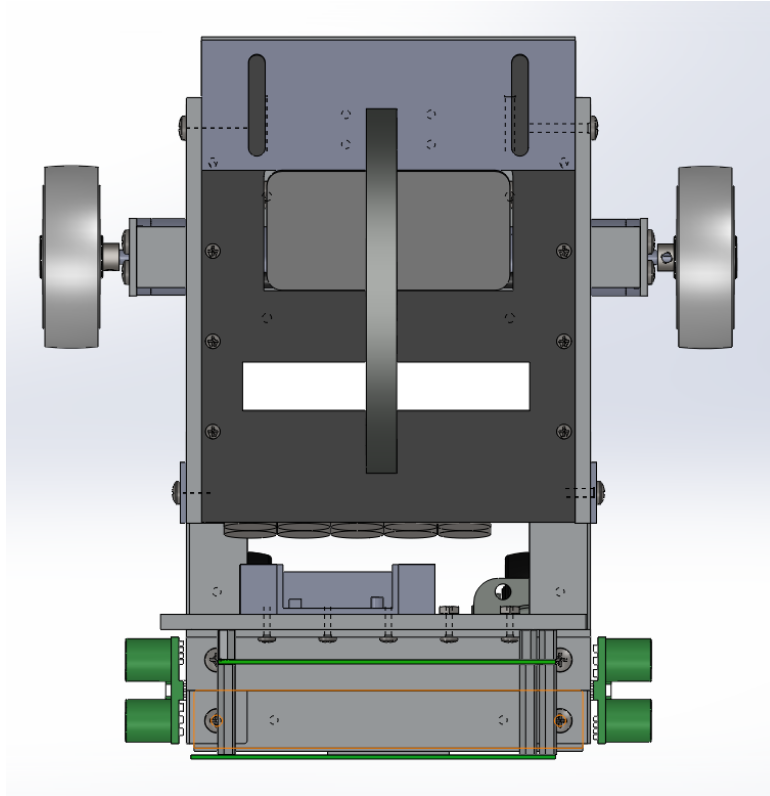


Figure 8: Top View

Our SB-RIO will be mounted in a vertical position so that we can minimize space and keep our electronics easily visible throughout the entire project. Our circuitry and wires will be wrapped around the backside of our given SB-RIO board so having this format allows for ease of access to all of the electrical components and allows us to change any components without having to disassemble everything.

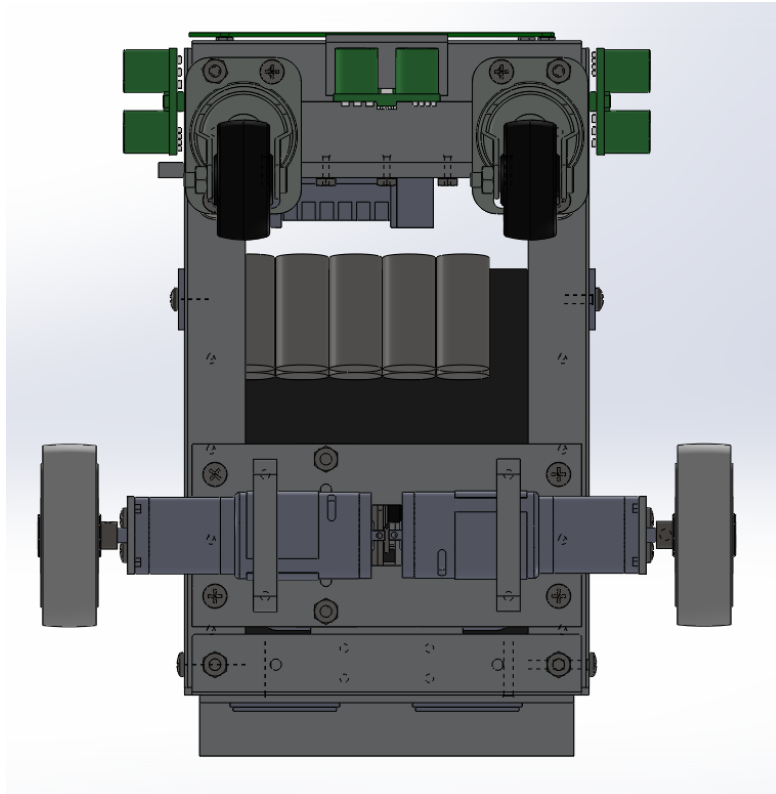


Figure 9: Bottom View

We kept our overall structure simple as well. Our structural base is an assembly of U-channels and L-channels. This allows for ease of attachment and assembly with all of the other components. The simplicity also allows for a larger tolerance because of the simplicity. Considering our entire robot was manufactured in a simple machine shop, this decision benefitted us greatly. We also encompassed handles into our design for ease of transportation and handling during the testing phase. Along the back of the structure is a extruding portion of our ramp. This part of the ramp will make contact with the edge of the track during unloading to prevent any possible tipping while unloading because the load itself is about the weight of the robot.

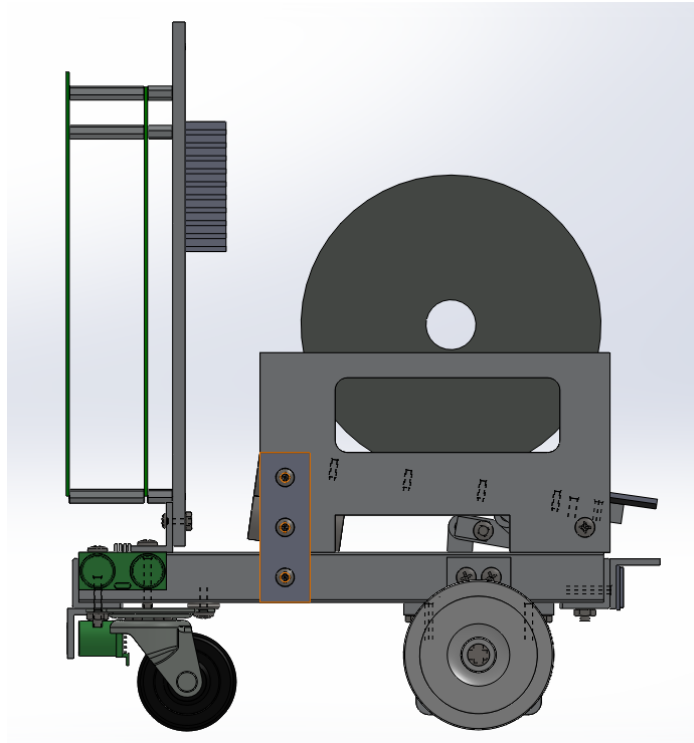


Figure 10: Side View

III. Systems Specifications

The Low-Level Design Requirements are the technical requirements that our team set for our robot. These are more of the specifics of how our robot will run on the competition day.

Our Low Level Design Requirements are as followed:

1. High load carrying capacity so that the maximum number of discs can be transported per run (6-8 discs).
2. Delivery system that can be loaded and unloaded with minimal complications.
3. A combination of sensors in order to follow the track and sense when the loading bay is emptied. If using an actuated unloading system a pressure sensor is needed.
4. At least one motor for rear or front wheel drive. All-wheel drive is considered in our conceptual designs. Front wheel steering is preferred, but not required.
5. 2 run minimum in the allotted 10 minute time frame.
6. Average speed of at least 5ft/minute in order to meet the minimum number of runs.
7. A maximum of 13 disposable batteries will be used.
8. The shape of the robot must be a rectangular prism in order to maintain simplicity and ease of accurate welding.
9. Unloading mechanism must use a minimum amount of power to actuate.
10. Wheelbase must be short enough to allow turning sharp corners.

Fortunately, we were able to satisfy most of our low level design requirements that are listed above. Our traveling time for going up the ramp is about 40 seconds. Time for turning and unloading takes about 6 seconds. When it is going down the ramp, the robot takes about 32 seconds to get to its initial position. The total traveling time for one round trip is approximately 78 seconds. During one round trip, we are able to carry up to 5 discs.

Our maximum velocity is 6in/s and dividing this by our wheel circumference we find our required motor revolutions per minute are 57.3RPM. Hence we decided to use the Gear Head Motor (GHM-13) from Lynxmotion [10].

Our motor is in a direct drive system and hence our drive torque is the direct torque from our motors. Our drive torque at 94RPM will be 76.375 lb-in per motor. Hence our total drive torque is this value multiplied by 2:

$$\text{Drive Torque} = \boxed{152.75 \text{ lb-in.}}$$

For our particular unloading mechanism, we only need one servo motor to control the force gate and the required force and torque values are 0.112 lb and 0.173lb-in. Since the initial potential energy is sufficient enough to fulfill require horizontal displacement, we don't need any additional subsystems. We used HD High-torque servo which has stall torque of 14.76lb-in at 6V and 13.45 lb-in at 4.8V.

To run our system, which includes motor, servo motor, and Sb-rio board, we choose to use two 12V battery packs and two 9V batteries. Although one 12V battery could be sufficient enough to power both motor and Sb-rio, we choose to individual 12V battery pack to power each component to be safe. One 9V battery is connected to the servo motor and another one is connected to the sensor.

IV. Overall System Design

We kept the original foundations of our second design concept which is to have vertical discs, held by a gate, unloaded off a ramp into the targeted area. Our changes included to have the discs be held together vertically and kept in place with an internal four-bar mechanized gate as shown in figure 11 below.

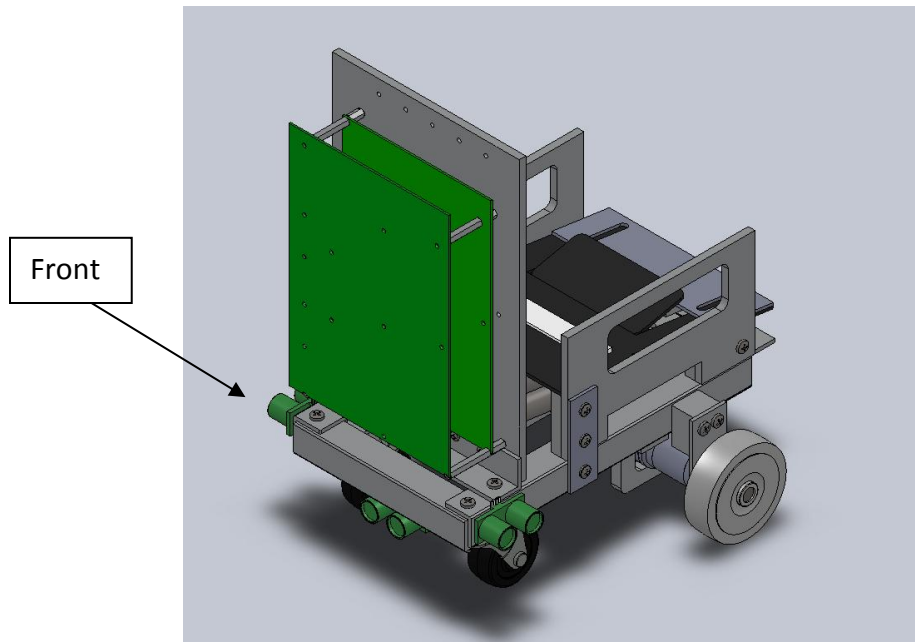


Figure 11: Isometric View of Developed Design without Discs

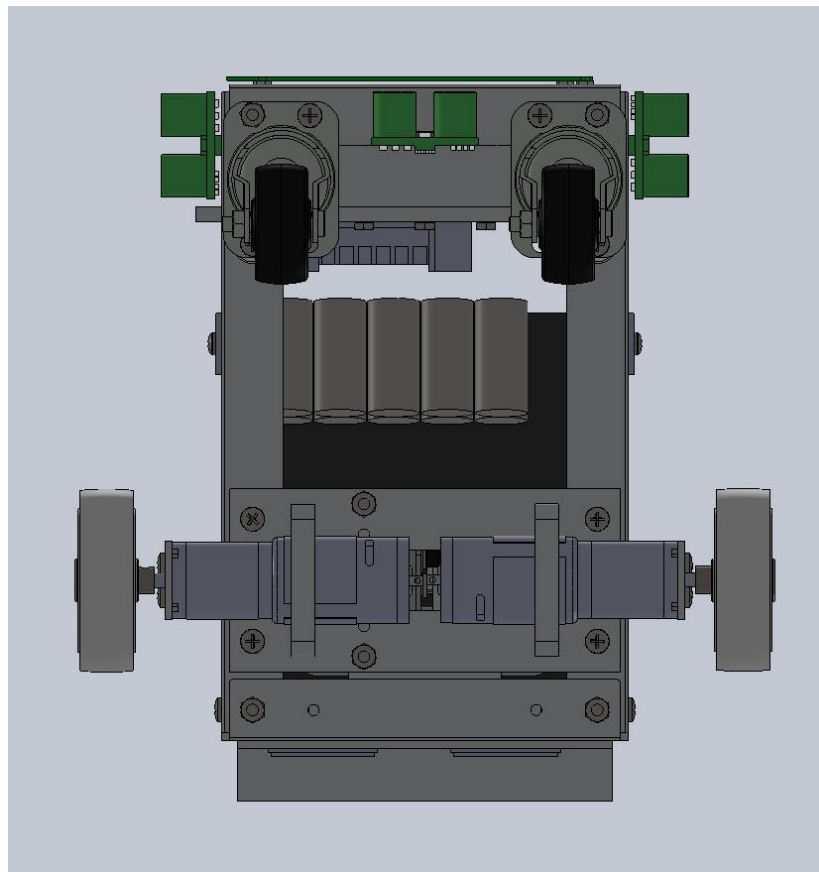


Figure 12: Bottom View of Developed Design

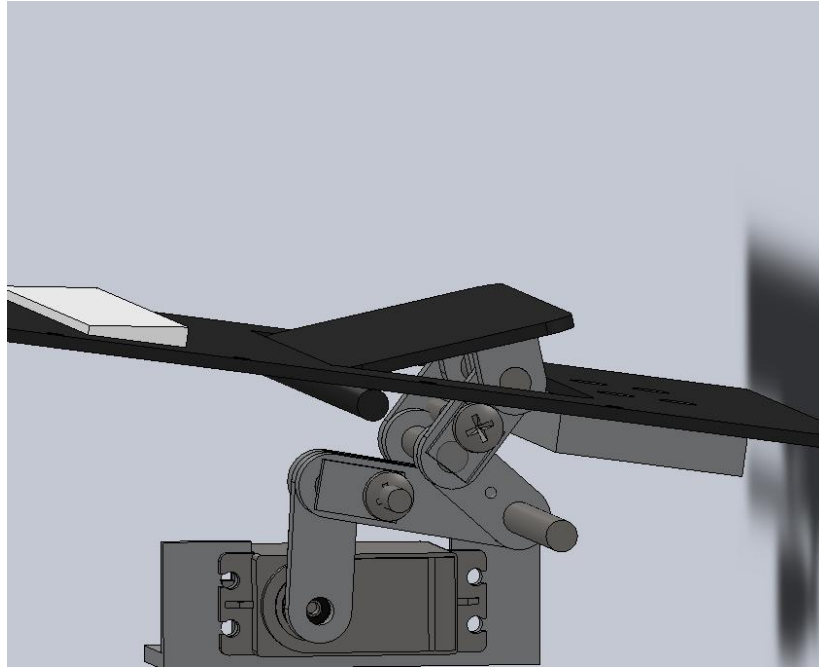


Figure 13: Internal Gate Mechanism Used to Hold Discs in Place

This overall design holds 6 lead discs held together on a ramp. The above internal gate mechanism holds the cargo in place while the robot travels up the track and to the delivery zone. Once at that point it will use its sensors to execute a 180 degree turn and then drop its external gate directly on to the unloading zone. Our robot is split into several subsystems that help obtain this goal: structural base, electronics, drive train, and the unloading mechanism.

Everything is attached to a structural base sub-assembly which is essentially a combination of U-channels that are readily available, Figure 14.

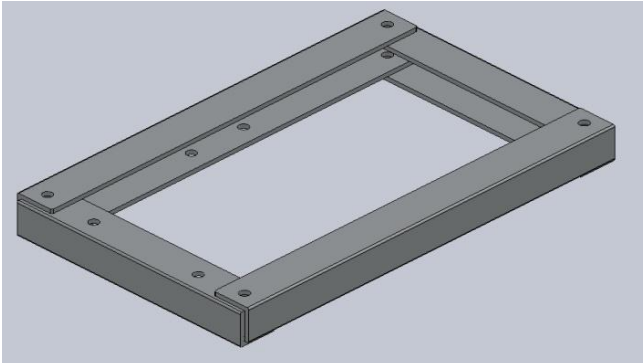


Figure 14: Isometric View of Structural Base for Developed Design

Using this as our main assembly point we can attach the electronics around the perimeter and the circuit board to the front in an upright vertical position so that we will be able to access any and all wiring easily.

The electronics and circuit board will be mounted to the front of the robot as depicted in Figure 11. Below is the sub-assembly of the electronics mount.

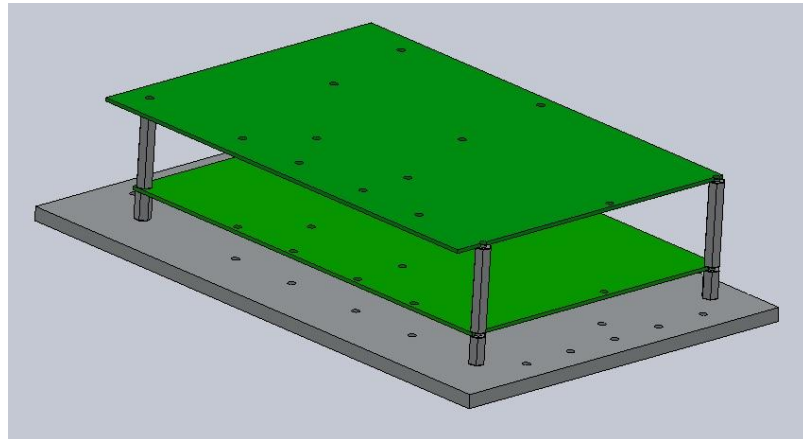


Figure 15: Isometric View of Electronics and Circuit Board Mount

The electronics is the brain of our robot. Here is where the programs are executed and hence all of our sensors will be wired to our board. We are utilizing three ultrasonic range finders located at the front, and one on each side. With this we are also using a force sensor in our cargo area to detect the presence of our load. Details of their function will be discussed in the subsystems section.

Our drive train is a rear wheel drive using two motors; one motor per wheel. Our wheels are 2 inch diameter wheels and are connected to the motor directly because our motor selection is powerful enough to propel our robot without a gearing system. The front wheels will be simply a pair of freely swiveling casters. Turning will be done by adjusting the speed of each motor individually allowing us to make our desired 180 degree turn at the end of the track.

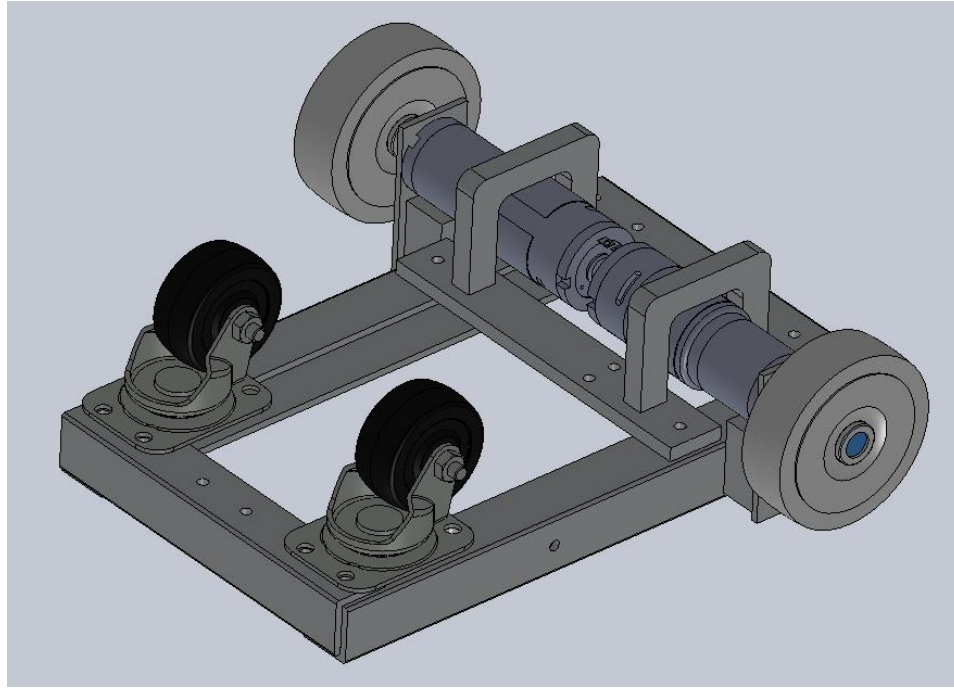


Figure 16: Isometric View of Drive Train for Developed Design

The last of our subassemblies is the unloading mechanism. We implemented a gate within the ramp that inclines in order to hold the lead discs in place. Once the robot is ready to unload the gate will recline and allow the load to roll off the ramp into the box.

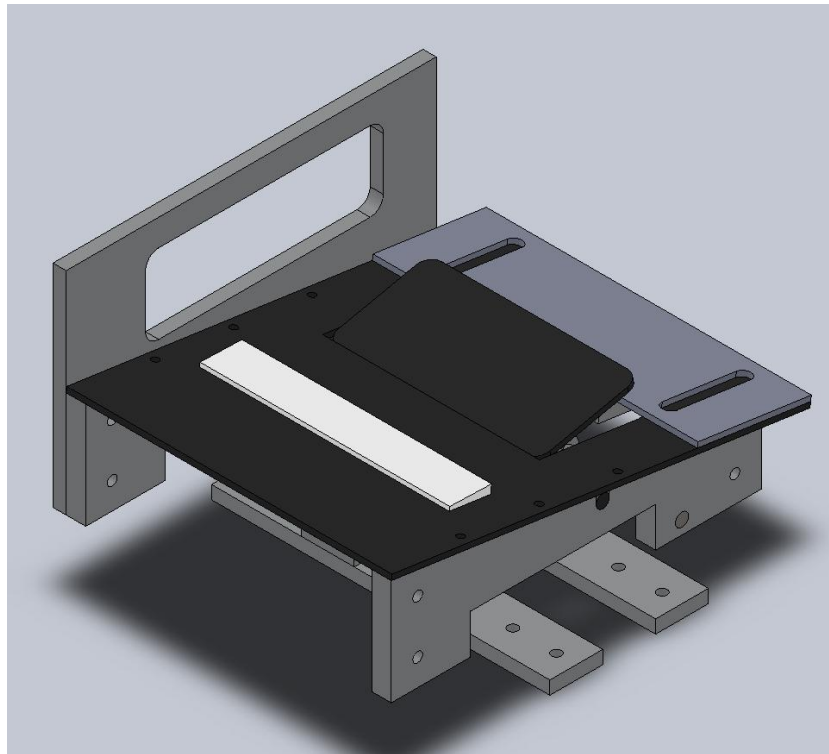


Figure 17: Isometric View of Unloading Mechanism for Developed Design

IV. Mechanical System Operation

Our mechanical systems include the drivetrain and the unloading mechanism. Our drivetrain uses two motors attached to a dual-motor controller, which determines speed and direction of our robot using voltage potentials across the motors. Since we are using the analog mode on the controller, we can vary the voltage applied to each wheel to independently make the wheels spin at various velocities, either forward or backward. Since each wheel's motion is independent of each other, our robot can turn by having each wheel spin in different directions or both forward at different rates. In the front of the robot are two casters to allow easy rolling and turning in all directions.

The unloading mechanism uses a servo attached to a toggle mechanism. This system is comprised of a four bar mechanism that either locks two sets of linkages parallel or allows them to fold. The parallel linkages are the basis for the force gate that protrudes from the ramp, as shown in figure 17. This allows us to apply force up to the yield strength of the aluminum linkages without needing much force from the servo. Our FPGA board sends pulse-width modulation signals to our servo, which translates into a specific position. These positions will be the reclined state, not supporting any weight, and the inclined state, supporting the discs due to the parallel linkages.

V. Control System Operation

The user control system consists of a LabVIEW program that is interfaced with SB-RIO, which acts as our FPGA. The LabVIEW programming is discussed in detail in section VI. Control System Design. The entirety of the robot navigation is written in the main statechart diagram that is linked to the main code. The SB-RIO is connected to three ultrasonic proximity sensors, which are located at the middle front of the robot, and the two sides near the front of the robot. Three connected contact sensors are placed at the area where the discs are loaded and two are on the rear where the robot contacts the ramp during unloading. The robot uses the ultrasonic sensor readings for the following actions: it uses the left sensor reading to wall follow at a certain distance along the ramp, it uses the right sensor reading to determine the correct wall following distance along the ramp, and it uses the front sensor reading to determine if there is an object in front of it so the robot has to perform a 180 degree turn. The robot uses the three contact sensors for the following actions: it uses the two rear sensors to determine whether or not it is in the correct position to unload the discs and it uses the button on the disc loading area to determine whether or not discs are currently loaded.

In order to control the mechanical devices on the robot, which are the two drive motors and the positional servo, the statechart outputs analog outputs from the FPGA to control the motors and the servo. For the motor, the command output is sent to the Sabretooth

dual motor controller, which receives separate analog voltages to set the speed and direction of each drive motor. Straight movement is induced by setting the motor speeds to the same value and turning is induced by creating a speed differential between the motors. To control the servo, a PWM signal with a pulse width high and low that corresponds to the servo's position is sent from the SB-Rio directly to the servo.

III. SUBSYSTEMS DESIGN DESCRIPTION

I. Electronics

Description

Our electronics will consist of the following components: SB-RIO 9632 electronics board, three ultrasonic range finders, two push button sensors, force sensor made from a spacebar, dual DC motor drive controller, 5V voltage regulator, a rechargeable 12V battery pack, 9V alkaline battery pack, on/off switch. The servo and drive train motors will be described in separate sections.

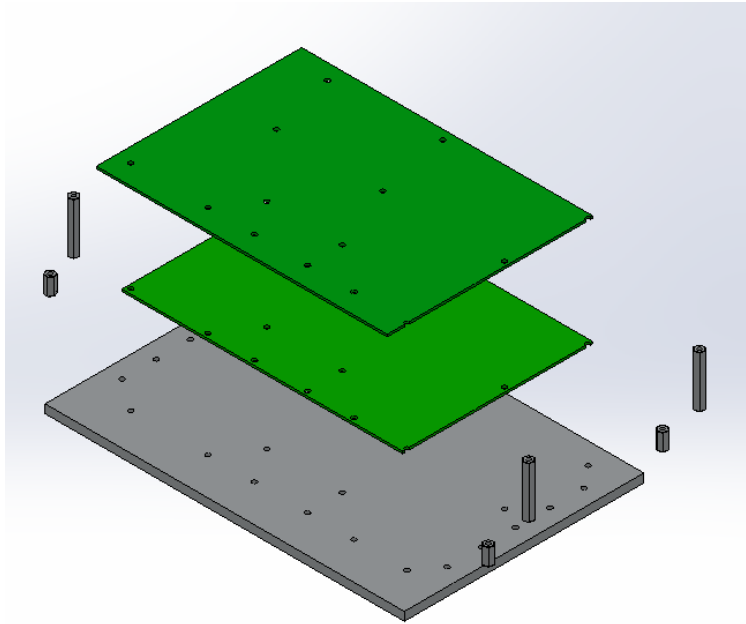


Figure 18: Exploded View of Electronics Board and Mount

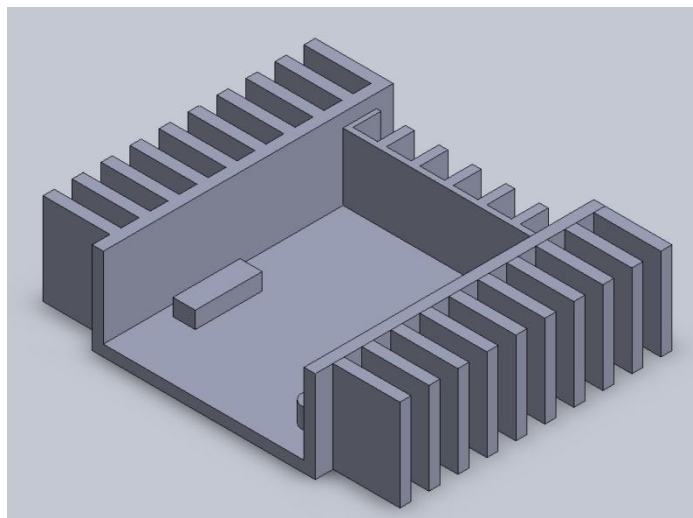


Figure 19: Motor Driver

The SB-RIO is our overall interface between the host pc and the entire system. It is the unit that incorporates our field-programmable gate array (FPGA) and our microcontroller. Our FPGA connects to our motor drive controller and then our drive train which will be described in the motor sizing portion of this report. Our 6.2V voltage regulator will be used for the drive train and servos. Our on/off switch will be attached to our board as well to serve as our point of main power and our batteries will be used to supply that power. We will be using the rechargeable battery pack during testing and hold the alkaline battery pack for our actual runs.

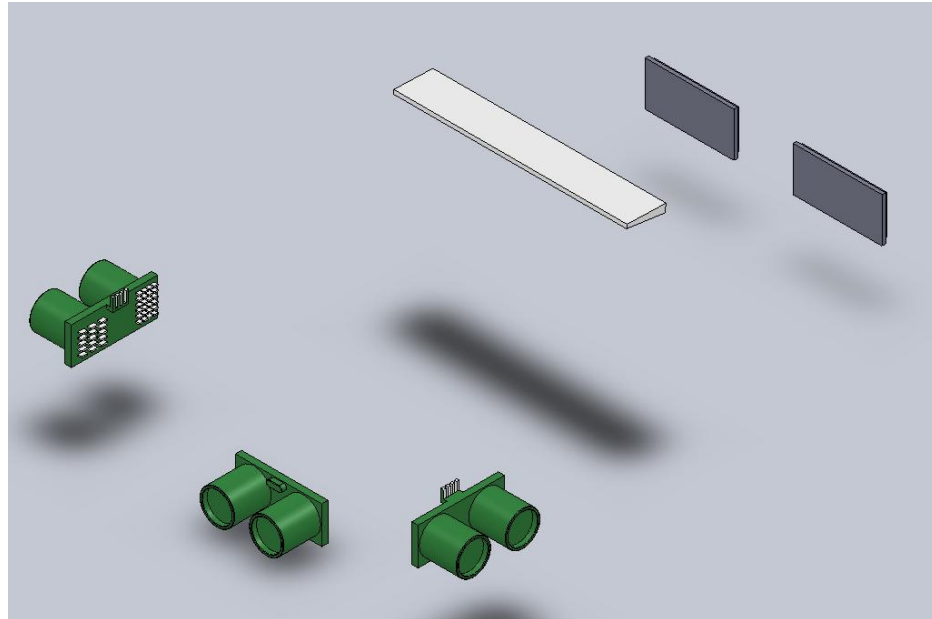


Figure 20: Exploded View of Sensors

Our three ultrasonic range finders will be used to locate the robot along the path. The two on the sides, as shown in figure 20 will be used to keep the robot in the center of the track. Though only one is needed we will be using two as a redundant system. One is mounted on the front to determine when there is a wall which will translate into a turning movement. Our two push button sensors on the rear beneath the unloading gate serve the following purpose. When the robot turns around, both buttons need to make contact with the ramp wall in order to unload the lead discs. This serves the function of permitting the force gate to drop down once the push buttons make contact with the ramp wall. Our sensors run with a voltage of 5V and this will be achieved using our 5V voltage regulators.

The force sensor will be placed on the loading bay, Figure 17. The concept of operation is simple. When the force button sensor is pressed, it closes a circuit and sends a signal to indicate that the robot is fully loaded. Once this occurs, it will start traveling. In this manner, we will not have to turn the robot off in order to reload the next run.

Requirements

The force button sensor is made out of a space bar and only requires to be pressed or not to serve its function. We followed the circuit diagram from the Electronics Lab to construct this sensor. We only require the correct resistor and 5V regulator for proper operation.

Our ultrasonic sensors are used to measure the distance from the side walls and keep our robot in the middle hence it will need an accuracy of a few centimeters. Our chosen HC-SR04 model has a minimum range of 2cm and a maximum range of 4m with an accuracy of $\pm 3\text{mm}$ which is a very tight tolerance and will allow our sensors to serve its purposes well.

Both sensors run off of a working voltage of 5V DC and hence we use a 5V regulator for all of our sensors. Our 9V alkaline batteries will be used to power all of the sensors because of the little power needed to operate them.

Because we set our round-trip time to 136.1 seconds we need a battery pack that can last the entire trip and can be recharged because of the testing that will be done. With this run time and the 12V voltage required by our motors we chose a rechargeable 12V battery pack with an energy capacity of 4200mA-h. Our robot will run at a current root mean squared value of 2.934A. This allows us to run for 1.4 hours which is much greater than the required round-trip time.

II. Unloading Mechanism

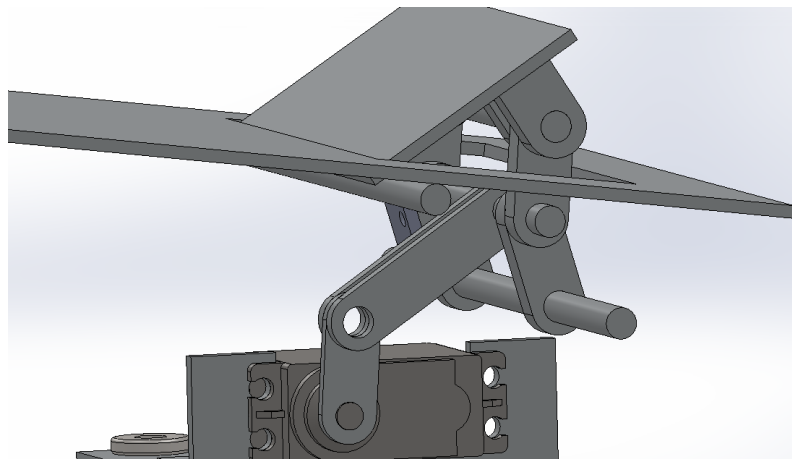


Figure 21: Isometric View of Unloading Mechanism

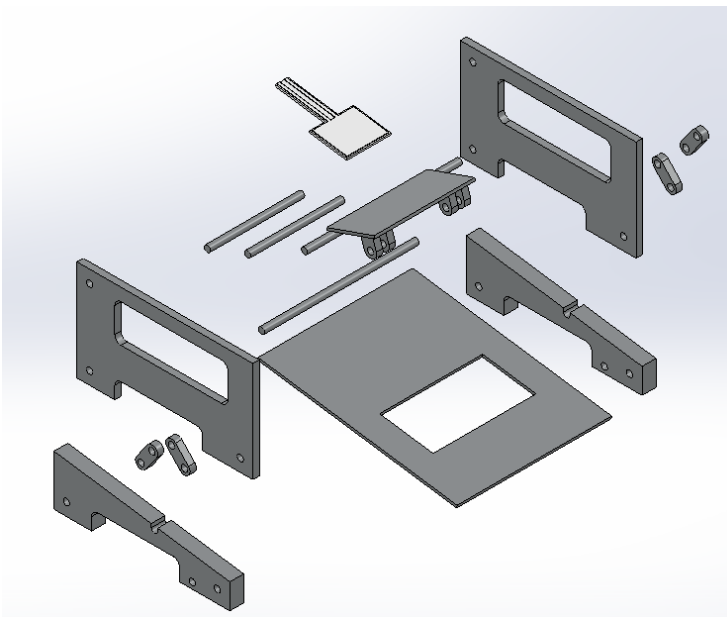


Figure 22: Exploded View of Unloading Mechanism

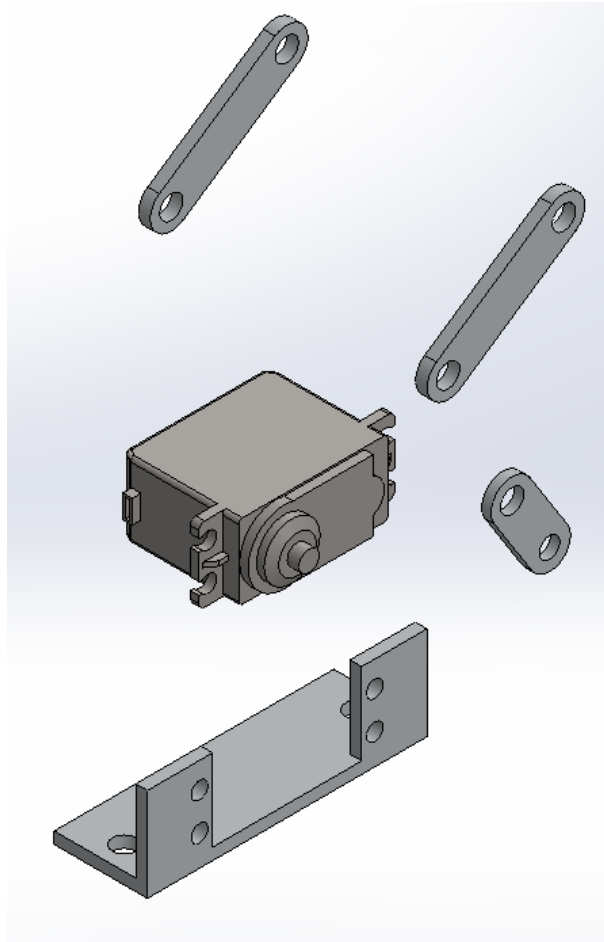


Figure 23: Exploded View of Unloading Mechanism Servo

Description

To reiterate our objective, we are aiming to deliver six lead weight discs up a defined path. From there we will have our robot execute a 180 degree turn and unload our cargo into the targeted area. Figure 17 shows our unloading mechanism and figure 21 shows our four bar mechanism under the gate. Our gate protrudes from the ramp in order to hold the cargo. Figure 22 shows the cargo area of the unloading mechanism in an exploded view. Figure 23 shows the exploded view of the servo mount under the platform. Once our force button sensor senses no discs, our gate will revert back to its starting position and the robot will travel back for the next load.

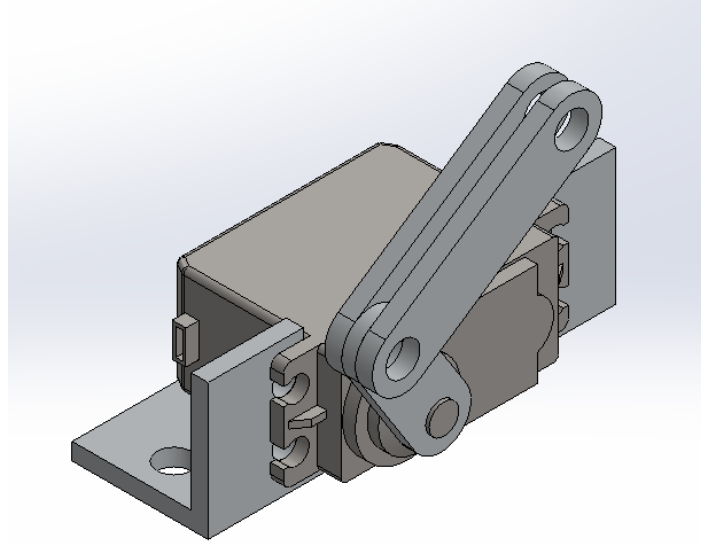


Figure 24: Isometric View of Servo Under Gate

Requirements

The unloading mechanism needed a method of holding the load in place and a method of unloading the load. Hence we used the internal four bar mechanized gate to keep the discs on the force button sensor. This portion needs to be able to hold up a weight of 36lb. The mechanism also has to be able to adjust to both the inclined and reclined position in appropriate time in order to achieve our desired round-trip time.

III. Direct Drive Train

Description

The direct drive train pictured in figure 16 encompasses two sets of motors, wheels, shaft support bars, and couplers. The overall function of this subsystem is to propel our robot. Using a direct drive train our outputted torque comes directly from our motors, which are described under the Power Requirements and Motor Sizing section of this report. Our selected motor, the Planetary Metal Geared Motor (PD264M) outputs 76.375 lb-in of torque, which is overcomes our needed propulsion torque of 14 lb-in up the steepest incline as derived later in this report. Because our wheel radius is 1 inch,

our outputted torque will be that provided by the motor. The coupler attaches the wheels to the gear shaft. Furthermore, the support bars will structurally strength our motor placement.

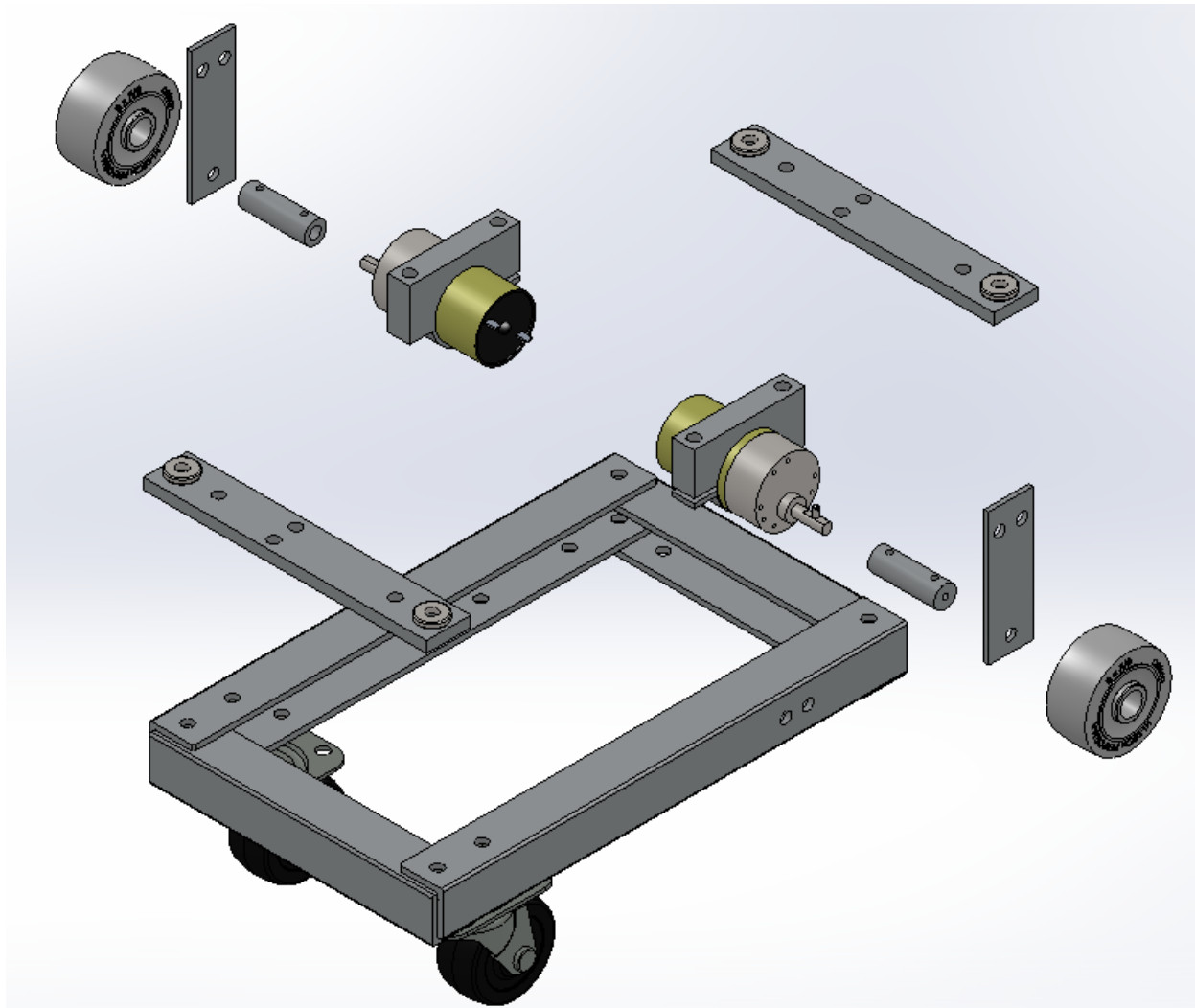


Figure 25: Exploded View of Drive Train

Requirements

This is our most important subsystem because it is the physical system that propels our robot up the track. Our requirements include the ability to run fast enough in order to achieve our round-trip time of 136.1 seconds for at least one trip and accommodate our maximum velocity. The subsystem must also be able to overcome friction and gravity forces to propel our system up the ramp in an efficient manner. Lastly, because our robot must be able to turn around the system must be capable of making a 180 degree turn.

IV. DESIGN ANALYSIS

After narrowing down a large selection of materials for our wheels, we decided on using rubber for our front and rear wheels to achieve the friction coefficient we desire. We found that our friction coefficient (μ_f) is 0.5 [7] and our rolling friction coefficient (μ_{rol}) to be around 0.01 [8]. These values will satisfy the minimum friction coefficient needed to sustain our robot up the ramp. Further explanation will be provided on the next few pages. On the next page is the comparison of the minimum friction coefficients if our robot was an all-wheel drive, a front-wheel drive, or a rear-wheel drive.

One formula used in the analysis is provided below [2]:

$$\mu_f = \frac{L \sin \theta}{(\gamma_r - \gamma_f)(h \sin \theta - L_c \cos \theta) + \gamma_r L \cos \theta} \quad (1)$$

This formula gives us a useful insight on the minimum coefficient of friction needed to sustain our robot. All formulas regarding the minimum friction coefficient, normal and traction forces are derived in the Appendix along with the corresponding free body diagram. For the all-wheel drive, we set $\gamma_f = 1$ and $\gamma_r = 1$, for the front-wheel drive, we set $\gamma_f = 1$ and $\gamma_r = 0$, and for the rear-wheel drive, we set $\gamma_f = 0$ and $\gamma_r = 1$. Provided on below are the values of the parameters used in the calculations as well as the final minimum friction coefficient values based on this procedure for both cases in which there is no load and a full load:

Table 1: Parameters used in friction coefficient calculation with and without load

Parameter	Without Load	With Load
Wheel Base Length (L)	5.84 in	5.84 in
CG from rear wheels (L _c)	3.19 in	2.00 in
CG height from ground (h)	5.13 in	7.23 in
Steepest Angle of Ramp (θ)	14.036°	14.036°

Table 2: Drive Systems and their respective friction coefficients with and without load

Type of Drive System	Minimum Coefficient of Friction without Load	Minimum Coefficient of Friction with Load
All-Wheel Drive	0.250	0.250
Front-Wheel Drive	0.765	7.583
Rear-Wheel Drive	0.371	0.258

In our analysis of choosing the wheel material, we used Table 2 as a guideline, being sure to select material that had a higher friction coefficient with plywood than the values above. This also helped us narrow our selection of which drive system would be best for our design. Since front-wheel drive required a large friction coefficient greater than 1.0, we concluded that front-wheel drive was not feasible, so we eliminated this type of drive system from our list of possible ones.

Another useful way that might be of interest is showing a plot of minimum friction coefficient vs. L_c. This analysis helps with deciding where to place our center of gravity to minimize how

much friction each wheel needs. Provided below are the formulas as functions of L_C used for the graph.

All-Wheel Drive:

$$\mu_{AWD} = \tan\theta \quad (2)$$

Front-Wheel Drive:

$$\mu_{FWD} = \frac{1}{\frac{L_C}{L} \tan\theta + \frac{h}{L}} \quad (3)$$

Rear-Wheel Drive:

$$\mu_{RWD} = \frac{1}{\frac{L-L_C}{L} \tan\theta + \frac{h}{L}} \quad (4)$$

Values for L , h , and θ are fixed values for this analysis, while we vary L_C . Figures 26 and 27 are the minimum friction coefficient comparison charts for the type of drive systems when the transporter is without the load and when it is with a full load, respectively.

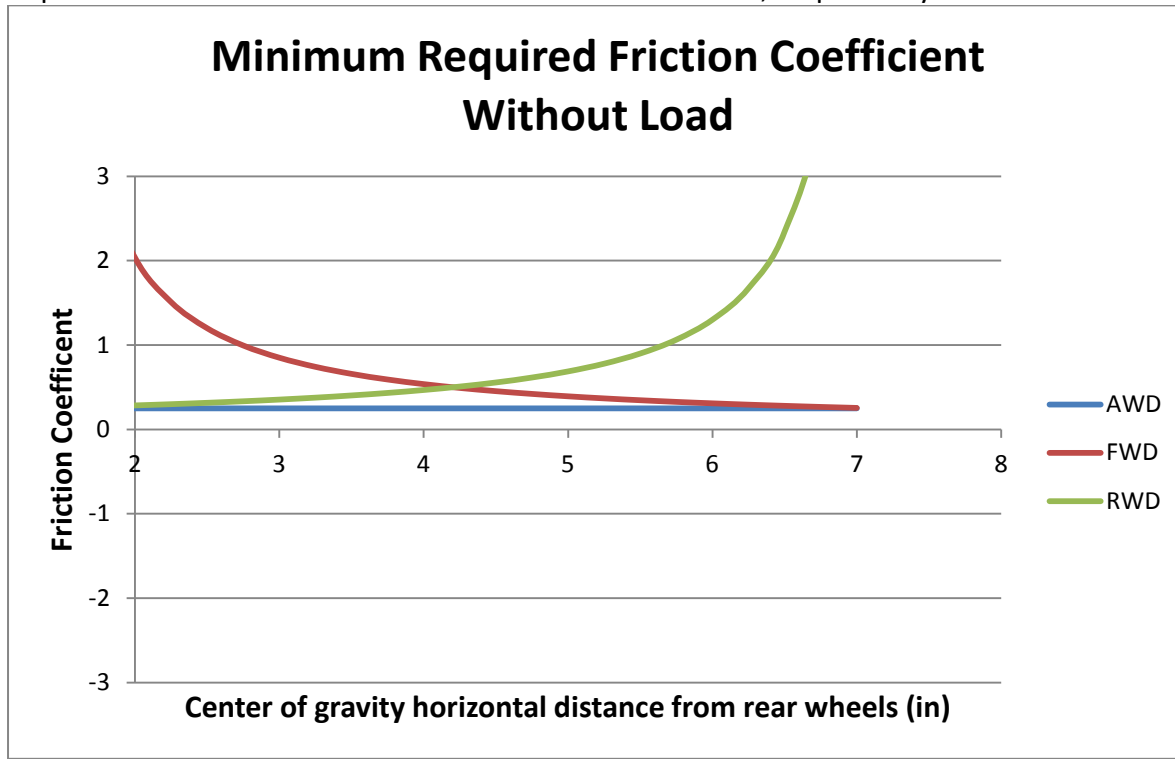


Figure 26: Friction Coefficient Comparison Chart without Load

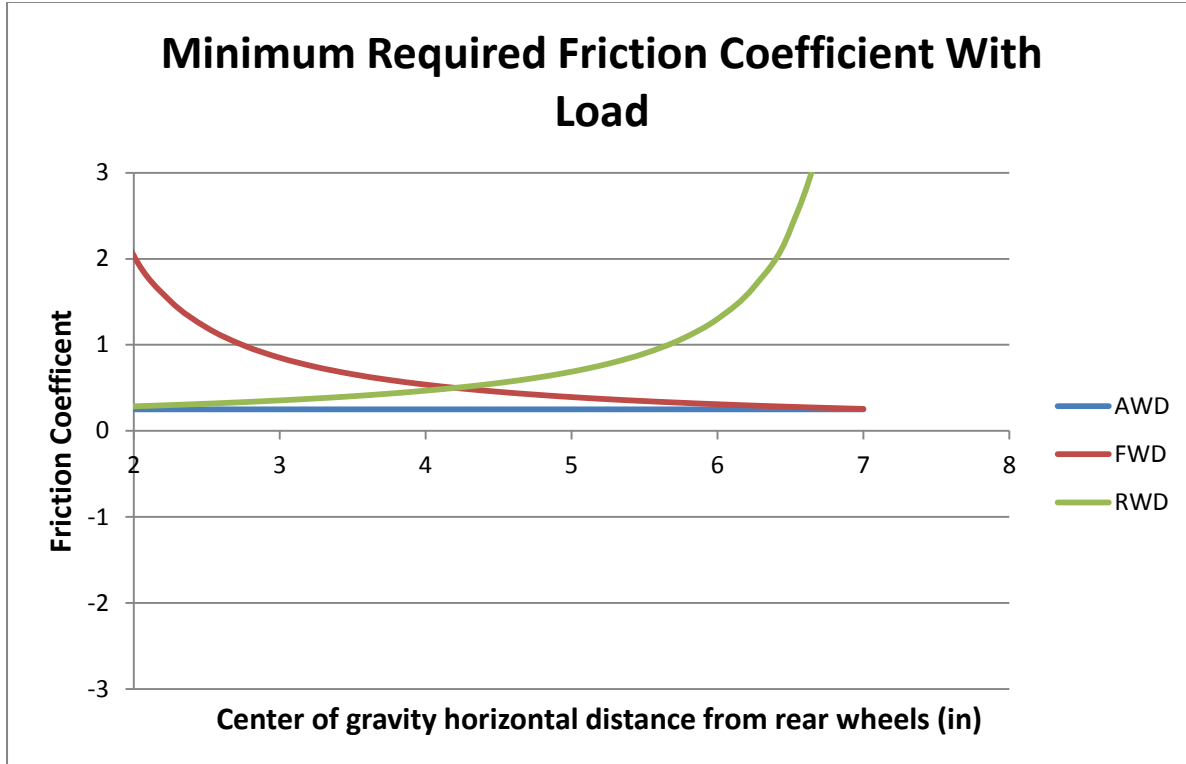


Figure 27: Friction Coefficient Comparison Chart with Full Load

Through observation of the plots, we see that they are very similar. This is due to the fact that only h in the formulas on the previous page is different, which just shifts the graph by a small amount. From both plots, we see that for equal rear-wheel drive and front-wheel drive friction coefficients, we get a value of about 0.5 at a center of gravity distance of about 4.1 inches from the rear wheel. These plots also show that front-wheel drive is not feasible due to the fact that it requires large friction coefficients if we were to concentrate most of our weight towards the back. Thus, confirming our previous conclusion. In addition, due to the complications of an all-wheel drive, we find that the rear-wheel drive system is best for our robot design. From there, we were able to choose a wheel material whose friction coefficient with plywood is greater than that of the minimum for a rear-wheel drive system.

Moving forward with the calculations, we now can calculate the normal force between the wheels and the ground. The front wheel and rear wheel normal forces are given by:

$$N_f = \frac{F_m L_C \cos\theta - F_m h \sin\theta}{L} \quad (5)$$

$$N_r = \frac{F_m (L - L_C) \cos\theta + F_m h \sin\theta}{L} \quad (6)$$

From here, we can calculate the maximum traction forces before slip on both the front wheels and rear wheels to find the total traction force on our robot's wheels. The formulas used to calculate the traction force is given by:

$$F_{Tf} = \mu_f N_f, \quad F_{Tr} = \mu_f N_r \quad (7), (8)$$

$$F_T = F_{Tf} + F_{Tr} \quad (9)$$

Below are Table 3 and Table 4 showing the parameters used to calculate the traction forces for our rear-wheel drive concept without and with the load.

Table 3: Normal and Traction Forces without Load

Wheel (front/rear)	Normal Force	Traction Force ($\mu=0.5$)
Front Wheel	5.406 lbf	2.703 lbf
Rear Wheel	11.145 lbf	5.572 lbf
Total	16.551 lbf	8.275 lbf

Table 4: Normal and Traction Forces with Full Load

Wheel (front/rear)	Normal Force	Traction Force ($\mu=0.5$)
Front Wheel	1.594 lbf	0.797 lbf
Rear Wheel	46.749 lbf	23.374 lbf
Total	48.343 lbf	24.171 lbf

When the transporter is not loaded, the force of gravity acting along the slope for the steepest angle ($\theta = 14.036^\circ$) is calculated as follows:

$$F_{wUnload} = F_{mUnload} \sin\theta \quad (10)$$

$$F_{wUnload} = (17.06 \text{ lbf}) \sin(14.036^\circ)$$

$$F_{wUnload} = 4.138 \text{ lbf}$$

Likewise, when the transporter is fully loaded, the force of gravity acting along the steepest slope is calculated using the same equation above:

$$F_{wLoad} = F_{mLoad} \sin\theta \quad (11)$$

$$F_{wLoad} = (49.83 \text{ lbf}) \sin(14.036^\circ)$$

$$F_{wLoad} = 12.085 \text{ lbf}$$

To conclude, when the transporter robot is unloaded, the force of gravity due to the steepest part of the ramp is 4.138 lbf, which means that:

$$F_{TUnload} > F_{wUnload} \quad (12)$$

So our robot will be able to climb the ramp when unloaded. Similarly, the force of gravity due to the steepest part of the ramp when fully loaded is 12.085 lbf, which leads to the same conclusion that $F_{TLoad} > F_{wLoad}$. Thus, our transporter robot will be able to climb up the ramp with a full load.

Figure 59 from the Appendix is used as a reference when applying the equations later on in this section. In the figure, the traction force, F_t , is facing up the ramp. This is the case when the robot is going up the ramp, and the direction is reversed when the robot is going down it.

The following equations are used to calculate the weight fractions, B_f and B_r , and are shown and derived in [2].

$$B_f = \frac{Nf}{Fm} = \frac{Lc \cdot \cos\theta - h \cdot \sin\theta}{L} \quad (13)$$

$$B_f = \frac{Nr}{Fm} = \frac{(L - Lc) \cdot \cos\theta + h \cdot \sin\theta}{L} \quad (14)$$

The following table contains the parameters used to determine the weight distribution between the wheels.

Table 5: Center of mass lengths for loaded and unloaded cases ($g = 386.088 \text{ in/s}^2$)

	Robot w/ Disks	Robot w/o Disks
L (in)	5.84	5.84
L _c (in)	1.34	3.17
L - L _c (in)	4.50	2.67
h (in)	7.14	5.12
2r (in) (drive wheel diameter)	2.00	2.00
m (lbm)	1.55	0.53
mg (lb)	49.83	17.06

The weight fractions, B_f and B_r, are shown in the following table for each section during the trip up and the trip down.

Table 6: Weight Fraction Tables

	A	B	C	D	E	F	G
B _f (%) going up	19.40	34.25	34.25	34.25	6.18	34.25	34.25
B _r (%) going up	80.60	65.75	65.75	65.75	93.82	65.75	65.75
B _f (%) going down	43.31	54.62	54.62	54.62	31.69	54.62	54.62
B _r (%) going down	56.69	45.38	45.38	45.38	68.31	45.38	45.38

Estimation of Required Propulsion Torque and Geared Motor Output Torque:

a_{inertia} is calculated using the same set of assumptions used to calculate the times for each section, which is shown in the set of equations above the velocity profile in part a. Since the velocity profile for each section is linear, the acceleration a_{inertia} for the robot traveling up the ramp is calculated using the equation:

$$a_{\text{inertia}} = (v_{\text{final}} - v_{\text{initial}})/t \quad (15)$$

When the robot is travelling down the ramp, we apply the modified equation below:

$$a_{\text{inertia}} = -(v_{\text{final}} - v_{\text{initial}})/t \quad (16)$$

We apply this equation because our notation for the velocities travelling down the ramp is to assign negative values for when the robot is travelling back to the starting point in order to be consistent with the velocity profile notation (negative velocity values when moving back to starting point). The values for v_{final}, v_{initial}, and t are shown in table 7 below. The calculated values for a_{inertia} are shown in the following table below:

Table 7: Inertial accelerations for each section

Section	v _{initial} (in/s)	v _{final} (in/s)	t (s)	a _{inertia} (in/s ²)
Going Up				
A	0.000	4.000	24.00	0.167
B	4.000	4.000	7.461	0.000
C	4.000	6.000	5.333	0.375

D	6.000	6.000	4.974	0.000
E	6.000	6.000	5.333	0.000
F	6.000	2.500	9.948	-0.352
G	2.500	0.000	11.20	-0.223
Going Down				
G	0.000	-4.000	7.000	0.571
F	-4.000	-6.000	9.948	0.201
E	-6.000	-8.000	4.000	0.500
D	-8.000	-9.500	6.283	0.239
C	-9.500	-7.500	4.266	-0.469
B	-7.500	-5.500	7.958	-0.251
A	-5.500	0.000	17.45	-0.315

Required/Propulsion Force ($F_{req} = F_{Propulsion}/\varepsilon$):

$$F_{req} = F_{inertia} + F_w + F_{rol} \quad (17)$$

This equation assumes that the robot has overcome the static friction term, given by $\mu_f mg\cos\theta$, so that is not included in the F_{req} calculations. The friction term is still included in the next table for reference purposes. The above equation can be substituted as: $F_{req} = ma_{inertia} + mgsin\theta + \mu_r mg\cos\theta$. The required force from the motors to propel the robot is dependent on the motor efficiency and is:

$$F_{req} = (ma_{inertia} + mgsin\theta + \mu_r mg\cos\theta)/\varepsilon \quad (18)$$

The required force from the motors needed to drive the robot through each section for up and down cases is shown in the following table.

Table 8: Propulsion Force for each Section: ($m = 1.856 \text{ lbm}$, $\varepsilon = 0.90$ [9], $\mu_r = 0.01$ and $\mu_f = 0.50$)

Section	ma _{inertia} (lbf)	$\mu_r mg\cos\theta$ (lbf)	mgsinθ (lbf)	$\mu_f mg\cos\theta$ (lbf)	F _{req} (lbf)
Going Up					
A	0.258	0.495	6.181	24.723	7.704
B	0.000	0.498	0.000	24.915	0.553
C	0.581	0.498	0.000	24.915	1.199
D	0.000	0.498	0.000	24.915	0.553
E	0.000	0.483	12.086	24.171	13.966
F	-0.545	0.498	0.000	24.915	-0.052
G	-0.303	0.498	0.000	24.915	0.217
Going Down					
G	0.303	0.171	0.000	8.530	0.527
F	0.107	0.171	0.000	8.530	0.309
E	0.265	0.166	4.138	8.275	5.077
D	0.127	0.171	0.000	8.530	0.331
C	-0.249	0.171	0.000	8.530	-0.087
B	-0.133	0.171	0.000	8.530	0.042
A	-0.167	0.169	2.116	8.464	2.353

Observing the table values, the robot does not require a lot of propulsion force for the non-inclined sections. For the inclined sections, it would require more because the weight force, F_w , has non-zero components along the inclined ramp. In addition, for section F going up the ramp, and section C going down the ramp, the F_{req} is negative. This indicates that in order to get the decreased velocities at the target values for those sections, the motors must effectively ‘brake’ or apply a torque in the opposite direction to help decrease it enough in the target time frame.

Total Propulsion Torque (T_{req})

$$T_{req} = F_{req} \times R_{DriveWheel} \quad (19)$$

Table 9: Required propulsion torque for each section ($R_{DriveWheel} = 1.00$ in)

Section	F_{req} (lbf)	T_{req} (lb*in)
Going Up		
A	7.704	7.704
B	0.553	0.553
C	1.199	1.199
D	0.553	0.553
E	13.966	13.966
F	-0.052	-0.052
G	0.217	0.217
Going Down		
G	0.527	0.527
F	0.309	0.309
E	5.077	5.077
D	0.331	0.331
C	-0.087	-0.087
B	0.042	0.042
A	2.353	2.353

I. Torque calculations

From our required torque and wheel radius we found a motor that matches our needed specifications. To begin our iteration we needed a motor selected to determine the exact center of gravity, weight, and several other parameters that would contribute to a motor selection. To circumvent this we considered that the majority of force needed to propel our robot will be due to weight. Because the weight of the motor is negligible compared to the rest of our robot we continued our first iteration neglecting the weight of the component. Our torque requirement is the torque to propel our robot with its maximum load up the steepest slope which is coincidentally where the maximum torque is needed. This is observed in path E of the track as designated in this report. Hence we need a motor that is strong enough to output 11.859 lb-in of torque, on a wheel of 1

inch radius, plus more to account for other factors including friction and the torque of the drive system. Eventually our motor selection is enough to overcome the actual propulsion torque of 13.966lb-in.

Table 10: Force and Torque Needed per Path Due to Weight (Forward)

Path	A	B	C	D	E	F	G
Force w/ load	6.065	0.000	0.000	0.000	11.859	0.000	0.000
Torque w/ load	6.065	0.000	0.000	0.000	11.859	0.000	0.000

Our maximum velocity is 6in/s and dividing this by our wheel circumference we find our required motor revolutions per minute are 57.3RPM.

Our maximum velocity is 6in/s and dividing this by our wheel circumference we find our required motor revolutions per minute are 57.3RPM. Hence we decided to use the Gear Head Motor (GHM-13) from Lynxmotion [10]. Below are the specifications provided by the manufacturer:

Table 11: Motor Specifications

Type: PK32KD3B2100-051
Model: PK32KD3B2100-051
Voltage Operation Range: 6-12VDC
Rated Voltage: 12VDC
Rated Load 12VDC: 15 Kg-cm = 13.02 Ib-in
Stall Torque: 88 kg-cm = 76.375 lb-in
No Load Speed 12VDC: 188RPM +/- 19
Speed at Rated Load: 163RPM +/- 16
No Load Current 12VDC: < 850mA
Current at Rated Load: < 5.0A
Outside Diameter = 36mm = 1.42in

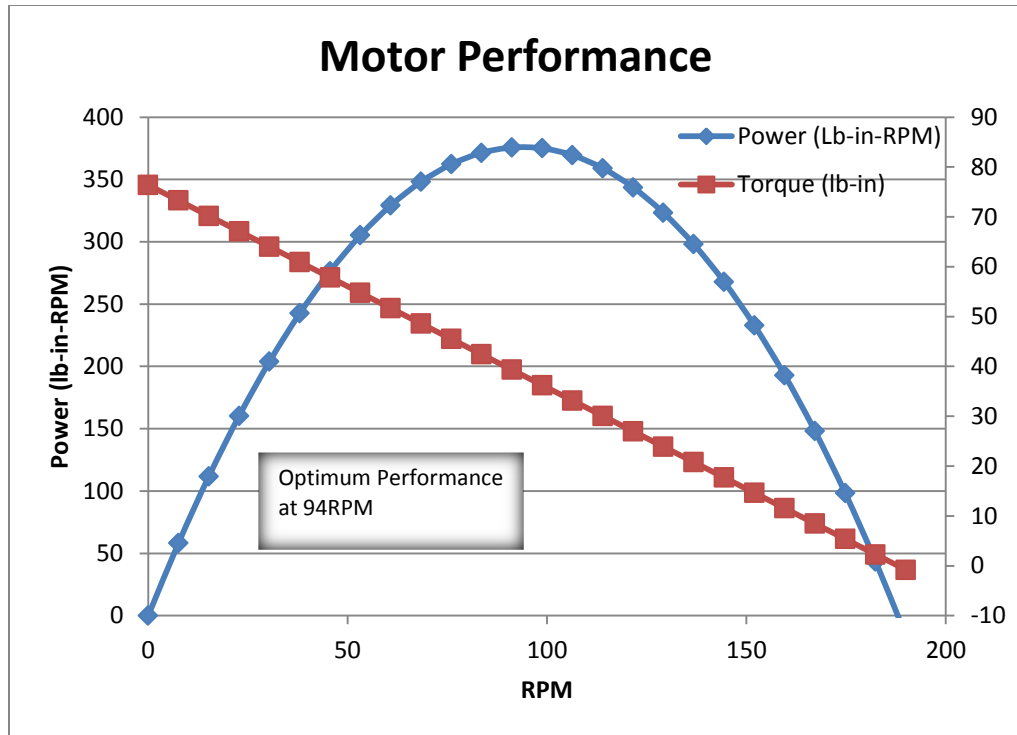


Figure 28: Motor Performance Curves

From selecting this motor we modeled this into our 3D drawing and used the overall model to calculate our propulsion force and propulsion torque that was described previously. We found this motor to satisfy the necessary torque conditions.

We will be using our motors in a direct drive system and hence our drive torque is the direct torque from our motors. Our drive torque at 94RPM will be 76.375 lb-in per motor. Hence our total drive torque is this value multiplied by 2:

$$\text{Drive Torque} = \boxed{152.75 \text{ lb-in.}}$$

The output torque is compared to the required propulsion torque for each section in the table below:

Table 12: Drive torque and required torque comparison table

Section	$T_{\text{Drive}} (\text{lb}*in)$	$T_{\text{req}} (\text{lb}*in)$	$T_{\text{Drive}} > T_{\text{req}}$ (Y/N)
Going Up			
A	152.75	7.704	Y
B	152.75	0.553	Y
C	152.75	1.199	Y
D	152.75	0.553	Y
E	152.75	13.966	Y
F	152.75	-0.052	Y
G	152.75	0.217	Y

Going Down			
G	152.75	0.527	Y
F	152.75	0.309	Y
E	152.75	5.077	Y
D	152.75	0.331	Y
C	152.75	-.087	Y
B	152.75	0.042	Y
A	152.75	2.353	Y

As seen from the table above, for every section, the output torque is greater than the required propulsion torque. This indicates that the selected motor is capable of supplying the necessary torque to drive the robot for this ramp.

Our system is a direct drive system so our required torque to overcome the motor mechanisms and the friction torque is calculated with the equations below:

$$T_{req} = J_t \alpha_{acc} + T_f = (J_l + J_m) \alpha_{acc} + T_f \quad (20)$$

$$J_m = (m_{shaft} R_{shaft})/2 = W_{shaft} R_{shaft}^2/(2g) \quad (21)$$

$$J_l = (m_{wheel} R_{wheel})/2 = W_{wheel} R_{wheel}^2/(2g) \quad (22)$$

$$T_f = F_f R_{wheel} \quad (23)$$

Where J_t is the total torque required which is equivalent to the sum of the load torque and the motor torque. α_{acc} is dependent on the portion of the track the robot is trekking. The weights and radii for the shaft and wheel are as listed:

Table 13: Wheel and Motor Dimensions

Wheel Radius (in)	1.000
Wheel Mass (lb)	0.090
Shaft Radius (in)	0.236
Mass Shaft (lb)	0.005
g (in/s^2)	386.000

Below are the tables listing the forces and torques required on both the trip forward and back.

Table 14: Torque Required per Track Path (Forward)

Path	A	B	C	D	E	F	G
Force Friction (lbf)	0.4945	0.4983	0.4983	0.4983	0.4834	0.4983	0.4983
Torque Friction (lb-in)	0.4945	0.4983	0.4983	0.4983	0.4834	0.4983	0.4983
alpha (rads/s^2)	0.167	0.000	0.375	0.000	0.000	-0.352	-0.223
Total Torque							
Motor (lb-in)	1.95E-05		4.39E-05		0	0	-4.1E-05
		0	05		0	-4.1E-05	-2.6E-05

Torque Required (lb-in)	0.5494	0.5537	0.5537	0.5536	0.5371	0.5536	0.5536
----------------------------	--------	--------	--------	--------	--------	--------	--------

Table 15: Torque Required per Track Path (Back)

Path	G	F	E	D	C	B	A
Force Friction (lbf)	0.1706	0.1706	0.1655	0.1706	0.1706	0.1706	0.1693
Torque Friction (lb-in)	0.1706	0.1706	0.1655	0.1706	0.1706	0.1706	0.1693
alpha (rads/s^2)	-0.5714	-0.201	-0.5	-0.2387	0.4688	0.2513	0.3151
Total Torque							
Motor (lb-in)	-6.7E-05	-2.3E-05	-5.8E-05	-2.8E-05	5.5E-05	2.95E-05	3.7E-05
Torque Required motor (lb-in)	0.1894	0.1895	0.1838	0.1895	0.1896	0.1895	0.1881

From Table 7 we can see where the highest accelerations are, but because the friction torque is 3 times the magnitude of our total drive torque we can estimate the location of our maximum required torques. From the values given in table 14 we find a $T_{req_motor} = 0.5537\text{lb-in}$ at part C of our track for the forward direction. For our backwards direction we use the motor to decelerate and for this the greatest required torque on the trip back is $T_{req_motor} = 0.171\text{lb-in}$ which is negligibly higher than on our forward trip. This puts the maximum accelerating torque that our robot needs at $T_{req_motor} + T_{prop} = 14.520\text{lb-in}$.

II. Unloading mechanisms

For the unloading mechanism, we are going to use motorized force gate. We are going to have one servo motor to unlock and relock the gate. The servo motor will be located at the bottom of the carrier. It will be connected to the force gate, which is used to hold the disk from falling. For our particular unloading mechanism, we first have to know the required force and torque to make this mechanism valid.

The servo motor that is located at the center bottom is connected to the carrier bottom surface through four bar linkage system. This allows more efficiency on generating the movement of the force gate through the motor. Once the robot reaches the unloading zone, the two push button sensors on the back of the robot will inform the motor to pull down the force gate which barely requires any force due to preexisting force caused by the weight of the disk. After unloading the disk, certain amount of force is required to pull up the force gate to its original position. The following figure shows the free body diagram after unloading disks.

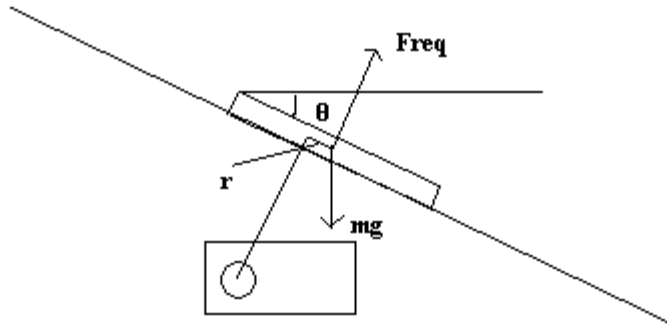


Figure 29: Free body diagram for forced gate after unloading disks

In order to reach the equilibrium the force acting in the vertical direction should add up to be zero.

$$\sum F_{\text{vertical}} = F_{\text{req}} \cos \theta + mg = 0 \quad (24)$$

When the gate is at the equilibrium position, that means it will move with constant velocity but since the gate is starting from the static position, we have to apply a stronger force in order to initiate the movement. The equation is given by:

$$F_{\text{req}} \cos \theta > mg \quad (25)$$

We were able to obtain values for the weight and angle θ using SolidWorks. Since the weight of the gate is 0.11 lb and angle θ is 8.13 degree, the minimum force required is 0.112 lb. This result is as predicted since the θ value is relatively small.

The following equation is the equation for the torque calculation.

$$T = F \times r \quad (26)$$

The r value is also obtained through the measurement tool in SolidWorks. Since the r value is 1.56 inch and force required is 0.112 lb, the torque required for the forced gate is 0.173 lb-in.

After knowing the force and torque requirement to activate the gate system, we also have to confirm that we have enough energy for the disk to move a certain amount of distance to reach to loading zone. In the case where the given energy is not sufficient enough to satisfy the distance requirement, we have to come up with some sub-system to achieve our goal.

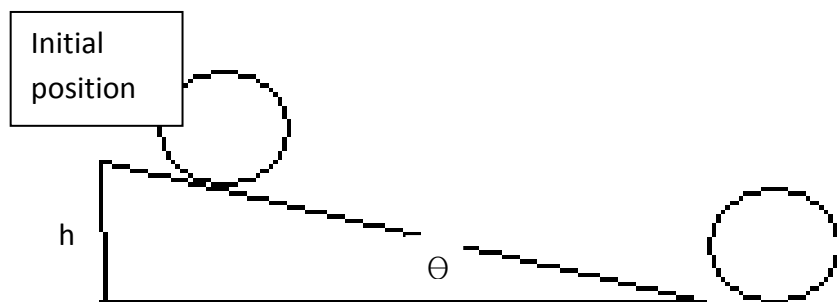


Figure 30: Disk rolling down the slope

The first procedure is to calculate the amount of energy we have at the beginning of unloading procedure. If we neglect minor energy that is induced, such as thermal, chemical...etc, we are left with two major energy types which are potential and kinetic. The following equation demonstrates the relationship between kinetic energy and potential energy.

$$E_{\text{total}} = E_{\text{kinetic}} + E_{\text{potential}} \quad (27)$$

In the beginning of the unloading procedure, there are no movements generated through disks. This implies that the kinetic energy in the beginning is zero so the total energy in the beginning is the potential energy. The major factor that determines the potential energy for our particular case is gravity and we can calculate the total energy using the following equation.

$$E_{\text{potential}} = m_d g h \quad (28)$$

As disks goes down the slope, total energy which is only potential energy gets transferred in to kinetic energy. When it reaches the bottom surface, all of the potential energy is transferred to kinetic energy. In other words, kinetic energy equals the potential energy of the beginning height when it gets to the bottom surface.

$$E_{\text{kinetic}} = \frac{1}{2} m_d v_d^2 \quad (29)$$

From the equation above, we can calculate the velocity of the disk when it gets to the bottom. If we set two equations equal to each other, we can derive an equation for the velocity of disks.

$$v = \sqrt{2gh} \quad (30)$$

For our case, height is 0.065 ft and g is 32.2ft/s^2 so we can calculate our velocity to be 2.05ft/s^2 . The y component of the velocity can be calculated to be -0.29 ft/s^2 with $\theta = 8.13^\circ$.

$$v_y = v_d * \sin\theta \quad (31)$$

The distance down to the edge of the box is 0.718 ft. By using the next equation, we can figure out the time it takes for the disk to get to its final position, which is about 2.02 s.

$$y_f = y_i + v_y t + \frac{1}{2} a_y t^2 \quad (32)$$

If we go through the similar procedure using:

$$v_x = v_d * \cos\theta \quad (33)$$

$$x_f = x_i + v_x t + \frac{1}{2} a_x t^2 \quad (34)$$

We can calculate the horizontal displacement which turns out to be approximately 0.41ft. This displacement is sufficiently large enough to fulfill the unloading procedure so we can conclude that we don't need any extra subsystem. For our particular unloading mechanism, we only need one servo motor to control the force gate and the required force and torque values are 0.112 lbf and 0.173lb-in. Since the initial potential energy is sufficient enough to fulfill require horizontal displacement, we don't need any additional subsystems.

With this requirement we chose the following servo motor:

Table 16: HD High-torque Servo Specifications

HD High-Torque Servo 1501MG	
Size	1.6 x 0.81 x 9.43 in
Weight	0.13 lb
Speed @ 6V:	0.14 sec/60°
Stall torque @ 6V:	14.76 lb-in
Speed @ 4.8V:	0.16 sec/60°
Stall torque @ 4.8V:	13.45 lb-in

Our servo motor's stall torque at both voltages greatly exceeds that which we require.

V. CONTROL SYSTEM DESIGN

I. Motor Selection from Torque Calculations

From our calculations we needed at least 640 oz-in to carry a maximum load of 6 discs and preferably a high enough RPM to have a 180 second trip. Our chosen motor, the Planetary Metal Geared Motor PD264M which provides 3471 oz-in of torque at a stall current of 35.0A. This motor goes well with our new driver because the maximum current on our driver per channel is 50.0A. In this respect, we know that our motor will not cause a current surge that would destroy our motor driver.

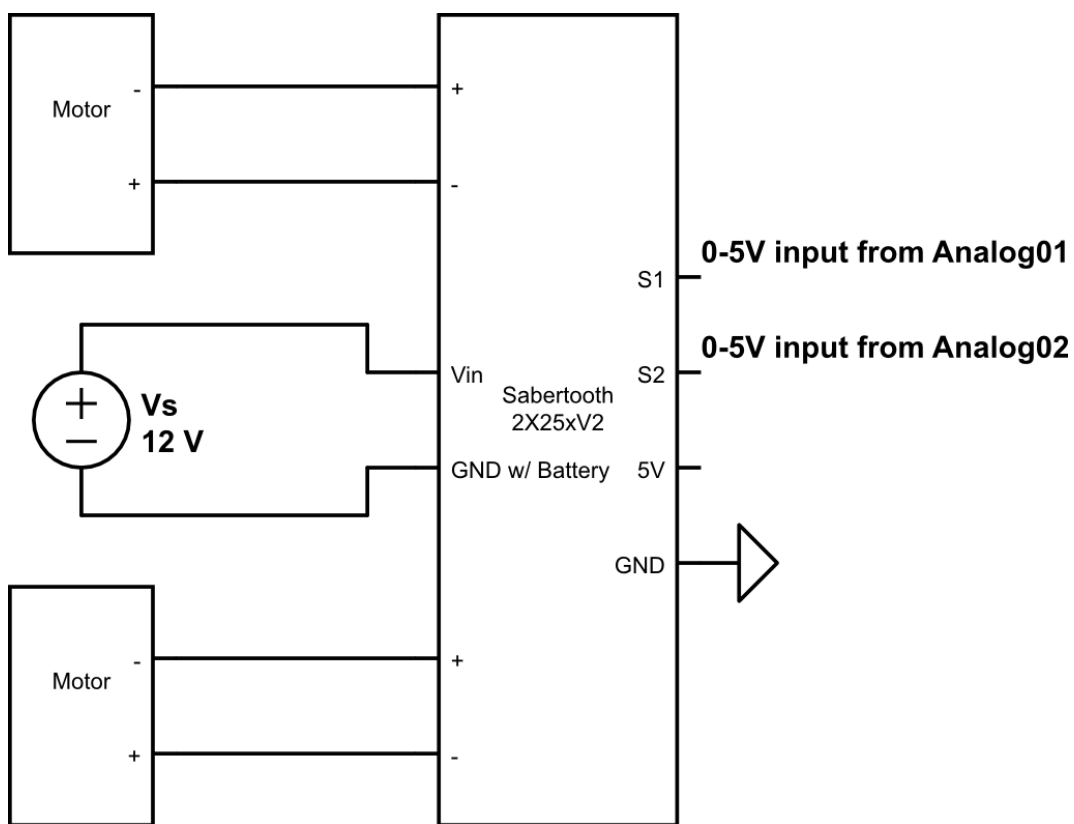


Figure 31: Motor Circuit Diagram

II. Unloading Mechanisms

Our unloading mechanism uses a four-bar toggle mechanism to make use of a smaller and cheaper servo. We are using one parallax standard servo to control our mechanism. Essentially, we have our four-bar mechanism attached to a small gate on a sloped ramp. The four-bar pushes the linkages into a linear position when the gate is up and when this occurs, all of the force from the weight of the discs act long that collinear path. This takes the entire load

off of the servo and allows us to have a smaller servo. At the beginning of the track, the mechanism will erect the gate up for someone to place the load on top. Then at the end of the track, the servo will retract the linkages and allow the gate to fall down. This allows the discs to roll off the ramp into the box. As a small modification, we added an extension to the ramp to ensure that our load overcomes the 3 inch gap between the ramp and the box.

III. Sensors and Theory of Operations

Our robot has 6 sensors: 3 ultrasonic sensors and 3 home-made push buttons. We use HC-SR04 ultrasonic sensors to navigate our robot through the track and adjust it during turns. The sensors are well apt for use in our range between 2cm to 20cm. Our push-buttons are homemade from a broken keyboard. We took advantage of our spare parts and the fact that there is an aluminum connection in the keys. After modifying the keys, a connection is completed whenever the button is pushed down and this applies 5V across our SB-RIO pin. We use this as a true and false Boolean. These push buttons are used for unloading and loading purposes.

For our navigation we used the ultrasonic sensors. At first when the robot is in the starting box, it will read that the sum of the left and right sensors reading the side walls will be greater than 20cm which tells the robot to follow this portion of the track at 12cm away from the left wall. Once the robot reaches the actual track which is narrower, the sum of the distance to the two walls will be under 20 and the robot will follow the left wall at 6cm away from the wall. This wall following applies all the way up the track. Whenever the left sensor reading is below 11 it will cause the motors to adjust so the robot will turn slightly to the right. When this reading is above 13 the robot will turn slightly to the left.

As a precaution, we added a feature in which when the left sensor is reading below 4cm, the right wheel will completely stop and the left wheel will continue to turn allowing the robot to make a very sharp turn. This is useful if the robot cannot adjust fast enough to turn away from the wall. This also avoids collisions with the wall.

Once the front sensor reads the wall by the unloading area at 2cm, the robot will back up and complete a 180 degree turn. During this 180 turn the left sensor is used to adjust by backing up whenever the sensor reads 2cm or below. Doing this allows for a tighter 180 turn and prevents collision with the wall if the robot is too close to the left all before it starts turning. Once a counter runs out, we will know that the robot has turned 180 degrees and the robot will begin backing up into the wall.

Both wheels will go in reverse at the same speed. The 2 push buttons on the back of the vehicle are essentially stop buttons for each motor. Once the robot hits the wall and the buttons are pushed, the Boolean that both buttons are pushed tells the unloading mechanism to drop and allow our discs to roll off the ramp into the unloading area. After a short time, the gate will lift itself up and the robot follows down the track using the left sensor again.

At the end of the track, in the starting area, the right sensor is used with the left sensor to tell that the sum of the distances measured to the two walls is greater than 20cm. This correlates again with being in the starting area which tells the robot to follow at a distance of 12cm rather than 6cm with the left sensor. Once the front sensor is within 2cm of the starting edge wall, another 180 degree turn is completed.

The robot is now ready for a second run and it is initiated once our last push button sensor, on the loading ramp, is pushed down by the weight of our lead discs. Once this Boolean is true, the robot sets off on another run through the entire cycle.

We have noticed issues with both sensors. Although the ultrasonic sensors give us the flexibility of setting Booleans correlating to varying distances, the sensors are more complicated and fragile. We have run into problems with the sensor readings and the physical integrity of the ultrasonic sensors which is a disadvantage. If our reading spikes then we can have logical issues in our programming if it is not accounted for. If our robot runs into a wall for some reason, this could damage the sensor physically. A push button has the advantage that it is very simple and is meant for physical contact so it holds those advantages. The disadvantage is that there is a lack of flexibility because it must make contact with something in order to trigger the Boolean. We have also had some connection issues because our buttons are homemade.

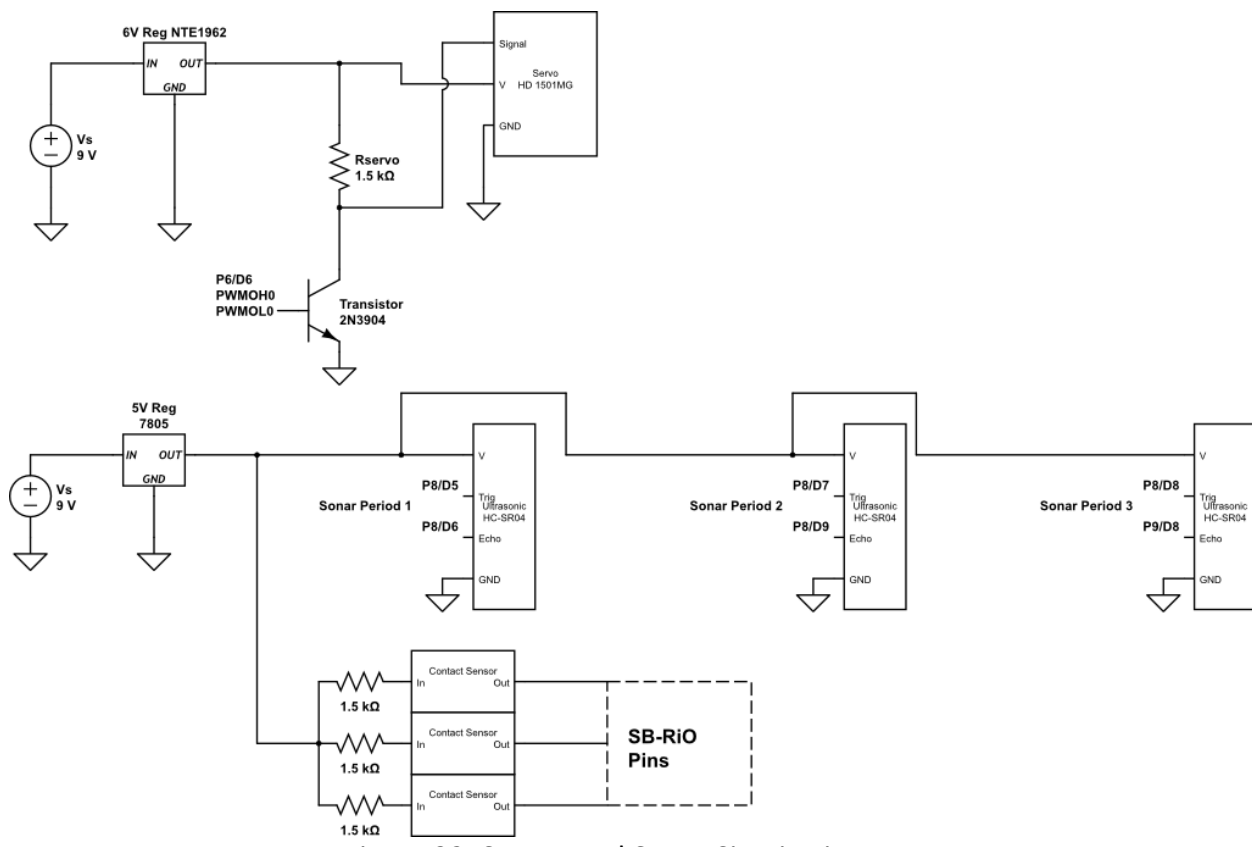


Figure 32: Sensor and Servo Circuit Diagram

IV. State Diagrams

The interface between the LabVIEW programming and the actions performed by the electronic systems is the Sb-RIO. The Sb-RIO is wired to the ultrasonic proximity sensors, the positional servo, the motor controller, and the contact sensors. The Sb-RIO takes in analog voltage inputs from the ultrasonic proximity sensors and the readings are converted to distance

in cm to use for convenience. The positional servo takes a PWM high and low in order to position itself. The PWM high and low values used are: 25000 for PWM high, 585 for PWM low for lifted gate, and 1010 for PWM low for dropped gate. The motor controller accepts analog outputs from 0 to 5 V from the Sb-RIO to control the motors. 0 V corresponds to full reverse for a wheel, 2.5 V corresponds to stop for a wheel, and 5 V corresponds to full forward for a wheel, and the Sb-RIO outputs two values since the motor controller can set two motors. The three contact sensors are digital inputs that are sent to the SB-RIO and send 0 V for false case and 3.3 V for true case.

The robot programming was entirely performed in LabVIEW. We used the skeletal code provided as the interface between the FPGA and the SB-Rio on the robot. In the appendix, the front panel and block diagram of the main code are screen-shotted. In the figure below, the screenshot of the LabVIEW statechart diagram is included. The two main states are: demonstration code and testing code.

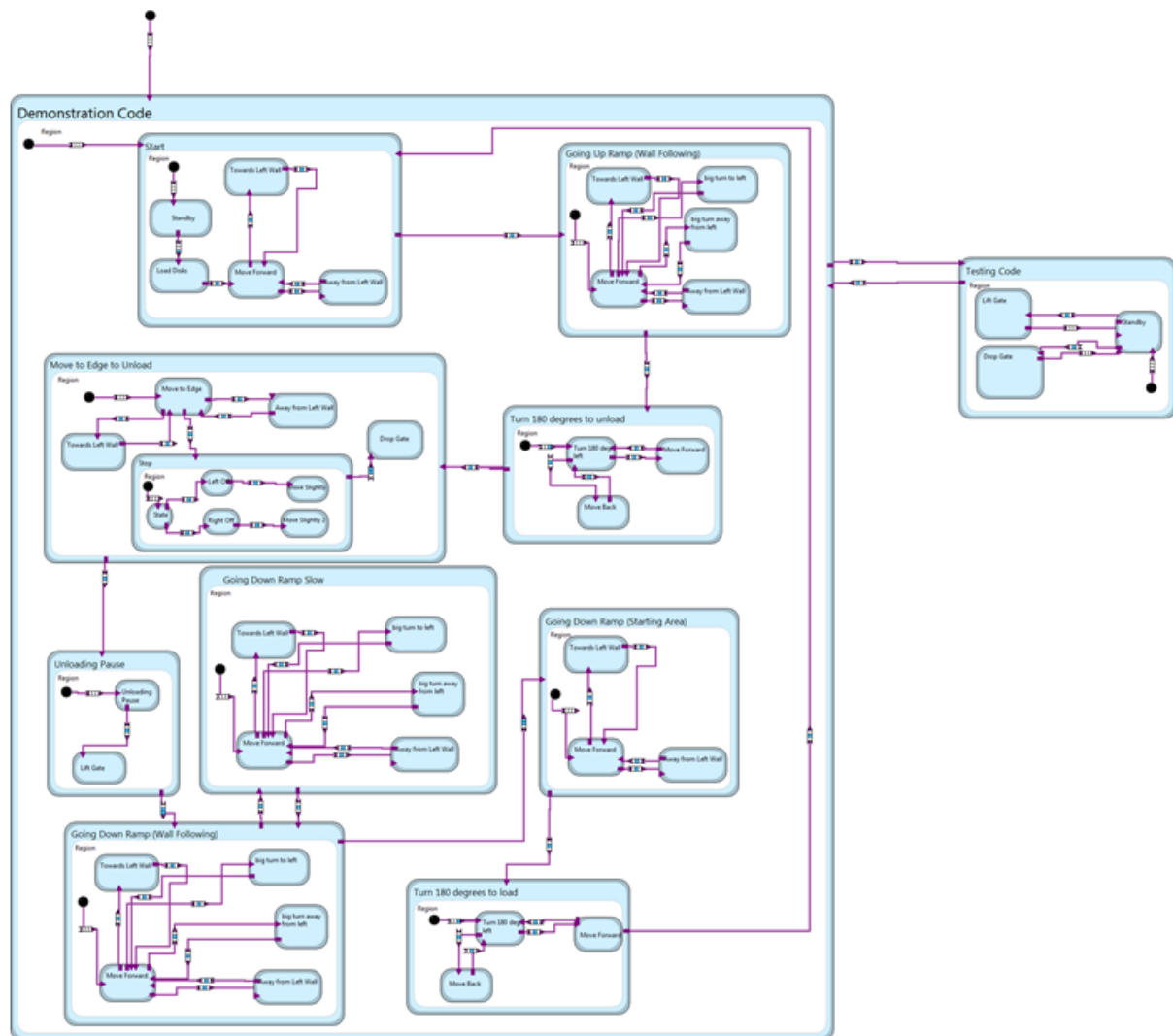


Figure 33: LabVIEW Statechart Diagram for Whole Demonstration Code & Testing Code

The figure below shows the state diagram for transitioning between the demonstration and testing code. Demonstration code includes all of the states and sub-states that are used to give output commands to the FPGA during the actual demonstration run of the robot. To transition to the testing code, BR 2 on the SB-Rio is pressed to enter the testing code state. In testing code state, the robot is in standby and the force gate can be lifted or closed by pressing BR 3 or BR 4. To transition to the start of the demonstration code, BR 1 is pressed.

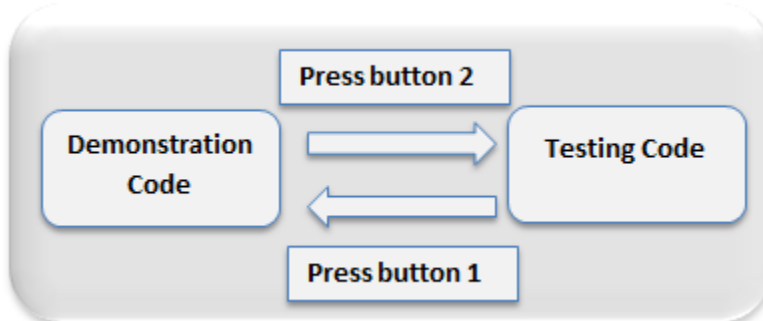


Figure 34: State Diagram between Demonstration Code and Testing Code

The figure below shows the simplified state diagram with the state transitions for the demonstration code state. When the code is run, the statechart begins at the start of the demonstration code. The demonstration code runs as follows: a PWM signal is sent to the servo in order to lift the force gate. Once the gate is in the lifted position, the robot is able to carry discs. The robot remains in standby until the force sensor is pressed by the weight of the discs. Then the robot will wall follow up the ramp in the starting area using the left sensor. The sum of the left and right sensors is used to determine whether or not the robot is in the starting area or the 16" wide ramp area. If the sum is greater than 34 cm, then the robot assumes that it is still wall following in the starting area at a greater distance from the left wall. If the sum is less than 34, then the robot will wall follow at a lesser distance that is appropriate for the thinner walls. The robot will wall follow up the ramp including for the turns and its wall-following state diagram is shown later on. Once the robot wall follows to the top of the ramp, it will turn around left for 180^0 when the front sensor reading is 8 cm or less. The 180^0 turn is in a countered loop that remains in the state and performs the turn until the counter reaches a certain value. We assume that the loop executes at the same time as the main loop, which is once per 60 ms. If we want to perform the turn for 2.4 seconds and increment the loop counter once per cycle, then the turn is finished once the loop counter reaches 40. Once the robot has finished turning 180^0 , it moves in reverse to the edge of the ramp to prepare for unloading the disks. The robot continues moving in reverse until both the left and right rear contact sensors are pressed, which stops the corresponding motor. Once both motors are stopped due to both contact sensors being pressed, a PWM signal to the servo drops the force gate and allows the disks to roll out and into the unloading bin. After a countered standby loop that lasts for 1.5 seconds, the robot uses the left sensor to wall follow down the ramp using the same method as going up the ramp. Using the sum of the left and right sensors, the robot will wall follow at the

starting area distance if the sum is greater than 34 cm or wall follow at the ramp wall distance if the sum is less than 34 cm. Once the front sensor reads 8 cm or less when wall following, the robot will turn in a counter-clockwise loop for 2.0 seconds to re-orient itself to go up the ramp and start the demonstration code loop from the beginning in the starting area.

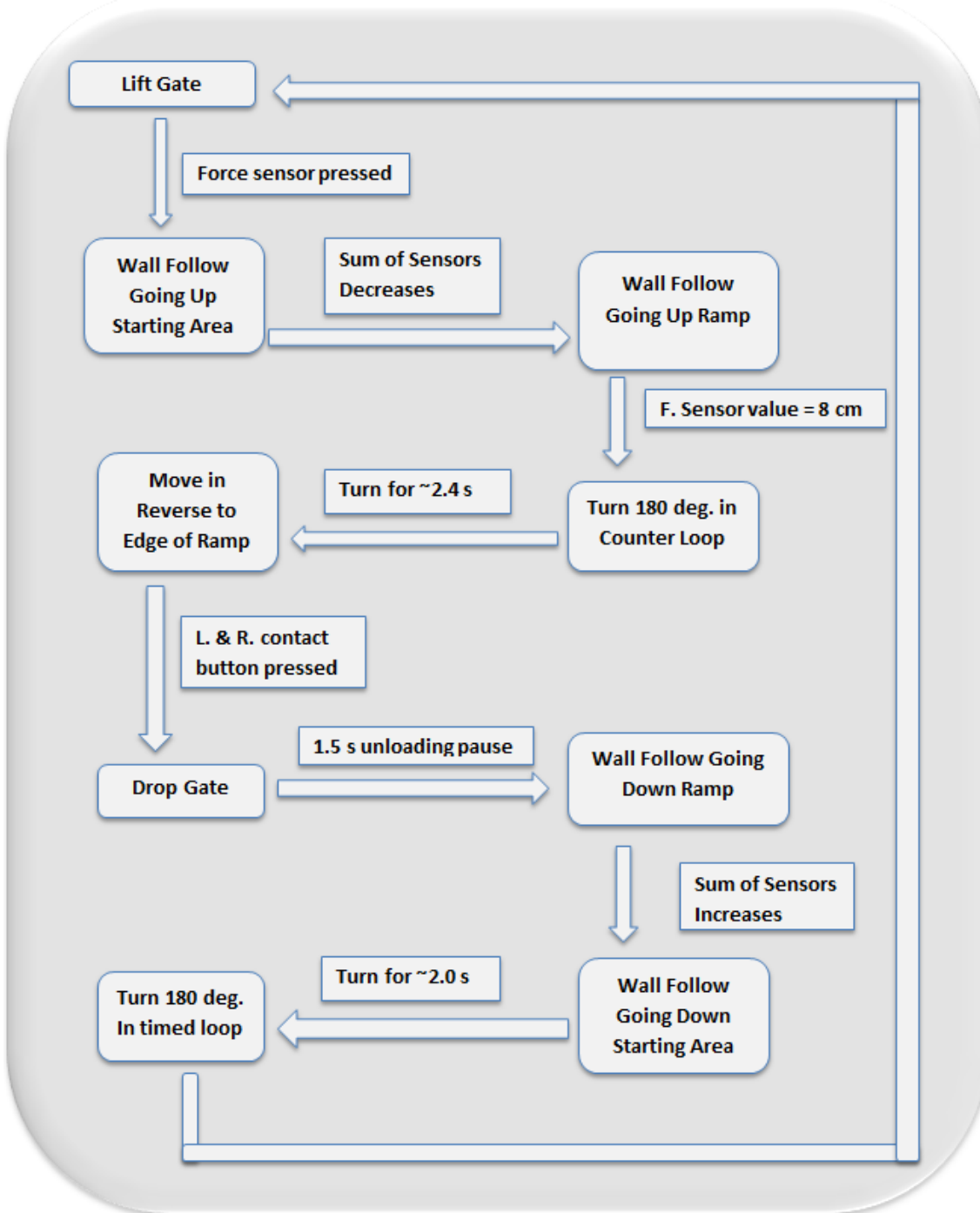


Figure 35: Demonstration Code Statechart Diagram

The figure below shows the state diagram for the testing code state. In testing code state, the robot starts in standby, where all counters are stopped and the motors are turned off. The unloading mechanism can be tested by pressing BR 3 to lift the gate and BR 4 to drop it.

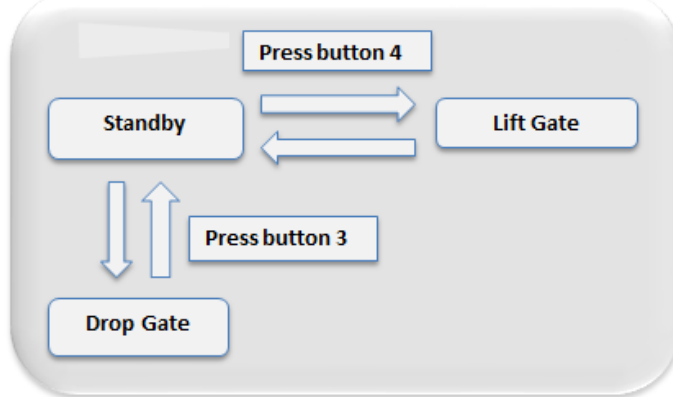


Figure 36: Testing Code Statechart Diagram

The figure below shows the ‘wall following going up the ramp in the starting area’ sub-statechart diagram. The robot starts in the move forward state and it maintains 18 cm from the left wall based on the left sensor reading. If the left sensor reading is 19 cm or greater, the robot turns to the left wall by applying a differential to the wheels with the left motor velocity less than the right motor velocity. The robot exits the turning state once the left sensor reading is 18 cm. If the left sensor reading is 17 cm or less, the robot turns away from the left wall by applying a differential with the left motor velocity greater than the right motor velocity. The state ‘wall following down the ramp in the starting area’ uses the same wall following state chart diagram.

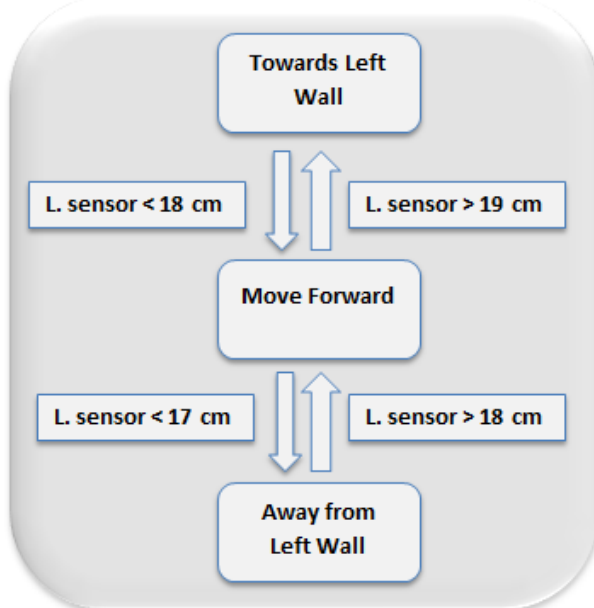


Figure 37: Wall Follow Going Up Starting Area Sub-Statechart Diagram

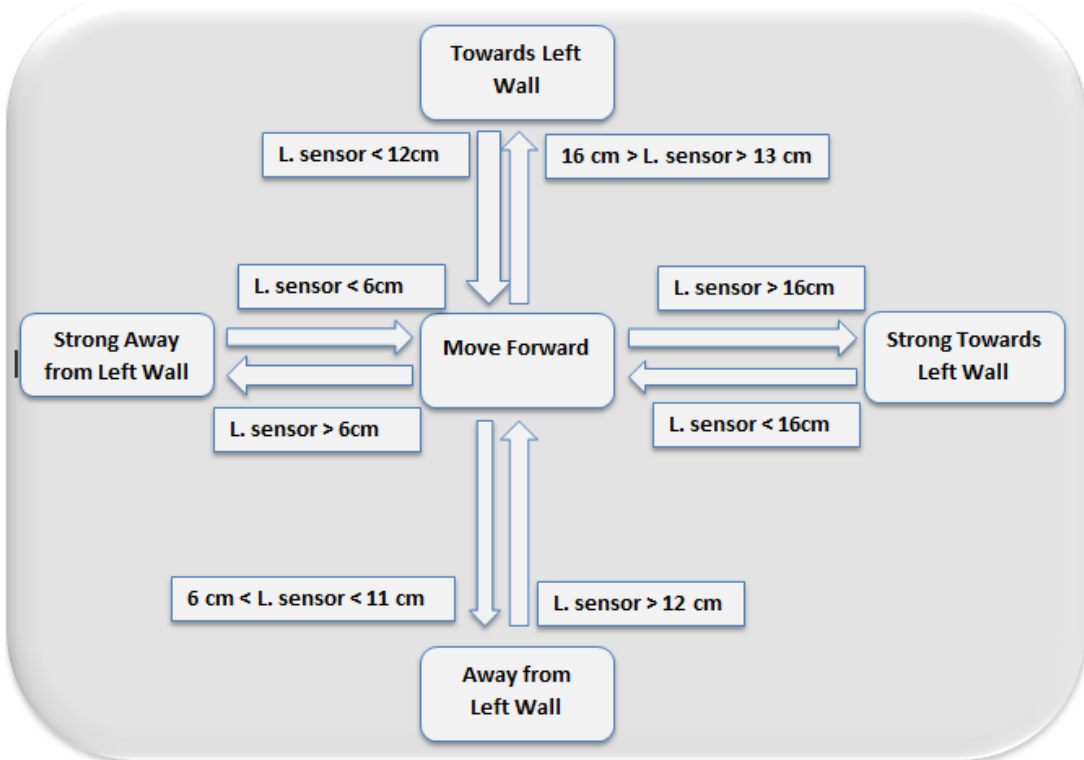


Figure 38: Wall Follow Going Up Ramp Sub-Statechart Diagram

The figure above shows the ‘wall following going up the ramp in the ramp section’ sub-statechart diagram. The robot starts in the move forward state and it maintains 12 cm from the left wall based on the left sensor reading. If the left sensor reading is 13 cm or greater, the robot turns to the left wall by applying a differential to the wheels with the left motor velocity less than the right motor velocity. The robot exits the turning state once the left sensor reading is 12 cm. For stronger turns, if the left sensor reads 16 cm or greater, an even greater differential is applied. If the left sensor reading is 11 cm or less, the robot turns away from the left wall by applying a differential with the left motor velocity greater than the right motor velocity. For stronger turns, if the left sensor reads 6 cm or less, a greater differential is applied to avoid the robot running into the walls. The state ‘wall following down the ramp in the ramp section’ uses the same wall following state chart diagram.

The figure below shows the ‘Turn 180° deg. In Counter Loop’ sub statechart diagram. The demonstration code statechart enters this state when the front sensor outputs 8 cm or less while it is wall following up the ramp. The robot will turn 180° by applying a differential where the left wheel is moving backwards at full speed and the right wheel is moving forwards at full speed in a counter loop. The counter is initialized at zero when entering the state and it increments by one every 60 ms. The code exits the ‘Turn 180° deg In Counter Loop’ state once the counter reaches 40. Also, the robot can move forwards and backwards to pivot itself in order to avoid bumping into the walls during the turning. Since the robot turns to the left, if the left sensor reads 5 cm or less, then it will back up until the reading is 8 cm. If the right sensor

reads 5 cm or less, then it will move forwards until the reading is 8 cm. This helps position the robot so that it does not bump the walls during the turning. Also, when the robot is pivoting, the counter does not increment. The ‘Turn 180° in starting area’ state is identical to this state.

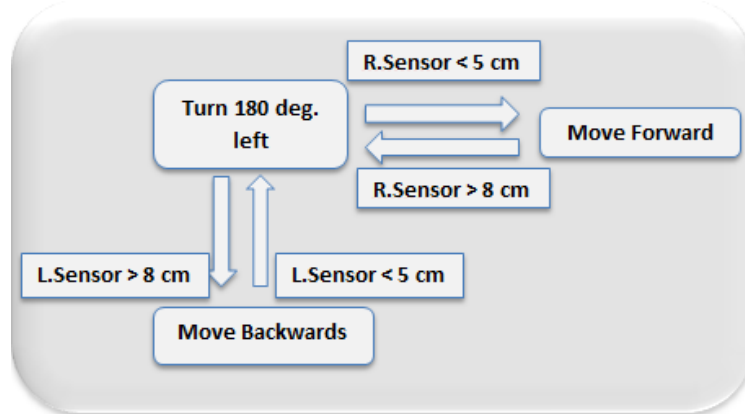


Figure 39: Turn 180° deg. In Counter Loop Sub-Statechart Diagram

The figure below shows the ‘Move in Reverse to Edge of Ramp’ sub-statechart diagram. The state begins in ‘Move Backwards’ and it can wall follow in reverse at 12 cm from the left wall in order to help orient itself. When the robot reaches the edge of the ramp, when a contact sensor is pressed, it will turn off that motor and pivot on that wheel until the other contact sensor is pressed and both motors are turned off. Once both buttons are pressed, the robot exits the state.

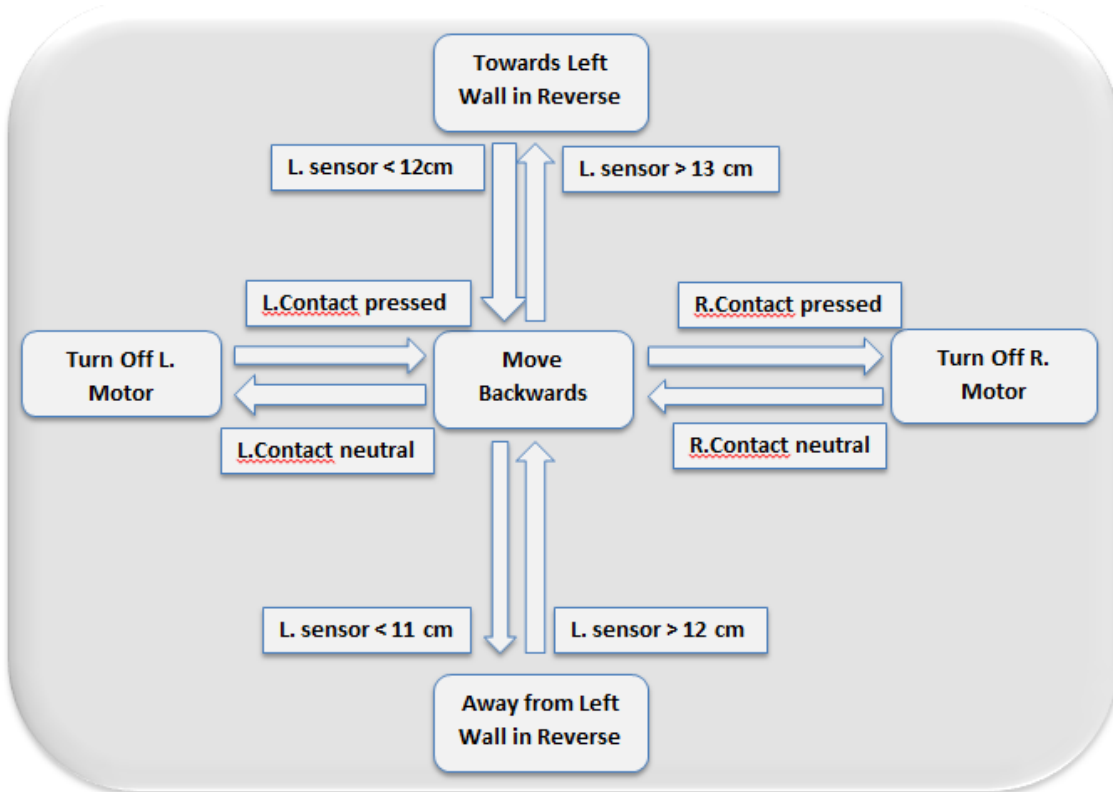


Figure 40: Move in Reverse to Edge of Ramp Sub-Statechart Diagram

VI. PRODUCT FABRICATION

I. Machining of Selected Parts

Provided in this section are details regarding our manufacturing of a select few parts and the assembly of our robot. Also included are some complications that we encountered in our design.

Section Wall:

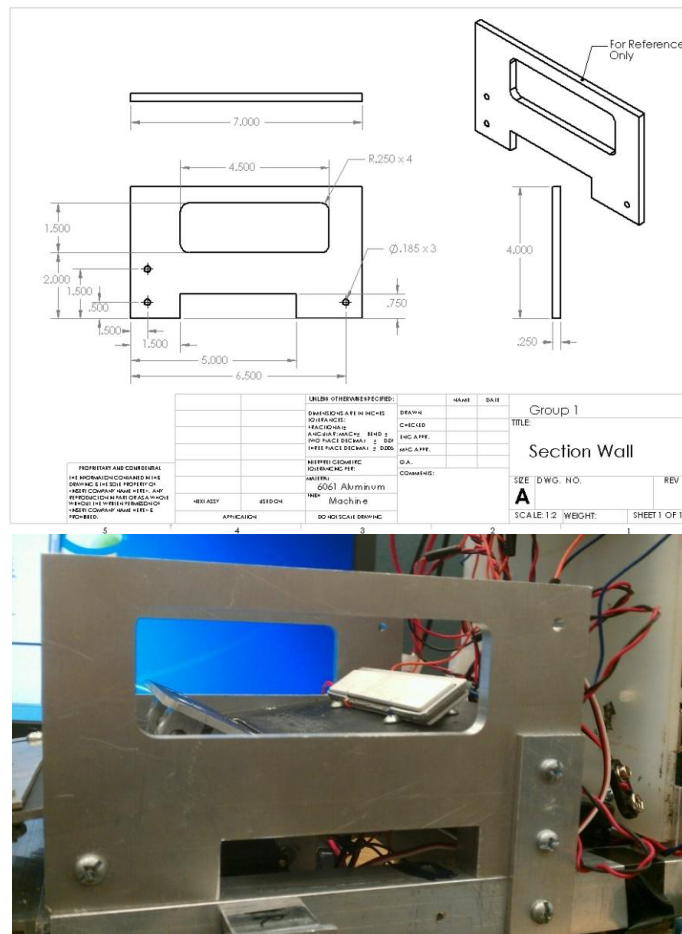


Figure 41: Section wall CAD drawing (top), Section wall finished piece (bottom)

The section wall was fabricated using the mill and band saw. Also, since our design contained two section walls, both were made simultaneously. First, we cut two pieces aluminum to around the outer dimensions indicated on the engineering drawing. Then, we clamped the two pieces together and used the mill to square the aluminum to the right dimensions. Then using the edge finder, the holes were drilled in the positions indicated. Once this had been completed, we cut the bottom opening using a band saw to around the specified dimensions and used the mill to achieve the exact dimensions. Then, the edge finder was used to make the slot. Then using a $\frac{1}{2}$ inch bit, the slot was cut out.

Motor Mount:

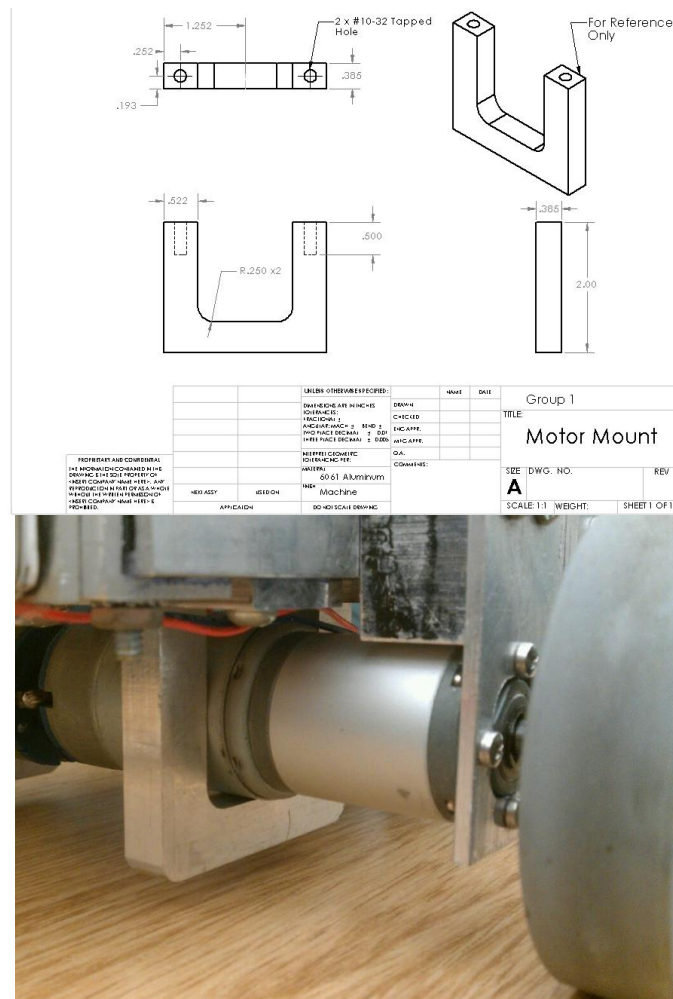


Figure 42: Motor mount CAD drawing (top), Motor mount finished piece (bottom)

The motor mount was actually modified from its original design. This was mainly due to making the machining easier. Since the purpose of the motor mount was to prevent the shaft of the motor from having a bending torque, our new design was sufficient. The motor mount was fabricated using the band saw, mill, and a hand tap. Since our design required two motor mounts, both were made simultaneously. First, the two aluminum pieces were cut to the approximate size according to the outer dimensions on the engineering drawing. Then the pieces were clamped and put onto the mill. The mill was used to square the aluminum pieces to exact dimensions. Then, the pieces were separated and the “U-shape” was cut out using the band saw. Once again, the pieces were clamped back together and the cut surface was milled to the exact dimensions. Once the outline of the motor mount has been milled, we drilled the two holes to the exact locations using the edge finder. Then, the hand tap was used to tap the two holes. We also eventually chose to round off the corners with the belt sander to avoid getting cut.

Ramp Extender:

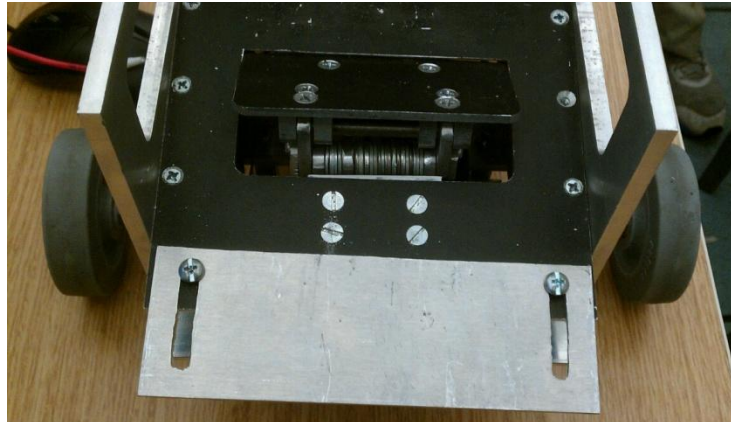


Figure 43: Ramp Extender

This part was not originally in our design. This part was made because the lead disks did not clear the receiving bin using our original design. This was made using a jigsaw and a hand drill. First, an aluminum piece was cut to size using a jigsaw. Then a hand drill was used to make four #10-24 holes; two on each side. Finally, a jigsaw was used to connect the holes on each side to make a slot. This allowed for easy sliding of the ramp extender, so that we could still follow the high level design requirements and clear the receiving bin.

II. Assembly

Our assembly consisted of multiple parts. Much of our holes were not tapped and, as a result, we used bolts, lock washers, and nuts for many of the connections. The problem with this was that we had a very hard time assembling it. This was due to the fact that it required us to put our hands into hard to reach places to lock the screws in place. Connecting the SB-RIO mount to the structural frame was the most difficult. Therefore, we made a modification and decided to tap a hole, so that we could just attach it by simply screwing it in.

In addition to difficulties involving nuts and bolts, the assembly had to be performed in a specific manner. First, the U-channels and L-brackets had to be connected to make the structural frame. This was followed by attaching the two casters to the bottom of the structural frame. Then the motor mounting strip and servo/servo mount was assembled onto the frame. Next, the motor was connected by screwing the motor mount onto the motor mounting strip. Also, the rear shaft support piece was connected to the frame and the motor to provide additional support, such that the motor was secure. The following figure shows how the motors are attached.



Figure 44: Drive train subsystem showing the attachment of the motors

After the mounting the motor, the rear wheel and shaft coupler was assembled. The shaft was actually press-fitted into the wheel using the press. The diameter of the shaft was slightly larger than the wheel's inner diameter, so that there would be a snug fit between the two. This was feasible since the bore of the wheel was plastic. This allowed the plastic to expand, such that the shaft could fit into the hole. The following figure shows the press-fit.



Figure 45: Two views of the shaft coupler press-fitted into the rear wheel

From here, the disc carrier sub-assembly had to be made separately. This involved first connecting each section base to the corresponding section wall and then putting two shafts along with their corresponding links and pieces (i.e. force gate attachment). Once this was done, the ramp was put on and screwed into the top of the section base. The ramp served as the piece that connected the two section walls and section bases.

After the disc carrier assembly was assembled, the toggle mechanism could be connected. This involved assembling the necessary shafts and links together to complete the unloading mechanism. Also, washers were used to keep the links from sliding away from one another. Furthermore, a piece was screwed into the links to keep the pins from falling out. Once the unloading mechanism was assembled the disc carrier assembly was connected to the structural frame using a connector piece. After the disc carrier assembly was attached, the battery L-bracket mount could be put on. The reason this had to be put on after was because it interferes with the hole that allows the connector piece to attach to the frame. The following figure shows the attached unloading mechanism.

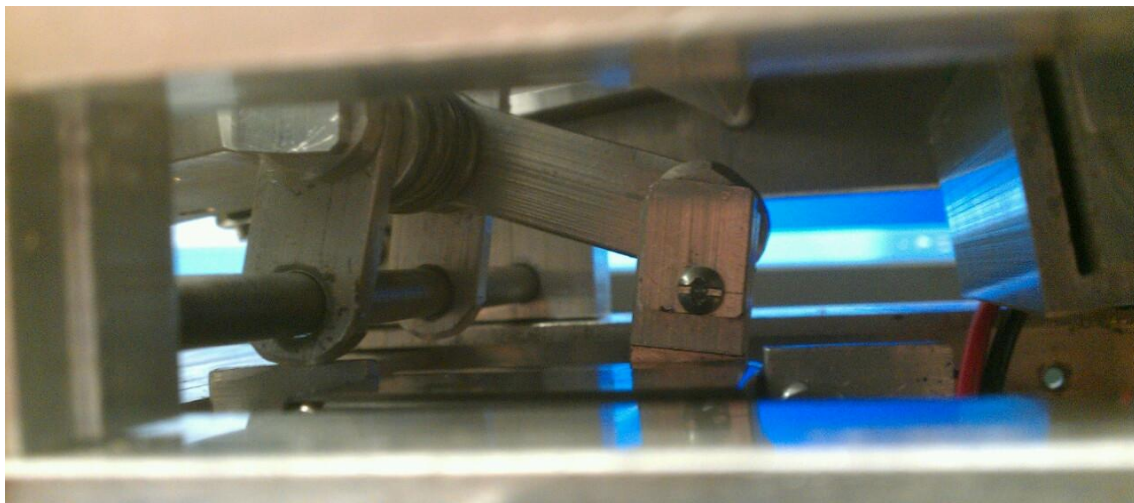


Figure 46: Side view of toggle mechanism used for unloading

Then the batteries were put into the robot. After this, the SB-RIO was connected to the mount. Finally, the SB-RIO mount was screwed into the frame.

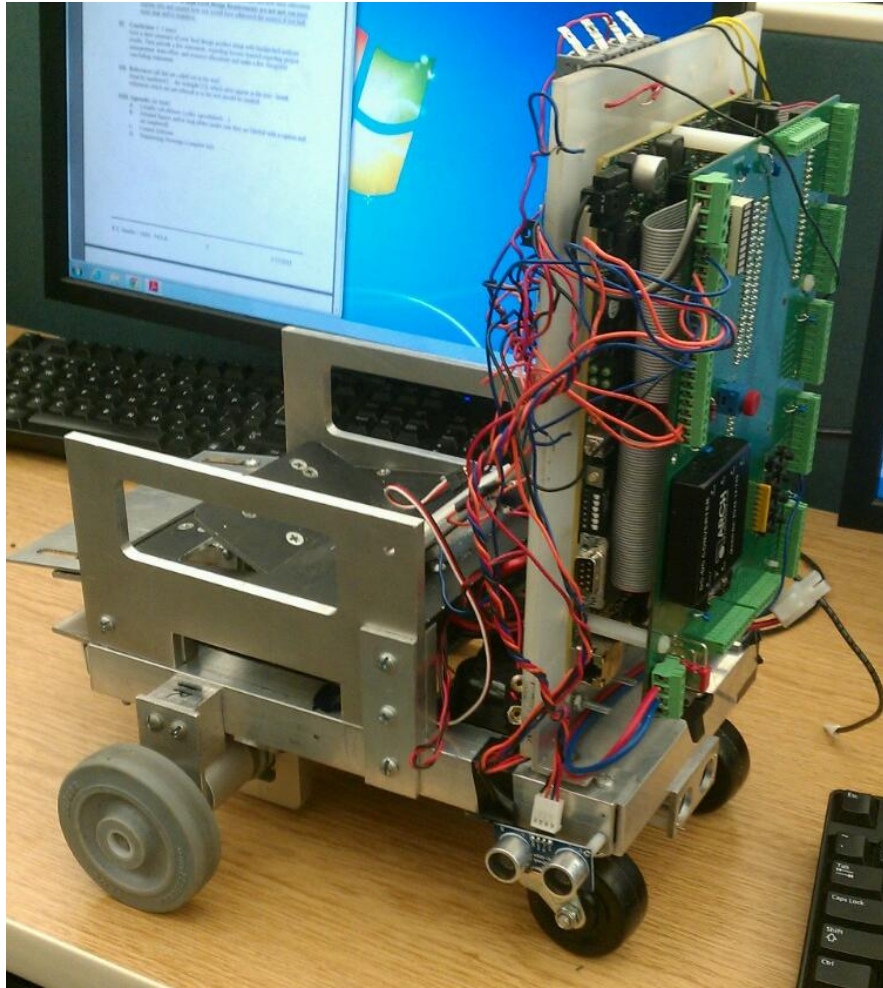


Figure 47: Fully Assembled Robot

VII. PRODUCT TESTING AND EVALUATION

To test the product performance of the robot, we ran the demonstration code on the demonstration ramp with five discs that are bolted through the middle (~ 31 lbs). For the first three runs, the robot runs continuously without restarting the code. For the last three runs, the code is re-run, but the motor battery and SB-RIO battery are not charged during the intercession. The following table indicates the run times divided by section for each of the six trials. Another run with three discs (load = ~ 19 lbs) is performed with three runs. The run times for the second run are shown in the table 19 below. The error analysis for the product run time sis performed using the following equations:

$$u = \sum x/n \quad (35)$$

where u is the mean average, x is the sample time value and n is the total number of runs.

$$\sigma = \sqrt{(x_1 - u)^2 + (x_2 - u)^2 + \dots + (x_n - u)^2}/n \quad (36)$$

Where σ is the standard deviation of the sample, x_1, x_2, \dots, x_n are the times for each run.

The relative error is calculated using the following equation:

$$\text{Rel. error} = \Delta X / X * 100 \% \quad (37)$$

Where $= \Delta X$ is the absolute difference in the time for each run from the mean time and X is the time for a particular run. A sample error calculations table for six discs is shown in the appendix section B under table 28. Based on the relative errors being less than 5 %, the performance using five discs was reliable and did not significantly deviate with successive runs.

Table 17: Miracle Robot Run-Times with Five Discs

Trial	Up Time (s)	Unloading Time (s)	Down Time (s)	Total Time (s)
1	37.6	5.5	35.0	78.1
2	38.0	5.6	35.0	78.6
3	38.0	6.0	35.5	79.5
4	37.5	5.5	33.0	76.0
5	38.5	6.0	35.0	79.5
6	38.0	6.0	36.0	80.0

The up, unloading, down, and total times for the run with five discs are shown in the following figures. For the up times, the times did not differ significantly, however based on the low correlation coefficient, R^2 , there is no predictability for the time for successive runs. The same is true for the unloading times, down times, and total run times.

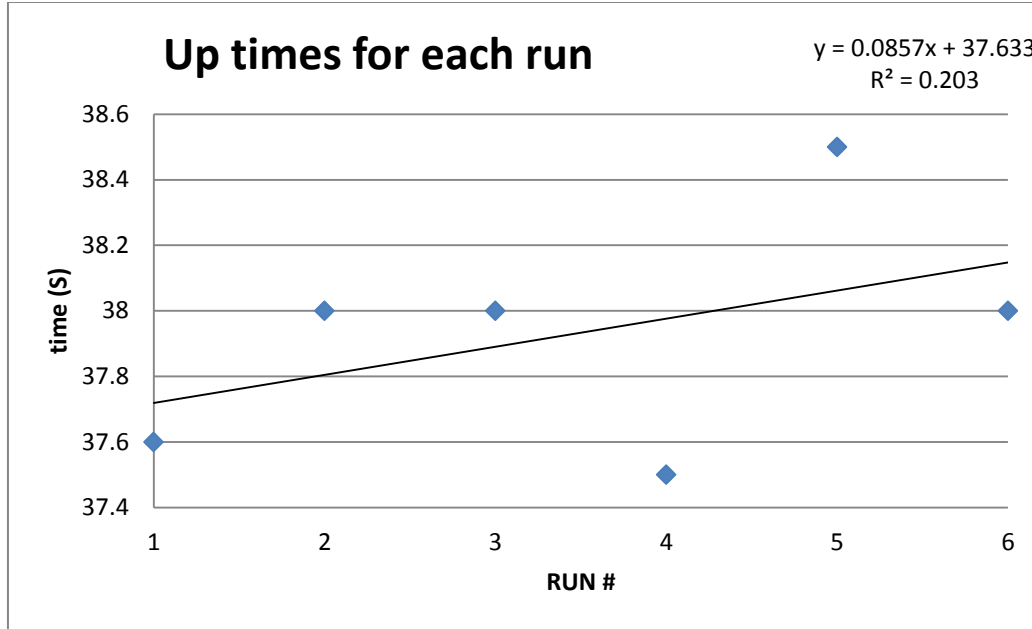


Figure 48: Up times using five discs

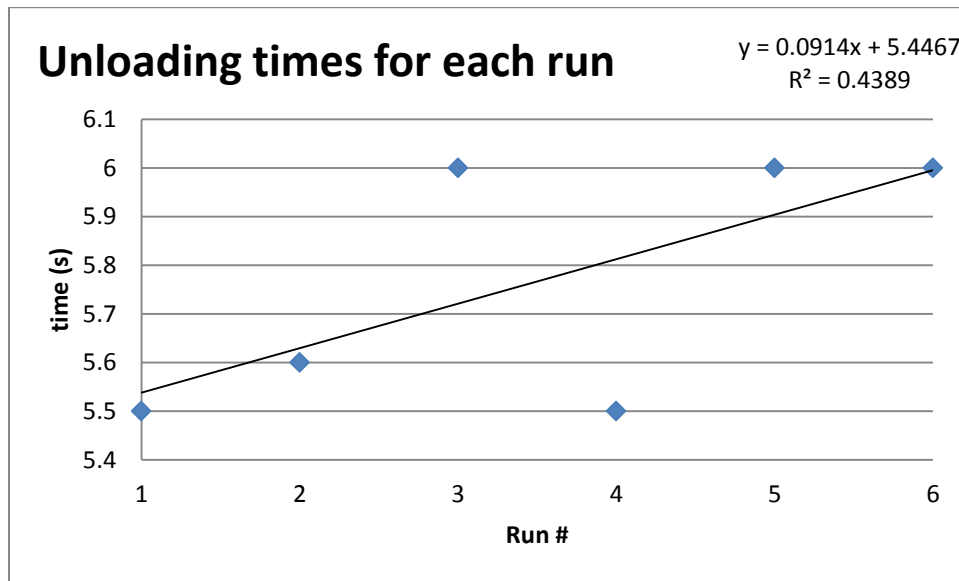


Figure 49: Unloading Times using five discs

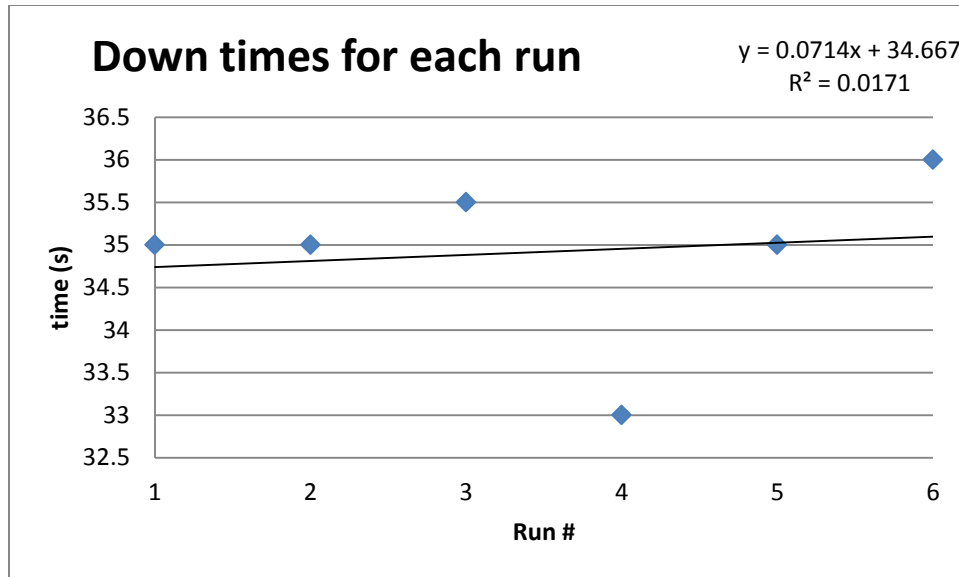


Figure 50: Down times using five discs

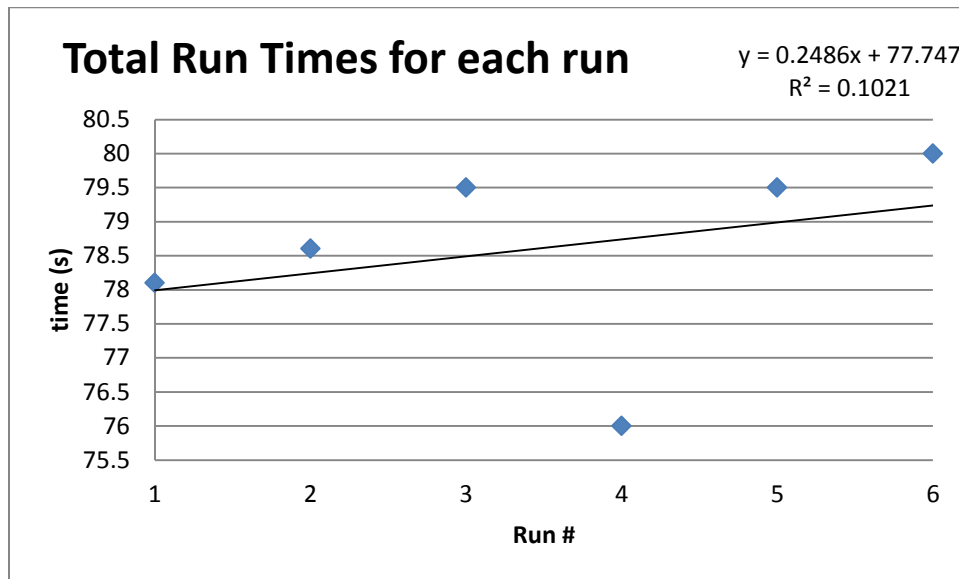


Figure 51: Total times using five discs

Table 18: Miracle Robot Run-Times with Three Discs

Trial	Up Time (s)	Unloading Time (s)	Down Time (s)	Total Time (s)
1	37.0	5.5	35.5	78.0
2	38.0	5.5	35.0	78.5
3	38.0	6.0	35.5	79.5

The up, unloading, down, and total times for the run with three discs are shown in the following figures. For the up times, the times did not differ significantly, however based on the low correlation coefficient, R^2 , there is no predictability for the time for successive runs.

The same is true for the unloading times, down times, and total run times. Compared to running with five disks, the run times are about the same because the mean complete run time for three disks is: 78.7 seconds, which is very close to the mean complete run time for five disks, 78.6 seconds, which is shown in table 28.

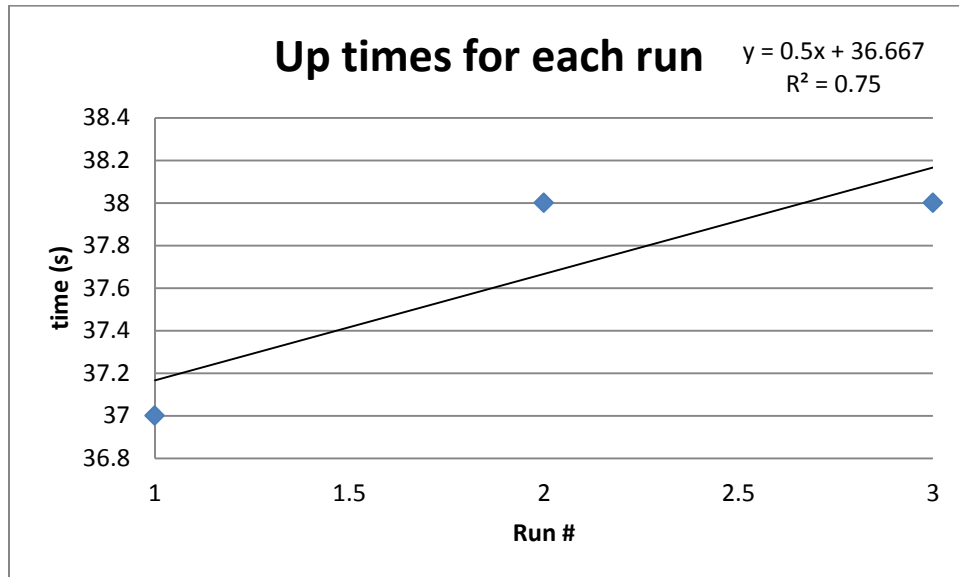


Figure 52: Up times using three discs

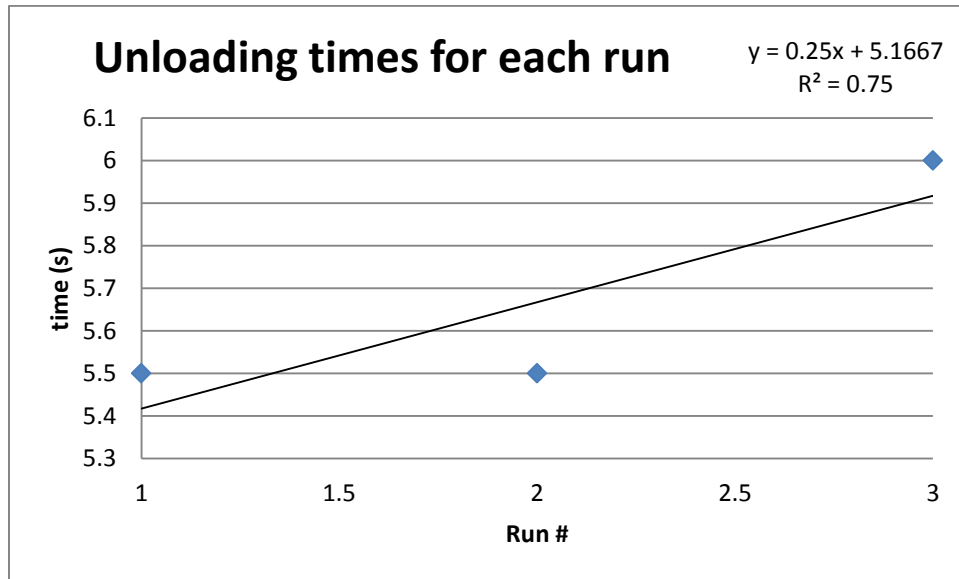


Figure 53: Unloading times using three discs



Figure 54: Down times using three discs

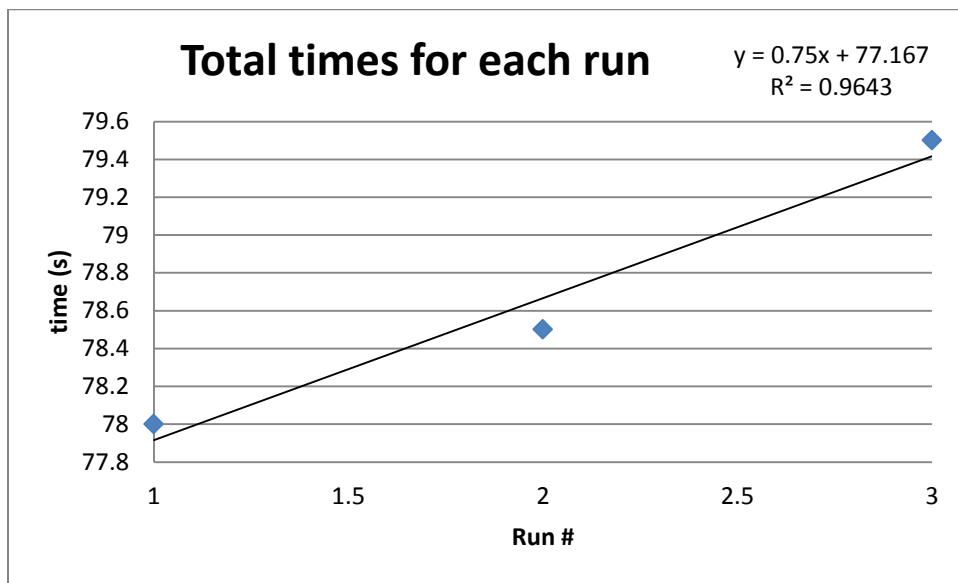


Figure 55: Total times using three discs

VIII. WORK BREAKDOWN SCHEDULE

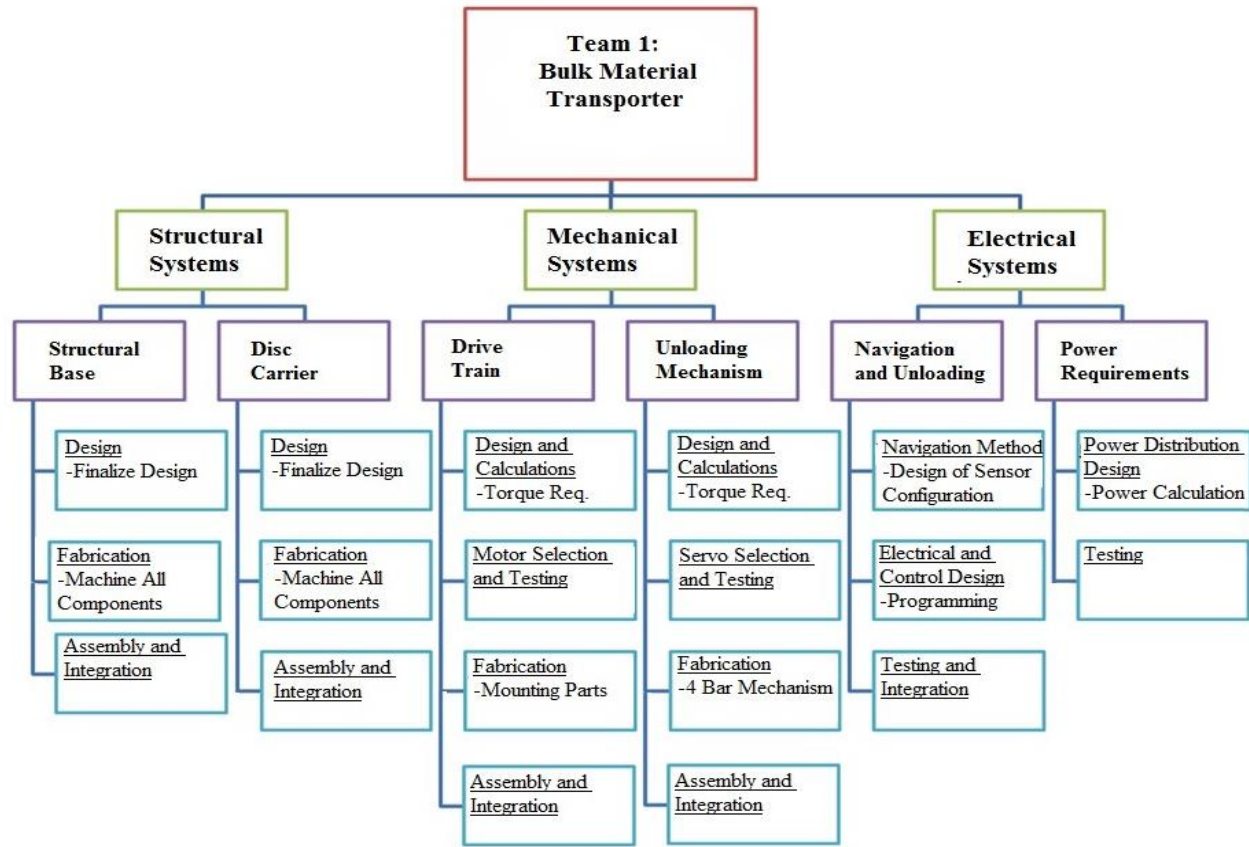


Figure 56: Work Breakdown Schedule

Table 19: WBS Dictionary

Index	Element Level	Description
	Level 1	The main deliverable of the project
	Bulk Material Transporter	Programmed and fabricated robot that loads/ unloads lead discs in an obstacle path.
A.)	Level 2	The Overall Systems for the Robot
	Structural Systems	Bases of the overall robot assembly.
	Mechanical Systems	Mechanical systems needed to produce movement.
	Electrical Systems	Electrical systems needed to operate the robot and achieve the objective.
B.)	Level 3	Subsystems Under Each General System
	Structural Systems	

	Structural Base	L-Channel and U-Channel bolted assembly that will be the mounting point of all other systems and subsystems.
	Disc Carrier	Cargo area that holds the entire lead disc loads. Works with the unloading mechanism.
	Mechanical Systems	
	Drive Train	Direct Drive Train system that propels the robot and allows maneuverability.
	Unloading Mechanism	A four bar mechanism that actuates a gate which unloads the cargo down a ramp.
	Electrical Systems	
	Navigation and Unloading	Assembly of sensors that allows the robot to navigate and determine when to unload the cargo.
	Power Requirements	Power distribution to allow the required current to each sensor and the appropriate voltage drop to each component.
C.)	Level 4	Each Individual Part and the necessary steps to ensuring operation.
	Structural Base	
	U-Channels	Design, procure materials, make drawings, and Machine components for the structural base.
	L-Channels	Design, procure materials, and Machine components for the structural base.
	Casters	Procure and ensure integration.
	Assembly and Integration	Ensure fitting of structural base to itself and other components later on.
	Disc Carrier	
	Section Walls	Design, procure materials, make drawings, and machine components for the disc carrier.
	Section Base	Design, procure materials, make drawings, and machine components for the disc carrier.
	Ramp	Design, procure materials, make drawings, and machine components for the disc carrier. Ensure that the incline will allow the lead discs to roll into the targeted area.
	Force Sensor	Select an appropriate force sensor that can detect the presence of a load reliably.

	Assembly and Integration	Assemble and integrate into the structural base.
	Drive Train	
	Drive System	Select appropriate drive system type for design. Calculate required torque and RPM needed for our velocity move profile.
	Motors	Select appropriate motors that have a torque greater than the required torque and accommodate our speed requirement. Procure and test the motors to ensure functionality.
	Wheels	Ensure radius and material are appropriate for the design.
	Motor Mounts	Design, procure materials, and fabricate mounts.
	Assembly and Integration	Assemble and integrate onto the structural base. Ensure that the system can maneuver so far.
	Unloading Mechanism	
	Mechanism Design	Design a four bar mechanism that is appropriate for our weight capacity.
	Servo Selection	Calculate the torque needed and select the appropriate servo. Test the servo on procurement.
	Servo Mount	Design, procure materials, and fabricate the necessary mounts to attach the servo and linkages to the robot.
	Linkages	Procure materials and machine linkages according to the four bar mechanism design.
	Pin Brackets and Force Gate	Design, procure materials, and fabricate the necessary components to complete the actuated gate for the four bar mechanism.
	Shafts	Procure materials and fabricate shafts for the unloading mechanism.
	Assembly and Integration	Assemble and integrate into the robot. Ensure the unloading mechanism can be actuated smoothly and can hold the allocated load.
	Navigation and Unloading	
	Sensor Assembly Design	Conceptually design a method of sensing the ramp walls to allow the robot to navigate. Also design a method to allow the robot to sense when it is able to unload.
	Electrical and Control Design	Design the circuitry needed to power all of the sensors. Procure materials and fabricate the needed circuitry. Test the circuit to ensure that all sensors are

		operating. Program the FPGA to take voltage readings from the sensors test the system.
	Testing and Integration	Integrate the sensor assembly into the robot and test the actual movement of the robot. Fine tune any necessary movements to ensure a smooth travel path.
	Power Requirements	
	Power Distribution Design	Select the appropriate batteries to power the servos, motors, sensors, and SB-RIO. Design any further circuitry to allow for the appropriate voltage across the servos and motors.
	Testing and Integration	Integrate the batteries and circuitry into the robot along with the servos, motors, sensors, and the SB-RIO and ensure that they can all be powered sufficiently.

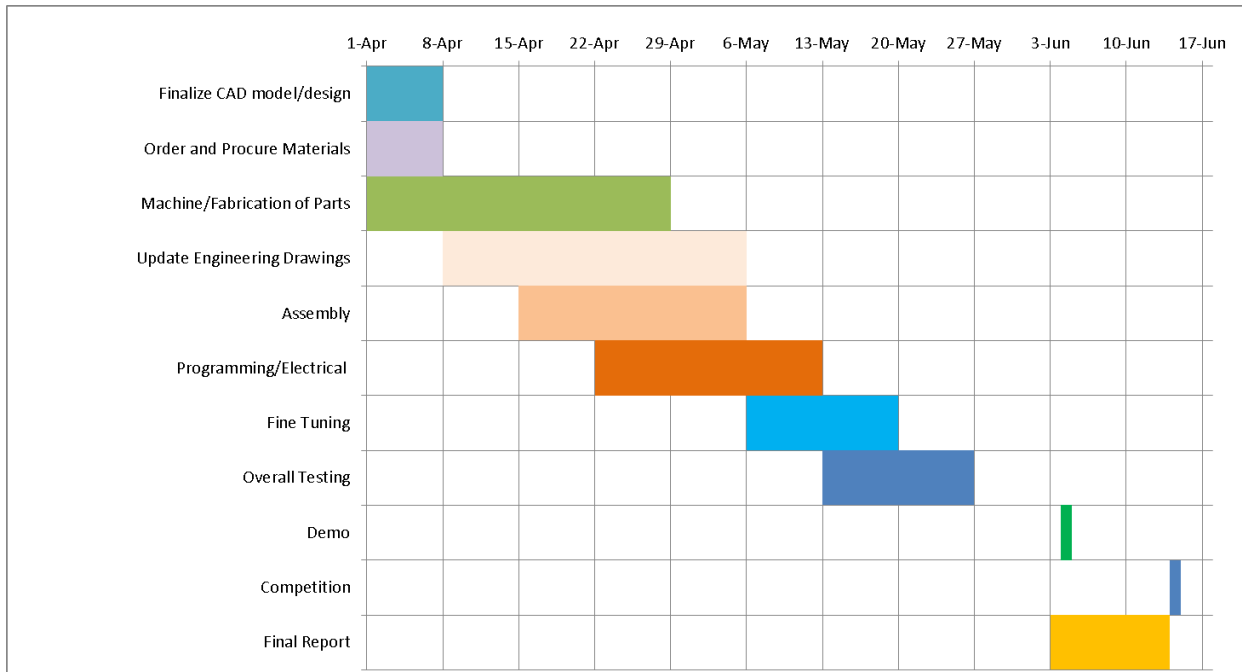


Figure 57: Gantt Chart

IX. BILL OF MATERIALS AND COST ANALYSIS

I. Bill of Materials

Below is our exploded view for our completed robot assembly. The numbered parts correspond to the actual parts that we will purchase in the bill of materials, which is shown in table 19. For our bill of materials, the majority of our structural components do not come pre-assembled and must be purchased as cut metals, and then fabricated into the desired part. Table 27 in the Appendix shows the Bill of Materials from the SolidWorks function that is shown according to individual parts that the final robot assembly will need. The exploded figure below corresponds to the Bill of Materials in table 20 below. In table 20, the materials are arranged by the purchased state of the parts before any fabrication.

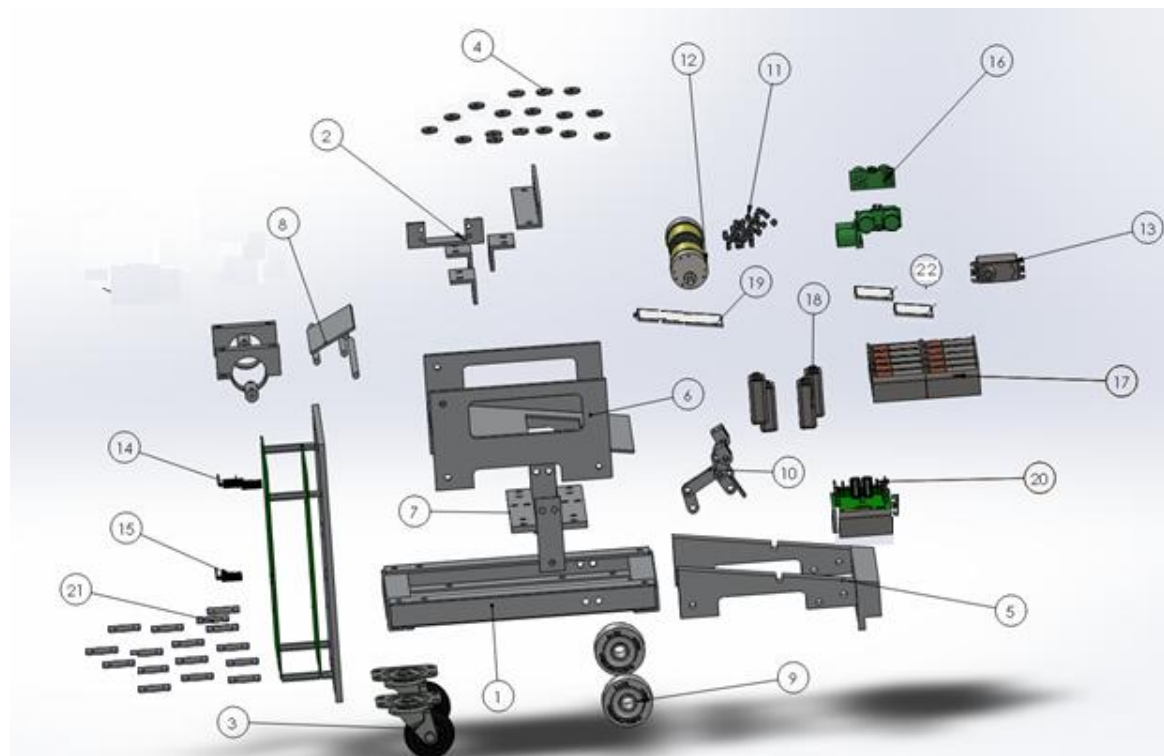


Figure 58: Exploded Robot Materials

Table 20: Bill of Materials

Part #	Description	Source	Unit Cost	Quantity	Total
Structural Components					
1	1" aluminum U-channel (4ft length) (C41616)	http://www.brunnerent.com	\$11.36	1	\$11.36
2	1" aluminum L-beam (3ft) 6061-T6	StainlessSupply.com	\$8.80	1	\$8.80
3	2" casters	Anawalt Lumber	\$2.99	2	\$5.98
4	Steel Ball Bearings (Flanged Open) (6383K213)	McMaster-Carr	\$3.17	2	\$6.34
5	6061-T651 Aluminum Plate 1/4" x 6" x 24"	StainlessSupply.com	\$22.65	1	\$22.65
6	6061-T6 Aluminum Sheet 1/8" x 6" x 30"	StainlessSupply.com	\$11.23	1	\$11.23
7	6061 Aluminum Flat Bar 1/2"x3"x 1"	StainlessSupply.com	\$7.41	1	\$7.41
8	6061 Aluminum Round Bar 1/2" x 3'	StainlessSupply.com	\$3.27	1	\$3.27
Mechanical Components					
9	Colson Wheels 2" x 7/8" (BPDWC02)	http://www.robotmarketplace.com/products/0W-BPDWC02.html	\$2.99	2	\$5.98
10	Everbuilt 1" zinc-plated hinge (2-pack) (15161)	Home Depot	\$1.97	1	\$1.97
11	Nuts/Bolts/Screws/Washers	HomeDepot/Anawalt	\$8.00	1	\$8.00
12	Planetary Metal Geared Motor (PD51M)	The Robot Marketplace	\$49.99	2	\$99.98
13	High-Torque Servo (1501MG)	ValueHobby.com	\$12.85	2	\$25.70
Electronics Components					
14	6.2V Voltage Regulator, 100 mA max (NTE988)	http://www.radioshack.com/product/index.jsp?productId=12673923	\$1.47	2	\$2.94
15	5V Voltage Regulator (For sensors) (LM2937)	https://solarbotics.com/product/lm2937/	\$1.50	1	\$1.50
16	Ultrasonic Range Finder (comes in lot of 5) (HC-SR04)	http://www.dhgate.com/5pcs-lot-ultrasonic-module-hc-sr04-distance/p-ff80808138bd39080138d59ebe0b1eb5.html?recinfo=8,1,3#cppd-3-1	\$2.60	5	\$13.00
17	Rechargeable NiMh Battery Pack 12V, 2000mAh (11621)	all-battery.com	\$9.95	1	\$9.95
18	9V Alkaline Battery (2 pack)	http://www.batteriesandbutter.com/MN16049V4ARP.html	\$7.00	4	\$28.00
19	Force Contact Sensor	Constructed	FREE	1	FREE
20	Sabertooth dual 25A motor driver	http://robokitsworld.com/index.php?main_page=product_info&cPath=73&products_id=342	Donated	1	Donated
21	Fuses (variable sizes and prices)	RadioShack	\$3.00	1	\$3.00
22	Contact Sensors	Constructed	FREE	2	FREE
					Tax/ Shipping
					8.75%
					307.76

II. Cost Analysis

All of our aluminum parts were found from scrap metal yards and hardware suppliers for a lower price. Since we only require a small amount of commonly found U-channels among other pieces, they should be easy to obtain in a cheaper manner. We were also able to obtain additional aluminum scrap metal from the scrap pile in the university machine shop. Other components such as the casters, ball bearing, and hinges will be ordered from their respective stores. Our nuts and bolts can be found at any hardware store. Electronics were obtained through their respective online stores. After the first servo was broken, the second servo was purchased at Fry's Electronics. We also purchased three ultrasonic proximity sensors from another group. All of our orders were done through our liaison and shipped to our own address for convenience.

X. DESIGN REQUIREMENT SATISFACTION

In this section, we show whether each subsystem design requirement is met. Shown below is a table illustrating the certain subsystems along with whether the design requirement is met and why. For more detail refer to the previous sections, since this table is meant to summarize our findings.

Table 21: Subsystem Design Requirement Satisfaction

Subsystem	Design Requirement Met?	Reason
Electronics	Yes	* <u>Force sensor</u> - Just needed to sense load <u>Ultrasonic sensor</u> - range: 2cm – 4m <u>Sensors</u> - require 5V; 9V used to power them <u>Motors</u> - require 12V; 12V battery pack satisfies this requirement.
Unloading Mechanism	Yes	Servo motor torque exceeds required torque for force gate. Initial potential energy sufficient enough to allow disks to roll out into collection bin: (Horizontal displacement = 0.41 ft > 0.33 ft)
Direct Drive Train	Yes	* $T_{drive} > T_{req_motor} + T_{prop}$ where $T_{drive} = 152.75 \text{ lb-in}$ and $T_{req_motor} + T_{prop} = 14.137 \text{ lb-in}$
Batteries (Run – Time)	Yes	Allows for a run time of 1.4 hours; much greater than our set run time of 136.1 sec.

*See below for more clarification.

Within our electronics subsystem, we have sensors and motors. We only need a force sensor to sense the lead disks, so precision is not needed. Therefore, a cheap force sensor

will suffice. Furthermore, our ultrasonic sensors can detect a range from 2cm to 4m, which is more than enough in terms of distances of the ramp. The sensors only require 5V needed to power them. Since we are using a 5 V voltage regulator and powering them using our 9V battery pack, this more than enough voltage needed, since the dropout voltage is typically 2V. For the motors, the 12V battery pack is sufficient to power our motors as shown in our Motor Specifications. With regard to the direct drive train subsystem, the drive torque includes both of our two motors. Thus, each motor provides a drive torque of 76.375 lb-in.

XI. CONCLUSIONS

We have completed the final design for the autonomous disc transporter robot and the result can complete the high and low level requirements that were initially set. The design specifications were changed as the new dimensions and weight of the robot is: 11.37 in x 8.64 in x 14.25 in and the loaded weight with 5 discs is 49.36 lb. We calculated the center of mass for the loaded and unloaded cases to be (2.00, 7.23, 5.00) inches and (3.29, 5.13, 5.24) inches by evaluating the completed final assembly in SolidWorks. We will use a RWD drive train system, which has minimum friction coefficients of 0.258 and 0.371 for the loaded and unloaded cases. The weight distributions, β , is calculated for the front and rear wheelbases using MATLAB. The maximum rear wheelbase weight distributions, β_R , are 93.82% and 68.31%, when the robot is travelling up and down respectively on the 14.036° incline. The corresponding required torque is 13.966 lb-in because our wheel radius is 1.00 inches. The required torque is less than the stall torque output, 76.375 lb-in per motor at 94 RPM, for our chosen drive motor, Hennkwell PD264M Planetary Gear Motor, for which we will use two of. In relation to our maximum velocity we obtained a value of 57RPM which relates to our drive torque per motor of 9.043 lb-in. Hence we have a total drive torque of 18.09lb-in which is greater than our maximum requirement torque of 14.520lb-in; which includes the required torque to overcome the mechanisms if 0.5537lb-in. The drivetrain system is currently a direct-drive system due to the low optimal RPM of the motor. The unloading mechanism consists of a motorized gate that unlatches to allow the discs to roll off and re-lifts the gate after unloading. For the forced gate that is attached at the bottom surface of the carrier, the required force is 0.112 lb and required torque is 0.173 lb-in. The user interface for the control systems consists of LabVIEW programming connected to the SB-Rio. From the product testing, we found that the average complete run time was 78.6 seconds and the deviation in times was relatively small. Overall, our calculations from the preliminary design led to a final design that works reliably and adheres to the design requirements.

XII. REFERENCES

1. "Bulk Transporter retraces three quarters of a century of covering the evolution of the tank truck industry." Bulk Transporter. 1 Jul. 2012. Web. 22 Mar. 2013.
http://bulktransporter.com/management/tank-truck/bulk_transporter_retraces_0712/

2. Shaefer, R.S., Mechanical & Aerospace Engineering Department, UCLA , 2013, Mechanical Engineering Based Design: Vehicle Climbing an Incline.
3. Shaefer, R.S., Mechanical & Aerospace Engineering Department, UCLA , 2013, POWER TRANSMISSION: Smart Motor Sizing for the Transporter.
4. Shaefer, R.S., "Ramp-Detail (01-23-13)." MAE Department, UCLA, 2013
5. "Spec Sheet PD264M" Robot Combat. 2013. Web. 17 Feb. 2013.
<http://www.robotcombat.com/products/images/0-PD64M.pdf>
6. Shaefer, R.S., Mechanical & Aerospace Engineering Department, UCLA , 2013, Senior Mechanical Engineering Design Project Description.
7. "Friction and Coefficients of Friction." Engineering Toolbox. 2013. Web. 22 Mar. 2013.
http://www.engineeringtoolbox.com/friction-coefficients-d_778.html
8. "Rolling Friction." Davidson University. 2013. Web. 22 Mar. 2013.
<http://www.phy.davidson.edu/fachome/dmb/PY430/Friction/rolling.html>
9. "Electric Motor Efficiencies." Engineering Toolbox. 2013. Web. 22 Mar. 2013
http://www.engineeringtoolbox.com/electrical-motor-efficiency-d_655.html
10. "PD264M Planetary Metal Geared Motor 51:1." Robot Marketplace. 2013. Web. 22 Mar. 2013.
<http://www.robotmarketplace.com/products/0-PD5264M.html>

XIII. APPENDIX

A. Lengthy Calculations

This section includes all the lengthy derivations for the minimum required friction coefficient needed for our robot to drive up the ramp. Then, we include our schematic of the ramp used in our move profile.

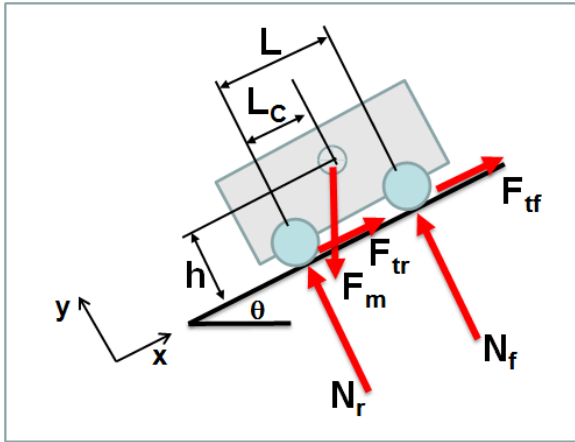


Figure 59: Free Body Diagram of Vehicle on Incline Plane [1]

$$\sum F_x = 0: \quad \gamma_r F_{tr} + \gamma_f F_{tf} - F_m \sin \theta = 0 \quad (1)$$

$$\sum F_y = 0: \quad N_r + N_f - F_m \cos \theta = 0 \quad (2)$$

$$\sum M_r = 0: \quad F_m \sin \theta \cdot h + N_f \cdot L - F_m \cos \theta \cdot L_c = 0 \quad (3)$$

From Equation (3),

$$N_f = \frac{F_m L_c \cos \theta - F_m h \sin \theta}{L} \quad (4)$$

From Equation (2),

$$\begin{aligned} N_r &= F_m \cos \theta - N_f \\ N_r &= F_m \cos \theta - \frac{F_m \cos \theta \cdot L_c - F_m \sin \theta \cdot h}{L} \\ N_r &= \frac{F_m \cos \theta \cdot L - F_m \cos \theta \cdot L_c + F_m \sin \theta \cdot h}{L} \\ N_r &= \frac{F_m(L - L_c) \cos \theta + F_m h \sin \theta}{L} \end{aligned} \quad (5)$$

Traction Force:

$$F_{tr} = \mu N_r \quad (6)$$

$$F_{tf} = \mu N_f \quad (7)$$

Friction Coefficient:

Substitute (6), (7) into Equation (1),

$$\gamma_r \mu N_r + \gamma_f \mu N_f - F_m \sin \theta = 0$$

$$\mu(\gamma_r N_r + \gamma_f N_f) - F_m \sin \theta = 0$$

$$\mu(\gamma_r N_r + \gamma_f N_f) = F_m \sin \theta$$

$$\mu = \frac{F_m \sin \theta}{\gamma_r N_r + \gamma_f N_f}$$

$$\mu = \frac{\gamma_r \cdot \frac{F_m(L - L_c) \cos \theta + F_m h \sin \theta}{L} + \gamma_f \cdot \frac{F_m L_c \cos \theta - F_m h \sin \theta}{L}}{\gamma_r \cdot \frac{F_m(L - L_c) \cos \theta + F_m h \sin \theta}{L} + \gamma_f \cdot \frac{F_m L_c \cos \theta - F_m h \sin \theta}{L}}$$

$$\mu = \frac{L \sin \theta}{\gamma_r [(L - L_c) \cos \theta + h \sin \theta] + \gamma_f [L_c \cos \theta - h \sin \theta]}$$

$$\mu = \frac{L \sin \theta}{\gamma_r L \cos \theta - \gamma_r L_c \cos \theta + \gamma_r h \sin \theta + \gamma_f L_c \cos \theta - \gamma_f h \sin \theta}$$

$$\mu = \frac{(y_f - y_r)L_c \cos \theta - (y_f - y_r)h \sin \theta + \gamma_r L \cos \theta}{L \sin \theta}$$

$$\boxed{\mu = \frac{(y_f - y_r)(L_c \cos \theta - h \sin \theta) + \gamma_r L \cos \theta}{(y_f - y_r)(L_c \cos \theta - h \sin \theta) + \gamma_r L \cos \theta}}$$

AWD: $y_f = 1, y_r = 1$

$$\mu_{AWD} \geq \frac{L \sin \theta}{L \cos \theta}$$

$$\mu_{AWD} \geq \tan \theta$$

FWD: $y_f = 1, y_r = 0$

$$\mu_{FWD} \geq \frac{L \sin \theta}{L_c \cos \theta - h \sin \theta}$$

$$\mu_{FWD} \geq \frac{1}{\frac{L_c \cos \theta}{L \sin \theta} - \frac{h \sin \theta}{L \sin \theta}}$$

$$\boxed{\mu_{FWD} \geq \frac{1}{\frac{L_c}{L \tan \theta} - \frac{h}{L}}}$$

RWD: $y_f = 0, y_r = 1$

$$\mu_{RWD} \geq \frac{L \sin \theta}{-L_c \cos \theta + h \sin \theta + L \cos \theta}$$

$$\mu_{RWD} \geq \frac{1}{\frac{(L - L_c) \cos \theta}{L \sin \theta} + \frac{h \sin \theta}{L \sin \theta}}$$

$$\boxed{\mu_{RWD} \geq \frac{1}{\frac{L - L_c}{L \tan \theta} + \frac{h}{L}}}$$

The ramp path that the robot must traverse is shown in the following figure. The ramp has 3 turns, and 2 inclined sections, and the rest of the sections are straights. The robot begins in the start area and moves up the ramp until it gets to section G. It must unload its disc cargo into the unload area and go down the ramp to collect more discs to unload again.

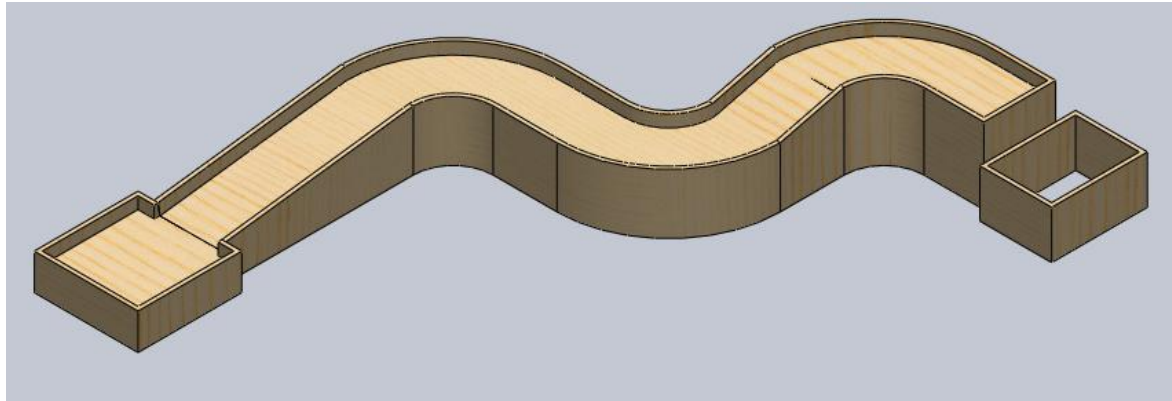


Figure 60: Ramp Isometric View [4]

Dimension are in inches
Scale 1:30
Radius is the same all around
Track width is 16 inches
Wall thickness is uniform

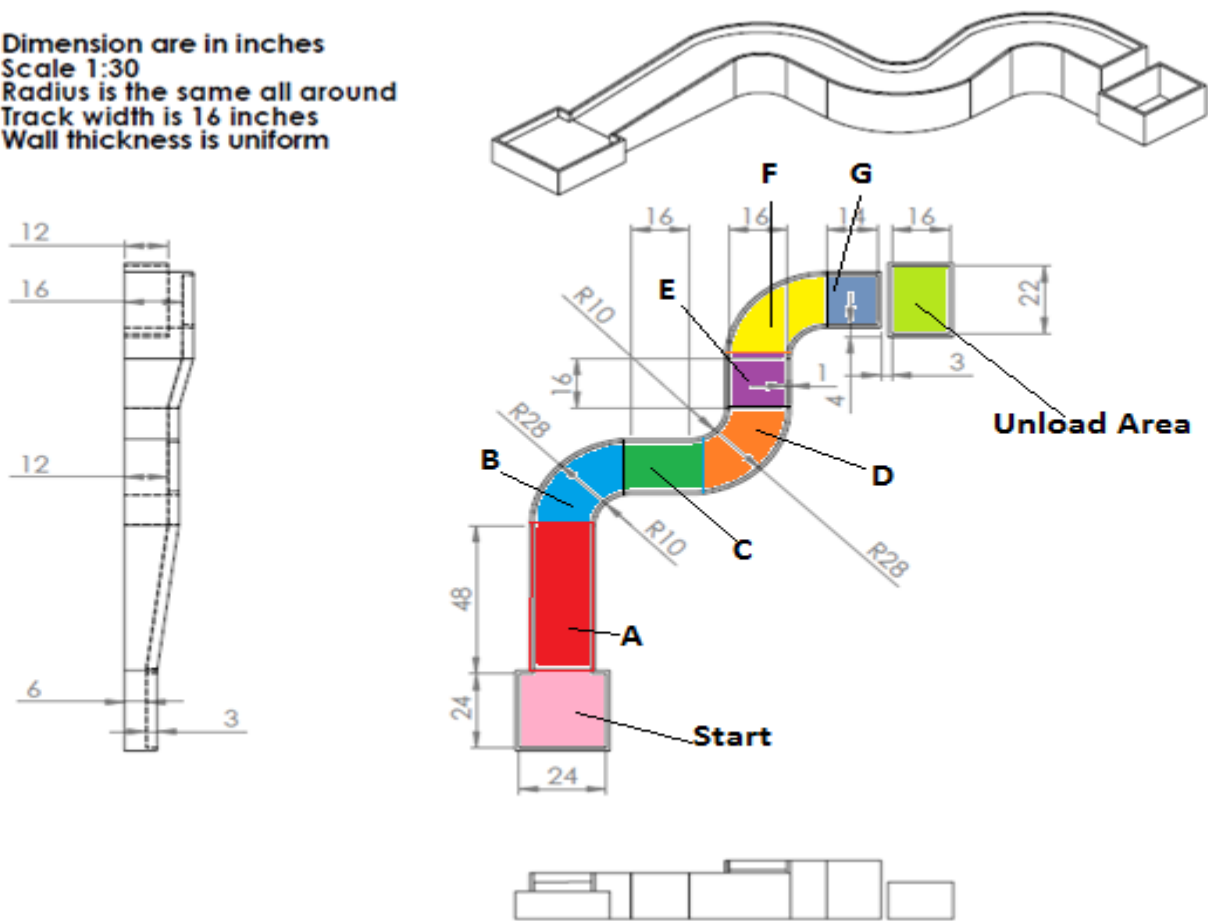


Figure 61: Ramp Engineering Drawing [4]

Ramp 1 (Section A):



Figure 62: Side Dimension of Ramp 1

$$\theta_1 = \tan^{-1}\left(\frac{6''}{48''}\right)$$

$$\boxed{\theta_1 = 7.125^\circ}$$

Ramp 2 (Section E):

Figure 63: Side Dimension of Ramp 2

$$\theta_2 = \tan^{-1}\left(\frac{4''}{16''}\right)$$

$$\boxed{\theta_2 = 14.036^\circ}$$

$$\therefore \boxed{\theta_{max} = 14.036^\circ}$$

Table 22: Ramp Section Parameters

	A	B	C	D	E	F	G
Type	Straight	Quarter Circle	Straight	Quarter Circle	Straight	Quarter Circle	Straight
Length (in)	48.37	29.84	16	29.84	16.49	29.84	14
Elevation Angle θ (degrees)	7.13	0	0	0	14.04	0	0
Radius I/O (in)	-	10/28	-	10/28	-	10/28	-
* = length of middle path ($r = (10 + 28)\text{in}/2 = 19 \text{ in}$)							

The length of the curved sections, B, D, and F are calculated by assuming that the robot will traverse the middle of the path, which has a radius of 19 in. The curved sections are assumed to take on the shapes of quarter circles.

B. Detailed Figures/Long Tables

This section includes all of our conceptual design tables used to evaluate which design was best. The tables below include everything related to our pairwise comparison chart and our objectives tree chart.

Table 23: Pairwise Comparison Chart

Pairwise Comparison Chart		# Designers (number of votes)									
Assets	Factors	Compared To							Total	Weight	
		Cost	Load Capacity	Power	Durability	Aesthetics	Speed				
		Cost	10	4	4	6	8	4	36	0.17	
		Load Capacity	6	10	6	5	8	5	40	0.19	
		Power	6	5	10	6	8	5	40	0.19	
		Durability	4	5	4	10	7	5	35	0.17	
		Aesthetics	2	2	2	3	10	2	21	0.10	
Sensitivity							8	10	39	0.18	
							Total Sum:		211	1.00	

*Note: Number of votes is 10 because each member is allowed 2 votes.

Table 24: Weighted Design Scores

Design Scores (arb. 1 to 10)			Weighted Design Scores			
Design 1	Design 2	Design 3	Design 1	Design 2	Design 3	
10	10	10	1.71	1.71	1.71	
6	7	8	1.14	1.33	1.52	
8	8	9	1.52	1.52	1.71	
9	9	6	1.49	1.49	1.00	
8	10	8	0.80	1.00	0.80	
8	8	7	1.48	1.48	1.29	
Total Score:			8.13	8.52	8.01	

Table 25: Types used in Objectives Tree Chart

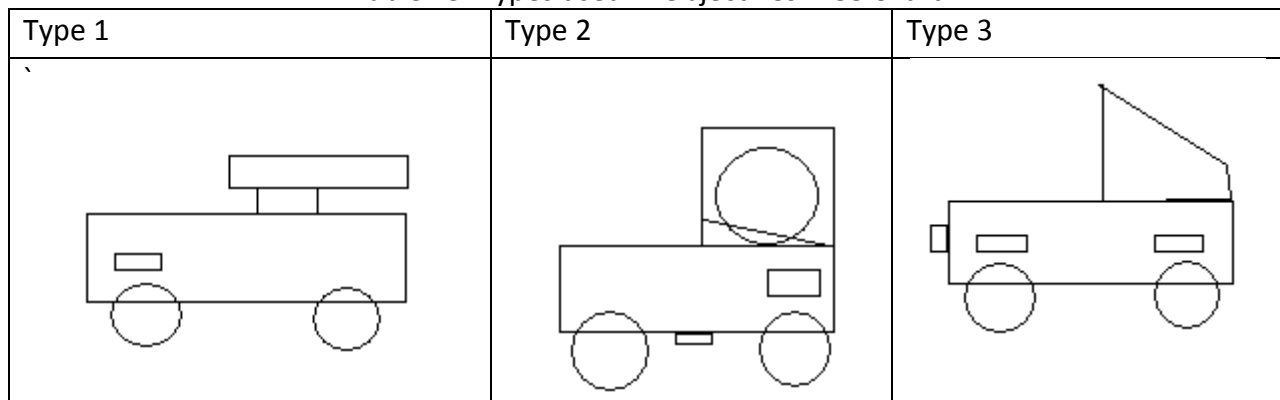


Table 26: Objectives Tree Chart

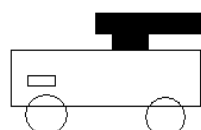
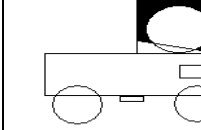
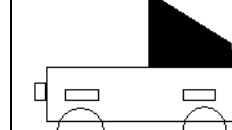
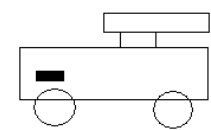
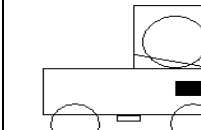
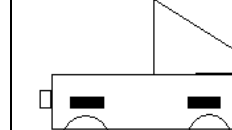
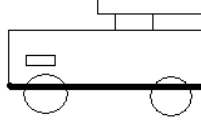
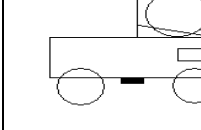
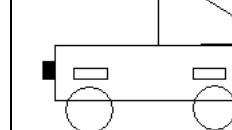
	Sub-function	Function Carrier	Task	Principle of Evaluation	Weight factor	Type 1	Type 2	Type 3
A	Offers space for the disks and unload disks	Delivery system/ container	Optimal size and shape/ mechanism	Load Capacity/ Unloading mechanism efficiency	0.19	6 	7 	8 
B	Generates the power for movement	Motor	Optimal placement/ number of motor(s)	Power	0.19	8 	8 	9 
C	Senses the obstacles and follows pathway accurately	Sensors	Optimal position/type	Sensitivity	0.18	8 	8 	7 
D	Aesthetic			0.10	8	10	8	
E	Durability			0.17	9	9	6	
F	Cost			0.17	10	10	10	
	Total Sum			1	8.13	8.52	8.01	
	Order of merit				2	1	3	
	<p>NOTES:</p> <p>(1) Evaluation marks: 0 – unacceptable, 1-3 still acceptable, 4-6 fair, 7-9 good, 10 very good [optimal solution]</p> <p>(2) Total sum of weighing factor is unity</p> <p>(3) Order of Merit: 1 highest; 3 least</p>							

Table 27: Bill of Materials Sorted by Parts

ITEM NO.	PART NUMBER	CORRESPONDING PART #	QTY.
1	U-Channel Right	1	1
2	U-Channel Front	1	1
3	U-Channel Back (No Gate)	1	1
4	U-Channel Left	1	1
5	washer	11	6
6	2in swivel caster	3	2
7	6.4x1x.25" motor mounting strip	8	2
8	ControlCover	-	1
9	Spacer_Plate-SBRio	-	4
10	SBRio	-	1
11	Spacer_SBRio-AddOnBoard	-	4
12	AddOnBoard	-	1
13	Board Assembly Mount L-Bracket	-	1
14	Ultrasonic Range Finder SRF-06	16	5
15	Ultrasonic Sensor Mount	5	3
16	Motor head	12	2
17	Motor body	12	2
18	Motor Mount	8	2
19	Rear Wheel Final	9	2
20	Shaft Coupler .25 to .125	8	2
21	Shaft Coupler Pin	8	2
22	Rear Shaft Support	2	2
23	Section Wall	2	2
24	Section Base (under disc)	7	2
25	Ramp	6	1

26	Force Gate	6	1
27	Pin Bracket	11	2
28	Force Gate Toggle Shaft Long	5	1
29	Force Gate Shaft	8	2
30	Forge Gate Toggle Bar	8	4
31	Force Sensitive Resistor SEN- 09376	19	1
32	Force Gate Link Limiter	10	1
33	Servo Mount	5	1
34	hs-311-hitec- standard- servo	13	1
35	Servo Bar	5	1
36	Servo Connecting Linkage	10	2
37	Back Edge Rest	6	1
38	cbatteryholder	17	10
39	C Duracell Body	17	10
40	Battery 9V	18	4
41	Motor Controller PCB	20	1
42	User Library- POWER MOSFET, NON- SURFACE- MOUNT	20	8
43	Terminal Block	20	6
44	CAPPR250- 630X1120	20	2
45	6 Pin Header	20	1
46	14 Pin SMT	20	7
47	M3 x 0.5 x 10_PHMS	20	12
48	#10-32 x	11	4

	0.3125_SSCUPSKT		
49	#6-32_MSHXNUT	11	16
50	TO-247H	4	3
51	1	21	8
52	tube	21	4
53	spiral	21	4
54	rocker switch 1	22	1

Table 28: Error Analysis Tables for Five Discs

Error Propagation	Up	Unloading	Down	Total
u (s)	37.93333	5.766667	34.91667	78.61667
σ (s)	0.355903	0.258199	1.020621	1.45522
ΔX_1 (s)	0.3333	0.2667	0.08333	0.51667
ΔX_2 (s)	0.0667	0.1667	0.08333	0.01667
ΔX_3 (s)	0.0667	0.2333	0.58333	0.88333
ΔX_4 (s)	0.4333	0.2667	1.91667	2.61667
ΔX_5 (s)	0.5667	0.2333	0.08333	0.88333
ΔX_6 (s)	0.0667	0.2333	1.08333	1.38333
$\Delta X_1/X_1$ (%)	0.886436	4.849091	0.238086	0.661549
$\Delta X_2/X_2$ (%)	0.175526	2.976786	0.238086	0.021209
$\Delta X_3/X_3$ (%)	0.175526	3.888333	1.643183	1.111107
$\Delta X_4/X_4$ (%)	1.155467	4.849091	5.808091	3.442987
$\Delta X_5/X_5$ (%)	1.471948	3.888333	0.238086	1.111107
$\Delta X_6/X_6$ (%)	0.175526	3.888333	3.00925	1.729163

C. Control Software

The screenshots below show the front panel and block diagram for the LabVIEW code that is used for the robot programming. Figures for the state diagrams are shown in section VI.IV. The front panel has multiple indicators to show: the analog commands given to each motor, the state of the Boolean contact sensors, the output of the ultrasonic proximity sensors, and the current state of the state chart diagram.



Figure 64: LabVIEW Front Panel

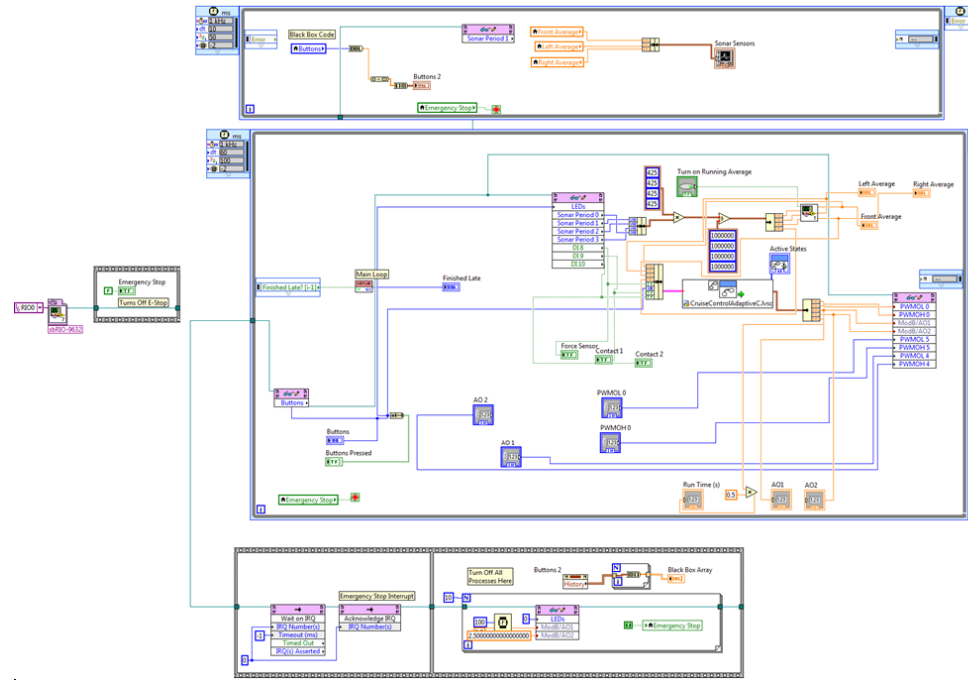


Figure 65: LabVIEW Main Block Diagram

D. Engineering Drawings

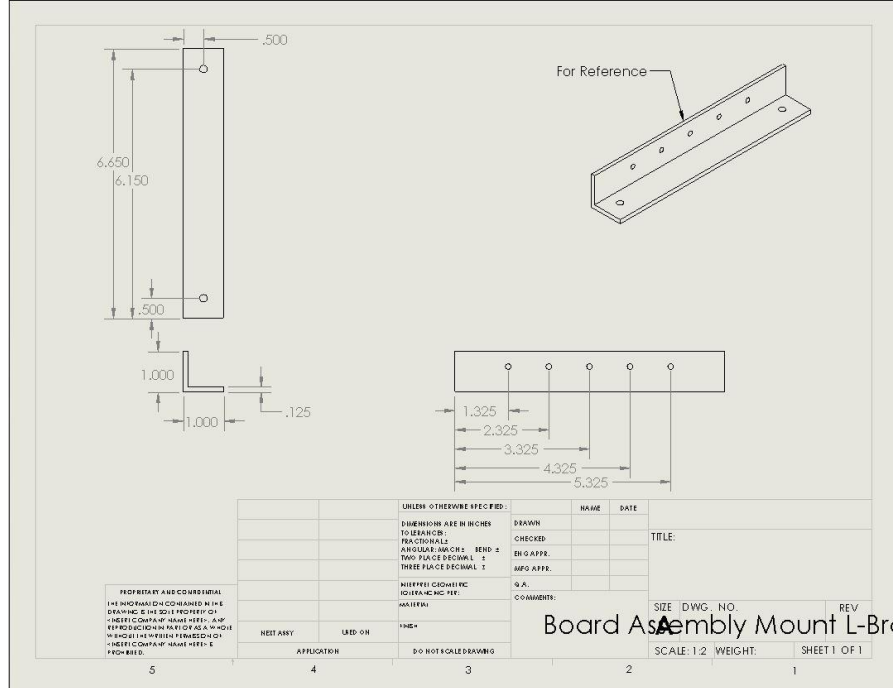


Figure 66: SB-RIO L-bracket Mount